THE EFFECT OF MECHANO-CHEMICAL ACTIVATION OF FLY ASH- NANOPARTICLE BLENDS ON PERFORMANCE OF CEMENT BASED COMPOSITES AND SELF-CONSOLIDATING CONCRETE

by

Rani Pradoto

A Dissertation Submitted in

Partial Fulfillment of the

Requirements for the Degree of

Doctor of Philosophy

in Engineering

at

The University of Wisconsin-Milwaukee

May 2016

ABSTRACT
THE EFFECT OF MECHANO-CHEMICAL ACTIVATION OF FLY ASH- NANOPARTICLE BLENDS ON PERFORMANCE OF CEMENT BASED COMPOSITES AND SELF-CONSOLIDATING CONCRETE

by

Rani Pradoto

The University of Wisconsin-Milwaukee, 2016
Under the Supervision of Professor Konstantin Sobolev

Other than water, portland cement concrete is the most used commodity. Major parts of civil and transportation infrastructure, including bridges, roadway pavements, dams, and buildings are made of concrete. Because of wide-scale applications of these important structures in different climatic zones and associated exposures, concrete durability is often of major concern. In 2013, the study of American Society of Civil Engineers (ASCE) estimated that one-third of America's major roads are in poor or mediocre condition [1]. The same article reports that annual investments of $170 billion on roads and $20.5 billion for bridges are needed to substantially improve the condition of infrastructure. In addition to durability concerns, the production of portland cement is associated with the emissions of approximately one cubic meter of carbon dioxide per ton (plus NO_x and SO_x). Therefore, replacement of portland cement with supplementary cementitious material is an important trend to improve the sustainability of concrete. Indeed, the consideration of these issues as well as proper and systematic design of concrete intended for highway applications is of extreme importance as concrete pavements represent up to 60% of interstate highway systems with heavier traffic loads.

The combined principles of material science and engineering can provide adequate methods and tools to facilitate improvements to concrete design and existing specifications. Critically, durability and enhancement of long-term performance must be addressed at the design stage. Concrete used in highway pavement applications has relatively low cement content and also can be placed at low slump. However, further reduction of cement (cementitious materials) content to 280 kg/m^3 vs. current specifications which require the use of 315 - 340 kg/m^3 of cementitious materials for concrete intended for pavement applications and 335 kg/m^3 for bridge substructure and superstructure needs a delicate proportioning of the mixture to maintain the expected workability, overall performance, and ensure long-term durability in the field. Such design includes, but is not limited to the optimization of aggregates and improvement of efficiency of supplementary cementitious materials (SCM), as well as fine-tuning of the type and dosage of chemical and air-entraining admixtures.

Self-consolidating concrete (SCC) is a new type of concrete which is characterized by its ability to fill the formwork under its own weight without the use of vibration, while maintaining the homogeneity at a very low segregation. Self-consolidating concrete can flow easily under its own weight and is characterized by near zero yield value. Therefore, the design of SCC needs to minimize yield stress parameter which is different from conventional concrete. Better understanding the workability and flow behavior of developed SCC requires the investigation of the rheological response (shear stress and viscosity) of cement pastes of the same composition as SCC.

For maintaining SCC workability it is essential to provide the adequate spacing between the aggregates in order to reduce friction between the particles. This is achieved by using mixtures with higher volumes of cement paste and the optimization of aggregates spacing, grading and

proportions. The cement paste between the aggregates depends on the aggregate packing and is known as a compact paste (so it can be minimized by effective aggregates grading) while the cement paste surrounding the aggregates is known as excess paste. This excess paste allows concrete to flow and maintain a uniform dispersion [2]. The application of self-consolidating concrete (SCC) is focused on high performance, dense and uniform surface textures, improved durability, high strength and faster construction.

The use of nanoparticles in SCC was a subject of interest for many researchers. Collepardi et.al [3] investigated low-heat self-consolidating concrete by combining supplementary cementing materials or SCM such as fly ash and limestone with colloidal nanosilica. In SCC, colloidal nanosilica acts as a viscosity modifying agent. Concrete was mixed, placed and consolidating without compaction and tested for slump flow and compressive strength. The performance of developed concrete was better in respect to slump flow and resistivity to segregation.

In this study, SCC was developed using nanoparticles such as nanosilica and the effect of nanomaterials on the fresh and hardened properties of nano-engineered SCC was investigated. Furthermore, the SCC mixtures were designed with different proportions of fly ash used as with nanosilica and superplasticizer. In addition, for selected SCC mixtures, the use of activated fly ash was investigated to enhance the fresh properties and mechanical performance. The aggregate optimization was based on a computer simulation as reported previously.

This research evaluated various theoretical and experimental methods for the design of the next generation of concrete for civil and infrastructure applications. For selected mixtures, reported research investigated eco-friendly concrete with cementitious materials content as low as 280 kg/m^3 and self-consolidating concrete containing a total of 400 kg/m^3 and 500 kg/m^3 of

cementitious materials, which can be an attractive alternative for the design of sustainable concrete pavements. This research demonstrated that nano-engineering of cementitious phase can be used as an effective tool to design a concrete with specific performance characteristics. For developed concrete, SCM, nanosilica and high range water reducing admixtures were selected based on the optimization study. The performance of different concrete mixtures was evaluated for fresh properties and compressive strength at the age from 1 and up to 90 days. The methods and tools discussed in this research are applicable, but not limited to wide range of concrete civil and transportation infrastructure.

This research demonstrated modern approach to incorporate nano admixtures, activated SCM, the optimization of SCM (e.g., Class F and C fly ash), the use of modern superplasticizers (such as polycarboxylate ether, PCE). In new sustainable concrete, this research proved that the optimization of concrete mixture proportions for specific performance characteristics can be achieved by the use and proper selection of modern superplasticizers, nanosilica and ultrafine SCM. This optimization can result in an effective use of cementitious materials and provide substantial enhancement of performance.

The effective use of supplementary cementitious materials (SCM) such as fly ash as partial replacement of portland cement is a very important strategy to reduce the environmental impact and improve the sustainability of conventional concrete. Many supplementary cementitious materials (SCM) are currently used in concrete improving the performance. Indeed, by-products such as fly ash can be recycled to produce “green” environmentally-friendly concrete with low cost.

The proposed method to improve the performance of SCM is based on the use of nanotechnology and nanomaterials by engineering effective materials at nanolevel. Nanoparticles were found to improve the structure of conventional concrete, accelerate the formation of C-S-H and the development of early age strength, as well as improve the durability of cement based materials.

To facilitate the distribution of nanoparticles, superplasticizing admixtures were investigated to reach the optimal dispersion. In order to increase the performance of cement systems with fly ash, the use of nanoparticles was proposed to boost the early age development.

In this study, the combination of nano-engineered cement (NEC) concept and mechano-chemical activation (MCA) of fly ash with chemical admixtures is realized. The optimization of grinding conditions with AC (activated cement) in the vibrating mill in order to realize MCA has been performed. Due to intensive milling, very effective forms of AC are produced, as proved by the acceleration of heat of hydration of cement systems with AC. The proposed technique for AC uses the liquid state activation in order to facilitate the efficiency of long-term milling. It was proved that the use of mechanically activated composition resulted in the increase of early age compressive strength. The microstructure of AC was characterized using X-ray powder diffraction and scanning electron microscope (SEM). The compressive strength of mortars with activated fly ash was tested and compared with reference. The overall objective of reported study was to develop a new binding material concept based on mechano-chemical activation (MCA) of fly ash with the use of nanoparticles and effective application of developed binders in self-consolidating concrete (SCC).

To analyze proposed concept, the following experimental steps were performed:

1. Optimization of the dosage of chemical admixtures using mortars;
2. Optimization of different types and sources of nanoparticles that can lead to the enhancement of properties of cement based materials;
3. Realization of NEC concept by activating of fly ash- nano particles blend in liquid state to produce finer activated blends;
4. Examination of the effect of activated fly ash on hydration, structure development and mechanical properties;
5. Development of an experimental matrix for comprehensive testing of chemical admixtures, SCM and activated fly ash blends in concrete including SCC;
6. Evaluation of the effect of fly ash and chemical admixtures on fresh properties and mechanical performance of reference (DOT-grade) concrete and SCC;
7. Investigation of the effects of fly ash – nanoparticle combination on flowability and resistance to segregation as well as strength development of eco-friendly SCC.

Based on the established correlations, it was concluded that the use of nano-engineering approach and mechano-chemical activation of fly ash can provide an improved performance of different types of concrete. The enhanced concrete performance can be used as a tradeoff to reduce the portland cement and increase the volumes of SCM to compensate for portland cement component. The optimized superplasticized concrete with nanoparticles and with up to 30% of activated fly ash demonstrated very exceptional workability and mechanical performance. The proposed approach to engineer new concrete provided the material with enhanced performance, extended of life cycle, improved sustainability and environmental benefits.

TABLE OF CONTENTS

1. INTRODUCTION 1
   1.1. MOTIVATION FOR THE RESEARCH 1
   1.2. PURPOSE AND OBJECTIVES 6
2. LITERATURE REVIEW 8
   2.1. NANOTEHCNOLOGY OF CONCRETE 8
   2.2. MODERN SUPERPLASTICIZERS 16
   2.2.1. Supplementary Cementitious Materials 23
   2.3. CONCRETE MIXTURE OPTIMIZATION 26
   2.4. DESIGN OF SELF-CONSOLIDATING CONCRETE (SCC) 27
3. MATERIALS AND METHODS 29
   3.1. MATERIALS 29
   3.1.1. Portland Cement 29
   3.1.2. Fly Ash 31
   3.1.3. Mechano-Chemical Activation 33
   3.1.4. Nanosilica: Colloidal SiO_2 Nanoparticles 36
   3.1.5. Chemical Admixtures 44
   3.1.6. Aggregates 45
   3.2. EXPERIMENTAL PROGRAM 49
   3.3. TEST METHODS 51
   3.3.1. Mini-Slump of Cement Pastes 51
   3.3.2. Rheological Investigation of Cement Pastes 51
   3.3.3. Mortars Tests 52
   3.3.4. Heat of Hydration 53
   3.3.5. Preparation, Mixing, and Curing of Concrete 53
   3.3.6. Slump 53
   3.3.7. Fresh Properties of SCC 54
   3.3.8. Density of Fresh Concrete 55
   3.3.9. Air Content of Fresh Concrete 55
   3.3.10. Temperature 55
   3.3.11. Compressive Strength 55

4. DESIGN OF NANO-MODIFIED COMPOSITES 56
4.1. OPTIMIZATION OF SUPERPLASTICIZERS 56
4.2. RHEOLOGICAL BEHAVIOR OF CEMENT PASTES 59
4.3. MORTARS: THE EFFECT OF SUPERPLASTICIZERS 65
4.3.1. Fresh Properties 65
4.3.2. Mechanical Performance 70
4.3.3. The Effect of SCM 73
4.3.4. Heat of Hydration 76
4.4. INCORPORATION OF NANOSILICA 78
4.4.1. Use of Cembinder Grade Nanosilica 78
4.4.2. The Effect of SP on Hydration and Strength of Mortars with SCM 82
4.4.3. The Effect of Nanosilica Derived from Hydrothermal Solutions 86
4.5. EFFECT OF MECHANO-CHEMICAL ACTIVATION 93
4.5.1. Microstructure of activated fly ash 93
4.5.2. Hydration Process 94
4.5.3. Compressive Strength 98
5. OPTIMIZATION OF CONCRETE MIXTURES 100
5.1. CONCRETE FOR PAVING APPLICATIONS 100
5.1.1. Target Properties 100
5.1.2. Fresh Properties 101
5.1.3. Strength Development 102
5.2. OPTIMIZATION OF SELF CONSOLIDATING CONCRETE 106
5.2.1. The Evaluation of SCC 106
5.2.2. Fresh Properties 106
5.2.3. Strength Development 109
6. CONCLUSIONS 113
7. FUTURE RESEARCH 116
REFERENCES 117
CURRICULUM VITAE 127

LIST OF FIGURES

Figure 1. The scale ranges related to concrete [10] 1

Figure 2. Concept of nano-binder [26] 4

Figure 3. The particle size and specific surface area scale related to concrete materials [21, 22]. 9

Figure 4. Nanosilica particles under the TEM [6, 51] 11

Figure 5. The process used by a geothermal power plant [43] 15

Figure 6. The effect of sulfonated melamine formaldehyde (smf) superplasticizer on the compressive strength of type I and V cement [61]. 17

Figure 7. Particle's dispersing mechanisms [64]. 18

Figure 8. Chemical structure and electrostatic repulsion mechanism of sulfonated ring superplasticizers [63]. 19

Figure 9. Selective sulfonated ring superplasticizers [63]. 20

Figure 10. Polycarboxylate superplasticizers: steric hindrance mechanism, adapted from Lubrizol [64] (left) and generic structure [69] (right). 20

Figure 11. Size and morphology of polycarboxylate SP, from Sakai et al. [68]. 22

Figure 12. Mixture proportioning method for high-performance concrete [103]..... 27

Figure 13. SEM images of portland cement at: a) 1000x magnification, and b) 2000x magnification 30

Figure 14. EDS spectrum of portland cement..... 31

Figure 15. SEM images and EDS spectrum of ASTM Class C fly ash 32

Figure 16. SEM images and EDS spectrum of ASTM Class F fly ash 32

Figure 17. Characteristic shapes of grinding media..... 35

Figure 18.The optimization of grinding media for 3-hour activation 36

Figure 19 PSD of the collected nanosilica samples of Cembinder 50 and Cembinder 8 (samples CnS-1 and CnS-2, respectively) [104] 37

Figure 20. The formation of C-S-H gel from nanosilica [105] 39

Figure 21. The effect of C-S-H formation on the surface of cement grain [105] 39

Figure 22. Particle shape of (a) Cembinder 50 and (b) Cembinder 8 [104] 40

Figure 23. The X-ray Diffractogram (left) and Scanning Electron Microscope image (right) of the N2 silica powder 42

Figure 24. The FTIR spectroscopy of silica nanoparticles (left) and model of the corresponding amorphous structure (right) 42

Figure 25. Particle size analysis of southern aggregates C1, F1, I1 (i) and optimization of aggregates proportions using 0.55 power curve and packing simulations (ii) [108] 48

Figure 26. The effect of portland cement and admixture type on mini-slump 57

Figure 27. The effect of SCM and type of admixture on mini-slump of pastes based on cements L1 (a) and L2 (b) 58

Figure 28. Shear stress vs. shear rate in cement paste W/CM = 0.3 61

Figure 29. Shear stress vs. shear rate in cement paste W/CM=0.375 62

Figure 30. Viscosity vs. shear rate in cement paste W/CM = 0.3 63

Figure 31. Viscosity vs. shear rate in cement paste W/CM=0.375 64

Figure 32. The effect of SNF (HR1 / HD1) and PCE (HAC / HG7) superplasticizers and mid-range water-reducer (RP8) on the flow of mortars 67

Figure 33. The effect of SNF (HR1 / HD1) and PCE (HAC / HG7) superplasticizers on the fresh density of mortars vs. mid-range water-reducer (RP8) 67

Figure 34. The correlation between the mini-slump of pastes and mortar flow 68

Figure 35. The effect of chemical admixtures on mortar flow 68

Figure 36. The effect of admixtures and SCMs on flow of mortars (based on cement L1 (a) and L2 (b) 69

Figure 37. Compressive strength of mortars with mid-range water-reducer (RP8) 71

Figure 38. Compressive strength of mortars with SNF superplasticizer (HR1) 72

Figure 39. Compressive strength of mortars with PCE superplasticizer (HG7) 72

Figure 40. The effect of SCM on strength of mortars based on cement L1 (a) and L2 (b) 75

Figure 41. The effect of mid-range water-reducing admixture (RP8) on cement hydration 76

Figure 42. The effect of SNF (HR1) admixture on cement hydration 77

Figure 43. The effect of PCE (HG7) admixture on cement hydration 78

Figure 44. Effect of cembinder 8 on heat of hydration of cement mortars 79

Figure 45. Effect of cembinder 50 on heat of hydration of cement mortars 79

Figure 46. The dosage and type of nanoparticles on mortar flow 81

Figure 47. Dosage and type of nanoparticles in mortar compressive strength 81

Figure 48. The effect of SP dosage on cement hydration a) heat flow, b) cumulative heat 84

Figure 49. The effect of SP dosage on the hydration of blended cement with class C fly ash and nanosilica. a) heat flow, b) cumulative heat 85

Figure 50. The effect of SP dosage on the compressive strength of mortars 86

Figure 51. The effect of SiO_2 nanoparticles on 88

Figure 52. The shift of C_3S and C_3A peaks due to the addition of nanosilica (left) and hydration energy of investigated systems (right) 88

Figure 53. The determination of setting time of nano-SiO_2 based mortars 90

Figure 54. The compressive strength of mortars with nano-SiO_2 particles 91

Figure 55. The correlation of compressive and splitting tensile strength for mortars with nano-SiO_2 91

Figure 56. Reference fly ash with large cenospheres 93

Figure 57. The SEM image for fly ash activated for different times, about 30% of small cenospheres are still present after 3-hour activation, 2000X magnification..... 94

Figure 58. The effect of activation on hydration of cement with fly ash..... 96

Figure 59. The effect of activated fly ash on cement hydration; a) class C fly ash; b) class F fly ash 97

Figure 60. The effect of activation time on compressive strength of cement systems with 30% of fly ash. 98

Figure 61. The effect of activated fly ash and nanosilica on compressive strength of mortars with 20% of fly ash a) Class C fly ash b) Class F fly ash 99

Figure 62. The relationship between the air content and fresh density of concrete mixtures..... 102

Figure 63. Strength development of concrete produced at cementitious material content of 280 kg/m^3 103

Figure 64. Slump flow of SCC with cementitious material content of 400 kg/m^3 (a) and 500 kg/m^3 (b)..... 108

Figure 65. Correlation between the slump flow and J-ring test 109

Figure 66. Strength of SCC produced at cementitious material content of 400 kg/m^3 (a) and 500 kg/m^3 (b)..... 110

LIST OF TABLES

Table 1. Structural factors affecting dispersibility and retention of dispersibility [68] 21

Table 2. Chemical composition of portland cement 29

Table 3. Physical properties of portland cement 30

Table 4. Chemical composition of fly ash 31

Table 5. Physical properties of fly ash 32

Table 6. Properties of Nanosilica 37

Table 7. The composition of the hydrothermal solutions [106] 41

Table 8. Characterization of Silica Nanoparticles 41

Table 9. Properties of chemical admixtures 45

Table 10. Designation and sources of aggregates 46

Table 11. Physical characteristics of aggregates in oven dry (OD) and saturated surface dry (SSD) conditions 46

Table 12. Bulk density and void content of aggregates in loose and compacted state 46

Table 13. Grading of coarse aggregates 47

Table 14. Grading of intermediate aggregates 47

Table 15. Grading of fine aggregates (sand) 47

Table 16. Rheological parameters of cement based materials [115] 52

Table 17. Mini-slump of cement pastes based on L1 at different W/C ratios 56

Table 18. Mixture proportions of cement pastes 59

Table 19. Effect of admixtures on flow of mortars 65

Table 20. Effect of admixtures on fresh density of mortars (limiting value are selected) 66

Table 21. The effect of admixtures on the compressive strength of mortars (w/c=0.45) 70

Table 22. Compressive strength of mortars designed with different SCM.....74

Table 23. Properties of investigated binders.....80

Table 24. The effect of PCE MP40 superplasticizer on performance of mortars with nanosilica 82

Table 25. The Effect of Nano-SiO_2 on Hydration of Mortars 88

Table 26. Compressive and splitting tensile strength of mortars with nano-SiO_2 92

Table 27. Experimental matrix and performance characteristics of mortar.....95

Table 28. Mixture proportions used for concrete with cementitious material content of 280 kg/m^3.....104

Table 29. Fresh and hardened properties of concrete with cementitious material content of 280 kg/m^3.....105

Table 30. Mixture proportions for SCC with cementitious material content of 400 kg/m3 and 500 kg/m3.....111

Table 31. Fresh and hardened properties of SCC with cementitious material content of 400 kg/m^3 and 500 kg/m^3 112

ACKNOWLEDGMENTS

I would like to gratefully acknowledge Professor Konstantin Sobolev for his guidance, his appreciation and his support throughout this research study, who first introduced me to the world of concrete nanotechnology. This study would not be possible without his guidance, countless encouragement and support.

I would like to thank Dr. Ismael Flores-Vivian for his endless helping to develop mix proportions and experimental protocols, and providing his guidance on many aspects of my research. I would also like to thank Marina Kozhukhova for numerous discussions related to this work. I would like to express a great gratitude to Dr. Habib Tabatabai, Dr. Ben Church, Dr. Michael Nosonovsky and Dr. Marina Kozhukhova for their support and contributions as members of my dissertation committee. I would like to express special thanks to all graduate and undergraduate students that assisted in preparation of concrete mixtures, tests and heavy work in the lab: Reza Moini, Scott Muzenski, Emil Bautista, Clayton Cloutier, Justin Flickinger, Kali Lorraine Phillips, Andrew Sinko, Emily Ann Szamocki, Nathaniel Havener, Leif Stevens Jackson, Brian Mullen, Katie LeDoux, Sara Dashti, Gaven Kobes, Jason Atchison, Chris Ball, Mark Moyle, Alper Kolcu, Jesus Cortes, Sunil Rao, Jayeesh Bakshi, Brandon Bosch, and Rahim Reshadi.

Finally, I would like to thank my parents and my family back home in Indonesia for their support and the love they give me and all my friends for their encouragement support and friendship.

1. INTRODUCTION

1.1. MOTIVATION FOR THE RESEARCH

There is an ongoing quest to modify and improve the properties of concrete which can be realized at different scale levels (*Figure 1*). At a macroscale, the optimization of aggregates is used to reduce the consumption of cementitious materials [3-7] and also to improve the performance of concrete mixtures [8, 9].

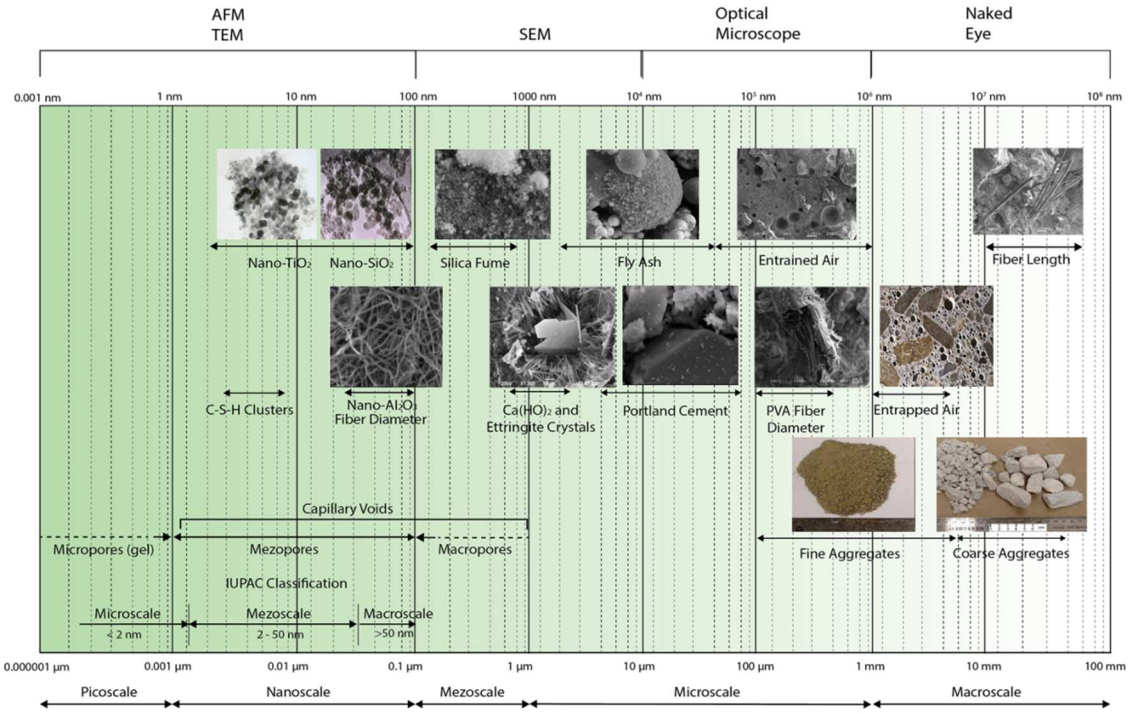

Figure 1. The scale ranges related to concrete [10]

The addition of air entraining admixtures and engineering of specific air-void structure are commonly used to enhance the resistance of concrete against freeze-thaw damage. At a sub-micro- and micro- scale, the addition of supplementary cementitious materials was used to improve the long-term mechanical response and durability of cement based materials [11, 12]. At

nanoscale, nanoparticles of SiO_2 were used in cement composites to modify the rheological behavior, to enhance the reactivity of supplementary cementitious materials, as well as to improve the strength and durability [13].

There is an urgent need for a paradigm change in current cement technology to reduce the environmental burden caused by cement production .This can be achieved by shifting to new sustainable products that perform more effectively, reduce energy consumption, use fewer raw materials, release less emissions and, also, are cost effective [14, 15] . The increasing global demand for cement can be partially met by the use of alternative cements and supplementary cementitious materials (SCM), and especially, by the utilization of industrial by-products, such as fly ash and granulated blast furnace slag [14-20] . The use of SCMs has already become one of the most important developments in modern cement and concrete technology. Replacing portland cement with such by-products, however, presents considerable challenges, including reduced rates of strength development.

Concrete, the most ubiquitous man-made *material*, is "a nano-structured, multi-phase, composite material which ages over time" [21]. The properties of concrete "exist in, and the degradation mechanisms occur across, multiple length scales (nano to micro to macro) where the properties of each scale derive from those of the next smaller scale" [16, 21-23]. The amorphous phase, calcium-silicate-hydrate (C–S–H) holds concrete together and is itself a nanomaterial [24]. With its "bottom-up" possibilities, nano-chemistry offers new products that can be effectively applied in cement and concrete technology. One example is related to the development of new admixtures for concrete, such as polycarboxylic ether (PCE) superplasticizers designed for extended slump retention [25]. It was proposed that, when nanoparticles are incorporated into conventional building materials, such materials can "possess

advanced performance required for the construction of high-rise, long-span or intelligent civil and infrastructure systems" [16, 22, 23]. The nanoparticles of SiO_2 can be used as an additive for high-performance and self-compacting concrete, improving workability and strength [16-19, 22]. The particle size and specific surface area scale related to concrete materials reflect the general trend to use finer materials [6, 22]. *Figure 1*, for decades, major developments in concrete performance have been achieved with the application of ultrafine particles such as silica fume, and now, with nanosilica. In cementitious systems with SCM, nanoparticles can boost the development of strength as the pozzolanic activity of SCM can be enhanced by the application of nano-SiO_2 [17, 19, 22].

Nano-binder was proposed as a material designed with a nano-dispersed cementitious component to fill the gaps between the particles of mineral additives as demonstrated by *Figure 2* [26]. The nano-sized cementitious component can be obtained by the colloidal milling of portland cement (the top-down approach) or by self-assembly using mechano-chemically induced topo-chemical reactions (the bottom-up approach) [26]. Chemically precipitated C-S-H was suggested as an effective admixture to improve the performance of concrete [27, 28]. It was proposed that nano-sized C-S-H particles with an average size of 5 - 10 nm act as nucleation seeds for the hydration products of portland cement. This bottom-up approach was used for commercial products such as x-seed [29]. In addition to accelerated hydration, the positive effect of the C-S-H seed material is attributed to the significant reduction of porosity, the size of the pores, and overall permeability.

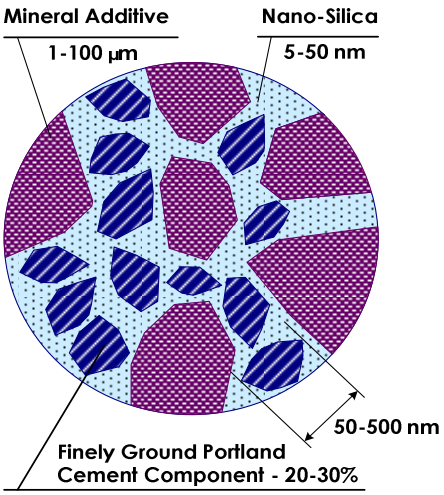

Figure 2. Concept of nano-binder [26]

Fine and ultrafine milling dry components can be used to boost the early strength of cement based materials and improve the efficiency of SCM [26, 30-36]. A well-established approach to improving cement performance includes the use of mechano-chemical activation, MCA [30-33, 37-39]. The term MCA is commonly used to describe the chemical conversions in solids induced by a mechanical process such as intensive milling [40-42]. Commonly, MCA is applied for processing of nano-powders, pigments, fillers, binders, ceramics, and ferromagnetic materials. The mechanical processing usually results in the formation of dislocations and other defects on the surface of particles [41]. In the case of MCA, the mechanical impacts cause the development of elastic, plastic, and shear deformations leading to fracture, amorphization, and even solid-state chemical reactions. In this way, intensive ball milling breaks down the crystallinity of solid reactants and provides a transfer of mass required for chemical reactions. The high pressure and shear stress facilitate both the phase transitions and the chemical transformations of solids. The energy in the form of various lattice defects, is accumulated by the solid particle during the mechanical processing, can support or even trigger various chemical transformations [41].

A significant improvement of cement strength was achieved with MCA [15, 30-33, 37-39]. For example, low water demand binder (LWDB) was produced by intergrinding of cement and a dry modifier in a ball mill [1, 32, 43]; The production of LWDB is based on the intensive milling of cement with sulphonated naphthalene formaldehyde (SNF) superplasticizer at a relatively high dosage (about 4%) resulting in a binder with reduced water demand and very high strength, up to 90 MPa [21]. The strength enhancing performance of complex admixtures such as supersilica, composed of a reactive silica-based sorbent, an effective surfactant (e.g. superplasticizer), and some minor corrective components (including nanosilica) was reported [15, 33, 38, 39]. The mechano-chemical activation of cement with supersilica results in a new type of high performance cement which can be used for concrete with high strength and extreme durability [15]. It was reported that developed approach can be used for engineering of eco-binders with high volumes (up to 70%) of locally available mineral additives such as natural pozzolanic materials, sand, limestone, granulated blast furnace slag, fly ash, glass cullet or ceramic waste [15, 38]. In addition to this, mechano-chemistry can be effectively used for bottom-up synthesis of nano-materials including C-S-H [28].

A top-down process which uses liquid-state activation accompanied with mechano-chemical transformations, accelerated hydration, and the formation of submicro- and nano-cement grains and nano-clusters of C-S-H was realized for nano-engineered cement (NEC) [26]. The complete effects of top-down technology are not yet completely understood; in particular, the effects of small quantities (0.01-0.1%) of nano-materials added during cement activation (e.g., nano-silica, nano-clay or SiO_2-rich reactive powder), remain unclear. However, it was demonstrated that the use of mechano-chemical activation, nano-particles, and nano-catalysts in cement technology can be used to tailor new cementitious materials with beneficial properties.

These developments can dramatically improve the performance of cement, as addressed by Sobolev and Gutiérrez [16, 22].

The feasibility of liquid-state milling, mechano-chemical activation and top-down synthesis of C-S-H to improve the properties of portland cement systems was reported [26]. Specifically, effective activation was achieved by vibro-milling of low-concentrated cement slurries with superplasticizer and small quantities of nano-silica. Microstructural analysis was used to detect the formation of the ultra-fine particles in activated cement and evaluate the effect of activated slurry on the early strength of the cementitious materials.

It was demonstrated that the use of small amounts (up to 20%) of activated cement can significantly increase the compressive strength of cementitious materials up to 125.6 MPa (vs. 92.2 MPa observed for reference mortar). The use of top-down process to synthesize the AC can provide an effective material to improve the microstructure of the cementitious matrix through densification with ultra-fine particles. Furthermore, the nano-sized products of cement hydration act as nucleation seeds accelerating the hydration and improve the early strength of nano-engineered cement (NEC). The implementation of proposed concept resulted in an increase of compressive strength up to 47 % and 36 % at 1- and 28- day age, respectively. Importantly, the boost of strength was achieved in binders of the same composition and at the same water to binder ratio, only due to effective modification of the production process [26].

1.2. PURPOSE AND OBJECTIVES

The overall objective of this study is to develop a novel concept based on the mechano-chemical activation (MCA) of fly ash with nanoparticles and superplasticizer. The developed

activated fly ash system can be beneficially used in self-consolidating concrete (SCC) characterized by enhanced properties in terms of flow and strength. The experimental results on SCC are compared with the reference (DOT grade) concrete to demonstrate the advantage of self-consolidating composites.

It was hypothesized that the developed activated fly ash concept can produce concrete of better performance vs. reference with regard to a) improved early strength gain; b) effective utilization of fly ash c) reduction of portland cement content; d) improved durability d) improved long-term mechanical performance.

To analyze the proposed concept, the following experimental steps were performed:

1. Optimization of the dosage of chemical admixtures using mortars;
2. Optimization of different types and sources of nanoparticles that can lead to the enhancement of properties of cement based materials;
3. Realization of NEC concept by activating of fly ash and nano particles blend in liquid state to produce activated components;
4. Examination of the effect of activated fly ash on hydration, structure development and mechanical properties;
5. Development of an experimental matrix for comprehensive testing of chemical admixtures, SCM and activated fly ash blends in concrete including SCC;
6. Evaluation of the effect of fly ash and chemical admixtures on fresh properties and mechanical performance of reference (DOT-grade) concrete and SCC;
7. Investigation of the effects of fly ash – nanoparticle combination on flowability and resistance to segregation as well as strength development of eco-friendly SCC.

2. LITERATURE REVIEW

2.1. NANOTEHCNOLOGY OF CONCRETE

While the science related to nanotechnology is new, nanosized devices and objects were used since ancient times with the use of nanoparticles in glass [44], to modern times where with film photography based on the use of silver nanoparticles sensitive to light. It has been proven that the exceptional mechanical performance of biomaterials such as bones or mollusk shells is due to the presence of calcium carbonate nanocrystals [45, 46].

Nanoparticle is the main building unit in nanomaterials; it can be represented as a cluster of tens to thousands of atoms of 1-100 nm in diameter[16]. When nanoparticles are created by the "bottom-up" approach, the size and shape of a particle can be controlled by production conditions. When the dimensions of a material are reduced from macro- to nano-size, significant changes occur in electronic conductivity, optical absorption, chemical reactivity, and mechanical properties. In reducing the size, more atoms are located on the surface of particle, and, in addition to a remarkable surface area of nanopowders (*Figure 3*), this imparts a considerable change on surface energies and surface morphologies. All these factors alter the basic properties and the chemical reactivity of nanomaterials [16, 44, 45, 47] . Currently, nanoparticles have been used to enhance the mechanical performance of plastics and rubbers [44-46], as these improve the ductility of ceramic and glass materials [16]. For example, new nano-ceramic materials based on metal and oxides of silicon and germanium demonstrate superplastic behavior, undergoing elongations up to 1000 % before failure [48].

The nanoscience and nano-engineering (nanomodification) of cement based composites are terms which describe two main directions related to nanotechnology of construction materials [22]. *Nanoscience* deals with the "measurement and characterization of nano- and micro-scale structure of materials used to understand how this structure affects the macroscale properties and performance through the use of advanced characterization techniques and atomistic or molecular level modeling" [21]. *Nano-engineering* encompasses the "techniques of manipulation at the nanometer scale to develop a new generation of multifunctional composites with superior mechanical performance and durability potentially having a range of novel properties such as: low electrical resistivity, self-sensing capabilities, self-cleaning and self-healing" [22]. Composite can be nano-engineered by the incorporation of nano-sized building blocks or objects (e.g., nanoparticles and nanofibers) to control material behavior and add novel properties, or by the grafting of molecules onto cement particles, aggregates, additives (including nano-sized additives) to provide surface functionality, which can be adjusted to promote specific interfacial interactions [21, 22].

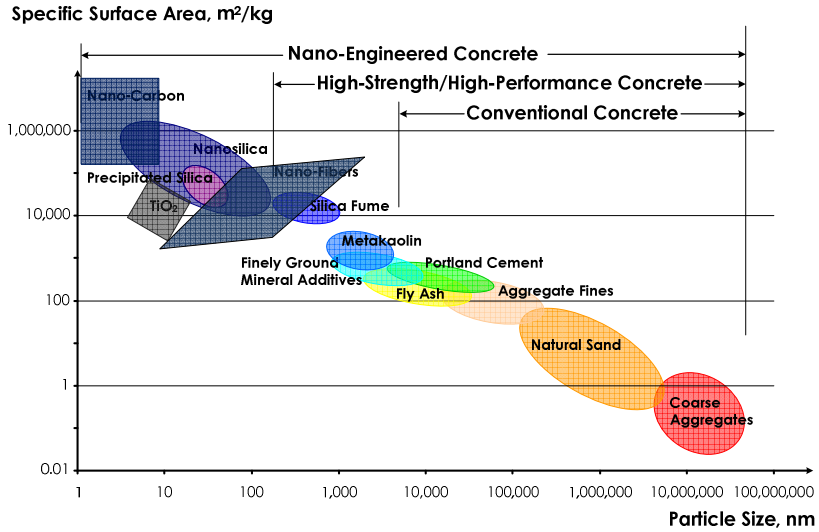

Figure 3. The particle size and specific surface area scale related to concrete materials [21, 22].

Better understanding the structure at nano-level helps to influence the important processes related to the production and use of construction materials: strength, fracture, corrosion and even tailoring the desired properties [22]. For instance, self-cleaning concrete, mortars, and water-based paints were developed based on the photocatalyst technology [49]. The self-cleaning effect related to the decomposition of organic pollutants and gases is achieved when TiO_2 photocatalyst thin film is set on a surface and can emit active oxygen under UV light. Another aspect of self-cleaning is provided by the hydrophilicity of the surface, which helps to rinse away dust and dirt. Photocatalytic properties can be also used to engineer cement based materials for energy harvesting applications [50]. Nano-SiO_2 and nano-Al_2O_3 have proved to be a very effective additives to polymers and cement-based composites to improve strength, flexibility, and durability [51, 52].

Nano-chemistry with its "bottom-up" possibilities offers new products that can be effectively applied in concrete technology. Mechano-chemical activation of cement with PCE based grinding modifiers was found to be very effective method to tailor the behavior of cement-based materials in fresh and hardened state [51]. The reported improvement of performance (up to 115 MPa vs. the strength of reference cements of 72 - 89 MPa) was achieved due to the formation of organo-mineral nano-layers or nano-grids on the surface of cement as well as surface amorphization.

Concrete with Nanoparticles

The most of the experimental work was conducted using nano-SiO2 particles (*Figure 4*). The nanoparticles of SiO_2 were extensively used to increase the strength and durability of concrete [3-5, 53] Björnström et al. investigated the effects of colloidal silica on the hydration process of Portland cement minerals C_3S (alite, Ca_3SiO_5) and β-C_2S (belite, β-Ca_2SiO_4) [4]. It

was demonstrated that nanoparticles accelerate the formation of C-S-H gel within the first 24 hours, especially when used at higher dosages of up to 2%.

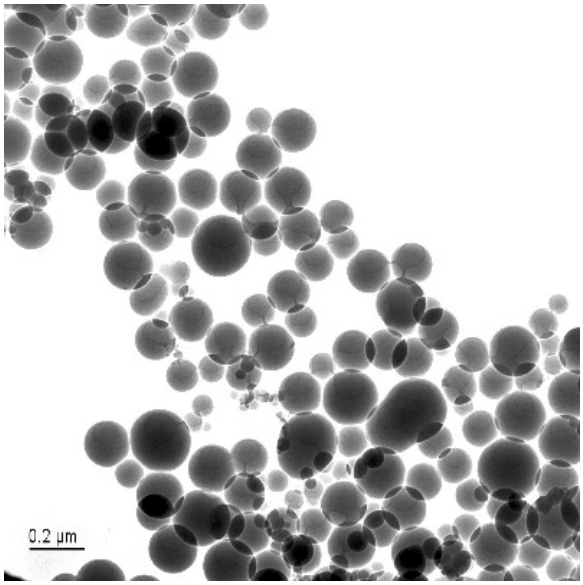

Figure 4. Nanosilica particles under the TEM [6, 51]

The team of Collepardi et al. was among the first to study the performance of low-heat self-consolidating concrete (SCC) produced with nano-SiO_2. Nanosilica with the size of 5-50 nm was used in a form of slurry as a viscosity modifying agent at a dosage of 1-2% of the mass of cementitious materials [3]. The design of SCC with low-heat emission was achieved by using blended cement (with 60% of blast furnace slag) and incorporating of limestone and fly ash powders. It was reported that the addition of nano-SiO_2 makes concrete mixture more cohesive and reduces bleeding and segregation. The best performance was demonstrated by concrete with ground fly ash, 2% nanosilica, and 1.5% of superplasticizer. The developed concrete had desired behavior in fresh state and also the highest compressive strength [3]. In another study, nano-SiO_2

was used as an effective viscosity modifying agent in high–density, high-strength cementitious grout [54].

Qing et al. investigated the development of $Ca(OH)_2$ phase in pastes and concrete with silica fume and nanosilica [55]. The addition of nanosilica increased the viscosity and reduced the setting time of pastes. In concrete, with addition of nano-SiO_2 the quantity and the size of $Ca(OH)_2$ phase crystals formed in the interfacial transition zone were considerably reduced and the mechanical performance at early ages was better than for specimens produced with silica fume.

Flores et al. [13] studied the effects of sol-gel synthesized nanosilica on strength of portland cement mortars. The addition of superplasticizer and an effective dispersion were employed to distribute these nano materials within the cementitious matrix and enhance the mechanical performance of mortars.

Gaitero et al. [56] demonstrated that the addition of nano-SiO_2 to cementitious systems can improve the strength by controlling the structure of C-S-H. Nano-SiO_2 with particle size between 5 and 50 nm was used in the field project as a viscosity modifying agent at a dosage of 1-2% of cementitious materials [3, 54, 57].

Based on the available data, the beneficial effects of nano-particles on the microstructure and the performance of cement-based materials can be explained by the following factors [21, 22]:

- Well-dispersed nano-particles increase the viscosity of the liquid phase, helping to suspend the cement grains and aggregates and improving the segregation resistance and workability of the system;

- Nano-particles fill the voids between cement grains, resulting in the immobilization of "free" water ("filler" effect);
- Well-dispersed nano-particles act as centers of crystallization of cement hydrates, thereby accelerating the hydration;
- Nano-particles favor the formation of small-sized crystals such as $Ca(OH)_2$ and AF_m and also uniform small-size clusters of C-S-H;
- Nano-SiO_2 participates in the pozzolanic reactions, resulting in the consumption of $Ca(OH)_2$ and formation of an "additional" C-S-H;
- Nano-particles improve the structure of the aggregates' contact zone, resulting in a better bond between the aggregates and cement paste;
- Crack arrest and interlocking effects between the slip planes provided by nano-particles improve the toughness, shear, tensile, and flexural strength of cement based materials.

The relatively small quantities, less than 1% (by weight of cement), of nano-sized materials are sufficient to improve the performance of nanocomposites [21, 22] ; yet, the commercial success of nanomaterials depends on the ability to manufacture these materials in large quantities and at a reasonable cost relative to the overall effect of the nanoadditives. Nanomaterial technologies, which could lead to the industrial outputs, involve plasma arcing, flame pyrolysis, chemical vapor deposition, electrodeposition, sol-gel synthesis, mechanical attrition, and the use of natural nanosystems [44]. Among chemical technologies, sol-gel synthesis is one of the widely used "bottom-up" production methods for nano-sized materials such as nano-silica. The process involves the formation of a colloidal suspension (sol) and gelation of the sol to form a network in a liquid phase (gel). Usually, tetraethoxysilane (TEOS) is applied as a precursor for synthesizing nanosilica [4]. The details of the "bottom-up" sol-gel

synthesis of nano-SiO_2 particles with the size range of 5–100 nm and the effect of this material on the performance of cement systems were reported [6, 51]. According to the XRD results, the manufactured nano-SiO_2 is a highly amorphous material with predominant crystallite size of 1-2.5 nm. The obtained nano-SiO_2 particles are forming highly agglomerated xerogel clusters with the size of 0.5–10 μm. The particles within the clusters are of the size of 5–70 nm and the BET surface area of 116,000-500,000 m^2/kg. It was demonstrated that the performance of nano-SiO_2 in cement system depends on the conditions of synthesis (i.e., molar ratios of the reagents, type of the reaction media, pH and the duration of the reaction). The best nano-SiO_2 products with particle size ranging from 5–20 nm were synthesized at highest molar concentrations of water. The addition of developed nano-SiO_2 to portland cement mortars improved the compressive strength. The distribution of nano-SiO_2 particles within the cement paste is an important factor governing the performance; therefore, the disagglomeration of nanoparticles is essential for the design of composite materials. The application of superplasticizer, ultrasonification and high-speed mixing was effective approach to incorporate nano-SiO_2 [6, 51].

Despite of attractive performance, the application of nanoparticles in concrete remains limited because of high cost associated with the production of nanomaterials. However, low cost silica nanoparticles can be obtained from natural sources such as hydrothermal solutions formed due to volcanic activities. Steam or hot water erupting from the earth surface due to geothermal activities has been used by Romans, Chinese and Native Americans for bathing and processing of food [58]. Currently, high-temperature steam and water are used for power generation and also as a supply of heat [59]. In a geothermal power plant (*Figure 5*), hot water rises to the surface, evaporates, and the steam is redirected to the turbines and a generator that produces energy. The steam is condensed into water in a cooling tower, where minerals (including

nanosilica) can be recovered and utilized for industrial applications. The minerals found in geothermal power plant water streams include zinc, silica, lithium, manganese, boron, lead, silver, antimony and strontium [59]. In geothermal plants, silica-particles cause clogging of pipes and, therefore, nanosilica extraction increases the efficiency of the plant [58]. Nanosilica present at high concentrations in hydrothermal solutions can be extracted for subsequent application in various products such as paint, paper, toothpaste, tires[59], chocolate slim shakes, solar panels [60] and also as a pozzolanic material for use in concrete.

In volcanic areas, orthosilicic acid is formed in hydrothermal solutions due to the dissolution of aluminosilicate minerals of rocks under elevated pressures and temperatures. Concentrated solutions travel to the surface, where the pressure and temperature is lower, and due to hydrolysis and polycondensation, spherical silica nanoparticles are formation. The use of hydrothermal solutions as a relatively cheap natural precursor for nano-SiO_2 production can reduce the costs associated with the production and application of nanomaterials.

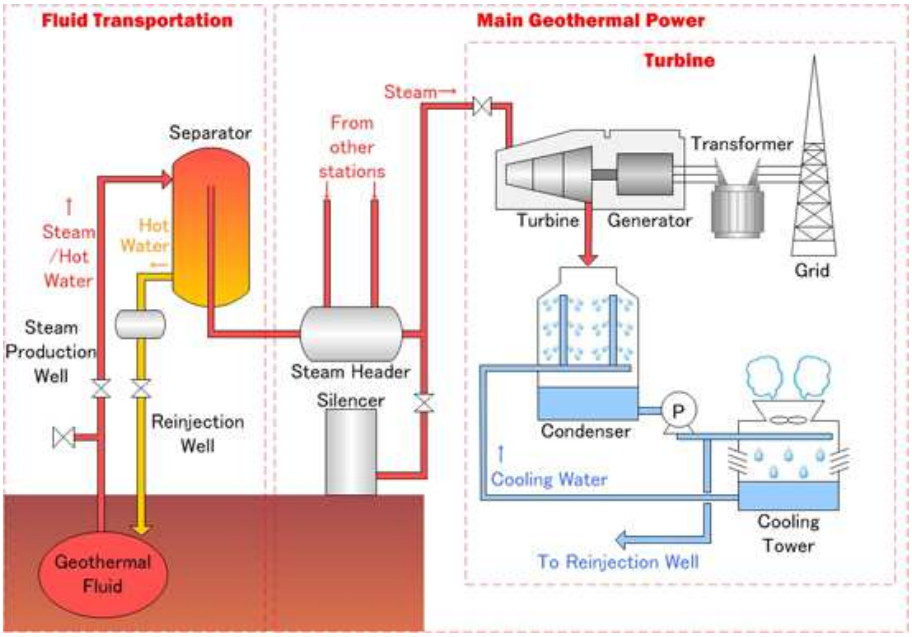

Figure 5. The process used by a geothermal power plant [43]

2.2. MODERN SUPERPLASTICIZERS

Superplasticized concrete has been effectively used for the production of heavily reinforced elements such as floors, foundations slabs, bridges, pavements, roof decks and others [61]. This type of concrete is characterized by reduced permeability, improved surface finish, reduced shrinkage, enhanced durability, and overall cost savings. Due to exceptional water-reducing properties, modern superplasticizers (SP) enable the production of very economical concrete with reduced cementitious material content without any detrimental effects on performance. Although superplasticizers introduce remarkable advantages in concrete, there are some limitations. For example, the compatibility of SP with other admixtures such as water reducers, retarders, accelerators and air-entraining agents must be investigated prior to application of superplasticizers. The combination of SP with air-entraining agents may alter the air bubble size distribution and spacing. In addition, reduced strength due to high porosity and retardation of hydration may occur when superplasticizer is mixed with Type V cement, (*Figure 6*) [61]. Workability and setting of superplasticized cement paste may change depending on the amount and type of sulfate (i.e., anhydrite or gypsum) used for cement production. The differences can be explained by different rates of dissolution of the sulfates [62].

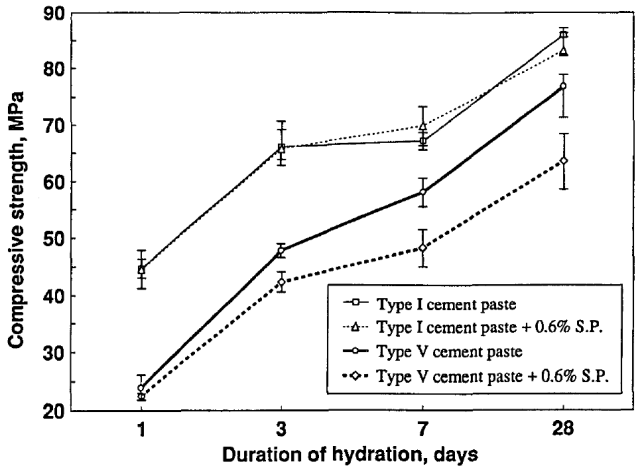

Figure 6. The effect of sulfonated melamine formaldehyde (smf) superplasticizer on the compressive strength of type I and V cement [61].

Admixtures of the same generic type may result in different effects in concrete because of the variations in the molecular weight, chain length, production technology, etc. Similarly, the same type of cement can be represented by a material with different fineness, mineral, alkali, and sulfate contents. In this way, each admixture combination must be evaluated before application. In addition, superplasticizers should be evaluated for side effects related to workability, setting, air content, and mechanical properties [61].

In terms of chemical structure, there are two main categories of superplasticizing polymers, also known as a surfactants, or dispersants: sulfonated ring structures and acrylic or polycarboxylate derivatives [61, 63]. There are two main dispersion mechanisms that explain the particle separation behavior: electrostatic repulsion and steric hindrance (*Figure 7*).

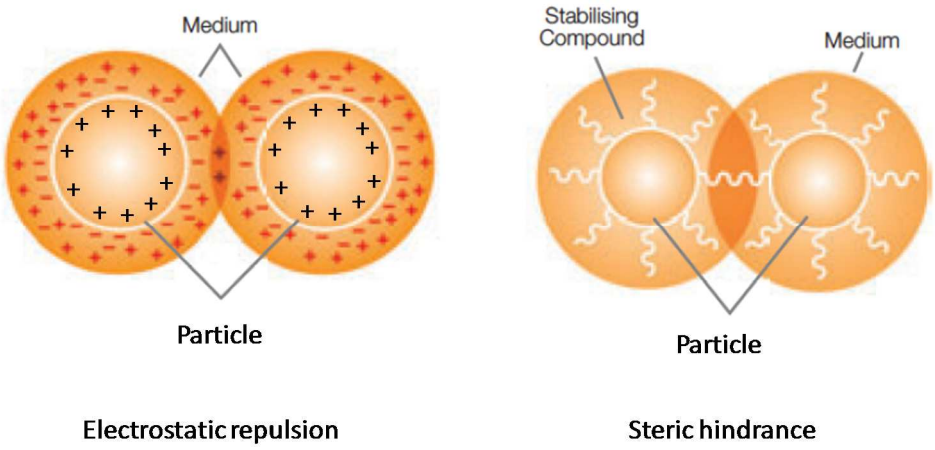

Figure 7. Particle's dispersing mechanisms [64].

In the electrostatic repulsion mechanism, the dispersant molecule has a localized negative ionic character at one region and a localized positive ionic character at another. The dispersant attracts to the particle surface and orients in a way that the outer layer of the film is now exclusively positive. As other particles are similarly coated, these are all essentially positively charged and cannot agglomerate. The steric hindrance mechanism similarly relies on portions of the dispersant to be attracted to the particle surface, but the outer regions of the dispersant chains tend to be long and non-polar (or partially polar) in character rather than ionic. Entanglement or crystalline-ordering of the outlying chains of different particles is thermodynamically unfavorable, so the particles tend to stay separated [63, 64].

Sulfonated ring polymers are anionic polymers with many $-SO^{3-}$ groups that attract to regions of positive charge on the cement particles, primarily Ca^{+2} (*Figure 8*). As particles are wetted with a film of polymer, these effectively become negatively charged and repel each other [63, 65]. Additionally, free water that would have been bound in particle agglomerates becomes available as a fluidizer, which reduces the viscosity of the paste or slurry [66, 67]. Selective structures for sulfonated ring polymers are displayed in *Figure 9*. The morphology of these

polymers can vary. Structures with more branching and less linearity can be produced that would be candidates for superplasticizers, as long as these have a sufficient number of anionic sites.

However, there are limits to the effectiveness of an increase in molecular weight and bulk. The gains in mini slump (as measure of workability) and polymer adsorption are limited by the molecular weight (MW, as indicated by polymer solution viscosity), as demonstrated for sulfonated naphthalene SP [67]. The basic structure of a sulfonated naphthalene formaldehyde (SNF) condensate polymer is well established, and it was demonstrated that similar effectiveness can be achieved by medium to high MW polynapthatlene sulfonate SPs [68].

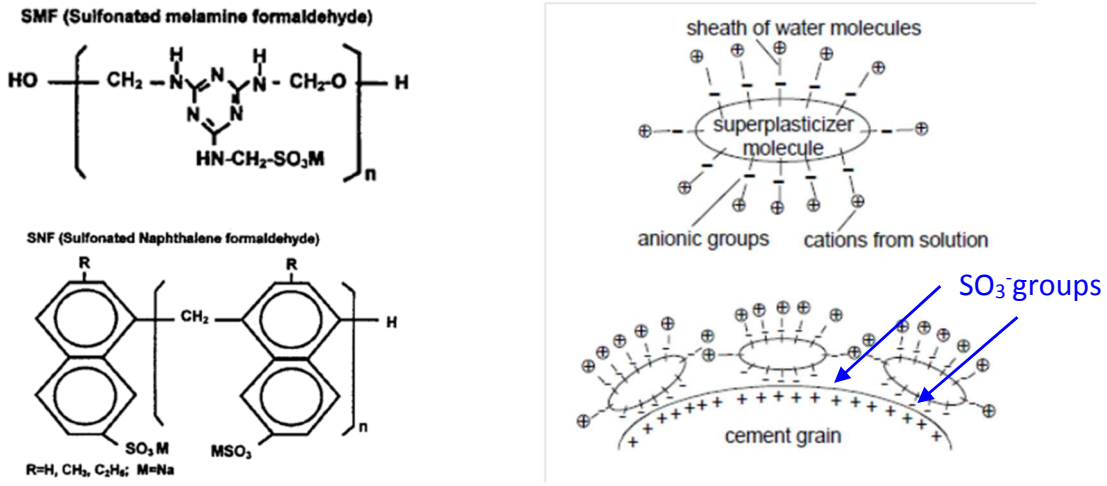

a) Sulfonated ring structures **b) Electrostatic repulsion**

Figure 8. Chemical structure and electrostatic repulsion mechanism of sulfonated ring superplasticizers [63].

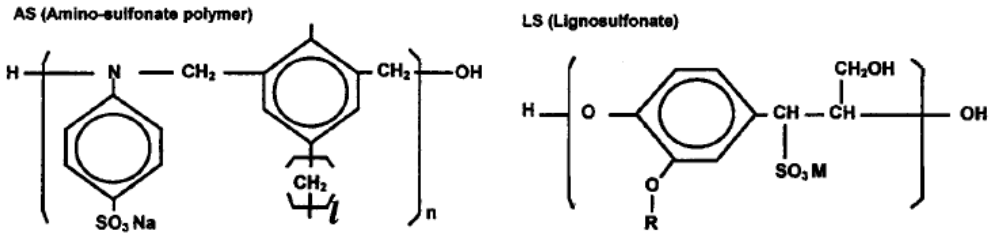

Figure 9. Selective sulfonated ring superplasticizers [63].

Polycarboxylate polymers have the main trunk of the molecule being the backbone and the ethoxy block polymer branches at the ends. The trunk contains carboxylate groups, which couple with Ca^{+2} sites on cement or hydration products. The branches, or side chains, contain ether oxygen groups (-C-O-C-), which form strong hydrogen bonds with water *(Figure 10)*.

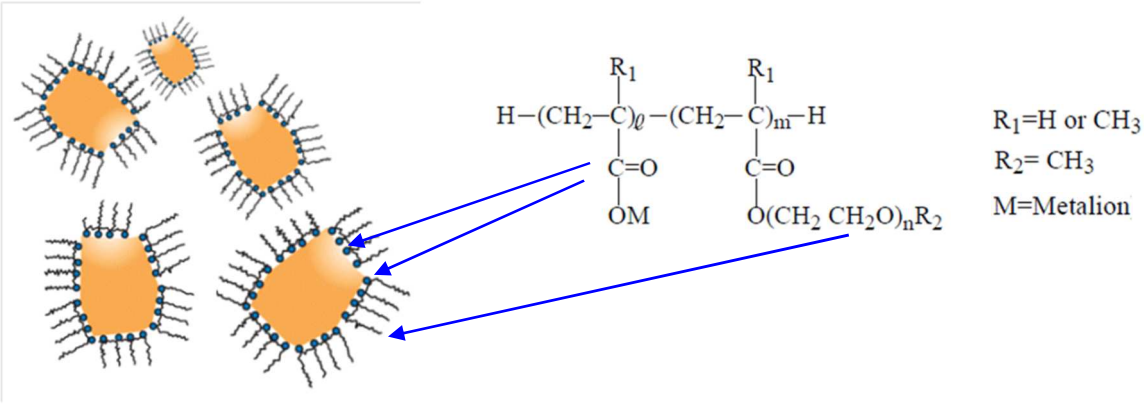

Figure 10. Polycarboxylate superplasticizers: steric hindrance mechanism, adapted from Lubrizol [64] (left) and generic structure [69] (right).

Sakai et al. [68] and Tanaka and Ohta [73] reported that the average molecular weight (MW) of the trunk polymer tailored for the best dispersion was 5,000 g/mol. For good dispersion, the maximum molecular weight for the trunk polymer was on the order of 10,000. With a 5,000 MW trunk, side chains containing twelve ethylene oxide groups (with each EtO

MW = 44) gave maximum dispersion, and it was believed that these groups also imparted a strong electrostatic repulsion effect [68].

Kirby and Lewis investigated the effects of the structure morphology using 5,000 MW trunk length and polyethylene oxide corresponding to 100, 700, 1,000, 2,000, and 3,000 MW [70]. It was reported that only a few ethylene oxide groups were needed to abate the aggregation and stiffening. The theoretical MW of developed polycarboxylate polymers ranged from 5,000 to 31,100 g/mol. Kirby and Lewis grafted the polyethylene oxide side chains to the trunk polymer with -C-N-C- bonds (imide bonding). Work by Magarotto et al. reported that polymer molecular weights of 30,000 to 50,000 or more were needed for better superplasticizer performance [68].

Generally, shorter trunk lengths and increased side chain length increase dispersibility and mini-slump retention (*Table 1*). The improved performance was believed to be due to increased SP film thicknesses. *Figure 11* demonstrates these assessments along with the approximations of polymer size.

Table 1. Structural factors affecting dispersibility and retention of dispersibility [68]

Structural factor / Dispersibility	Relative chain length of trunk polymer	Relative graft length	Relative number of grafts
Low dispersibility and short dispersibility retention	Long	Short	Large
High dispersibility	Short	Long	Small
Long dispersibility retention	Shorter	Long	Large

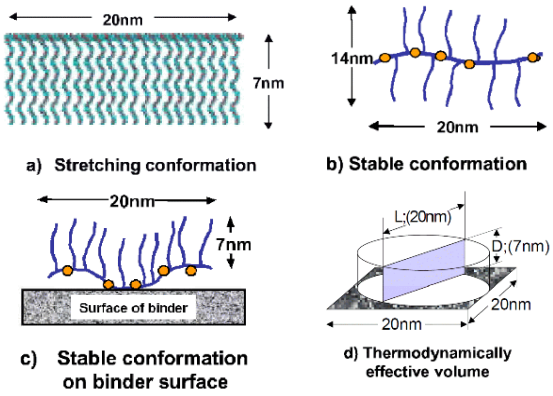

Figure 11. Size and morphology of polycarboxylate SP, from Sakai et al. [68].

The dosage of superplasticizers (SP) is typically less than 1% of the cement weight. A number of studies reported on the use of less than 0.5% by weight of the cement, based on the solid content [63, 68]. The effectiveness of SP can be influenced by a number of factors such as cement particle size (or surface area), cement composition, SP dosage, and time of addition. Products of hydration can interfere with SP by sequestering the SP polymer directly or by associating SP on the particle surface. As hydration takes place, the SP polymer becomes incorporated into the hydrating matrix and is completely consumed [63, 65, 68, 70].

Although the general practice to dissolve the SP in water allows easy addition and a more homogenous cement paste mix, based on the mini slump test, Collepardi [63] demonstrated that making a paste (by mixing water and cement) first, before adding SP, was a preferred method of incorporation. Sakai [68] quantified the SP dosage and response for various cement compositions. It was reported that the critical dosage, which is the minimum dosage of SP where flow begins to increase, and dispersibility, as the rate of response to additional SP, are the key parameters for effective application of SP admixtures.

2.2.1. Supplementary Cementitious Materials

One of the modern trends in infrastructure development projects is related to the application of high performance concrete with supplementary cementitious materials (SCM). The use of supplementary cementitious materials (SCM), including industrial by-products such as ground granulated blast furnace slag (GGBFS, also known as slag cement) and fly ash, can reduce the consumption of portland cement by up to 50% and 30%, respectively, as well as enhance workability, mechanical performance, durability, service life, and other performance characteristics of concrete. One of well investigated SCM is fly ash, a by-product from power generation plants [71]. Fly ash is widely used in concrete technology for replacement cement as supplementary cementitious material (SCM) since 1930s and it helps to reduce the cost of concrete and environmental problems associated with landfilling. Many researchers were investigating the effect of fly ash as supplementary cementitious materials (SCM) [16, 17, 19]. There are two types of fly ash used in concrete: low-calcium fly ash (ASTM class F) and high-calcium fly ash (ASTM class C). Fly ash class F (FAF) is typically produced by burning of anthracite or bituminous coal and generally is an effective pozzolanic material consisting of silicate glass modified with aluminum and iron. At the same time, fly ash class C (FAC) is produced by burning of lignite or sub-bituminous coal. Class C fly ash contains higher amounts of lime, more than 10%. Fly ash suitable for concrete applications is defined by ASTM 618 and its classification is based on the total proportion of Si_2O, Al_2O_3, and Fe_2O_3.

Therefore, fly ash is a material based on aluminosiliceous, ferric oxide (Fe_2O_3) and calcium oxide (CaO) compounds and which also may contain carbon, other metallic oxides as impurities. Class F Fly ash is a pozzolanic material containing a siliceous or aluminosiliceous material in a finely divided form which can react with calcium hydroxyde to form a calcium

silicate hydrate and other cementitious compounds. The size of fly ash is varies from less than 1 μm to more than 100 μm with typical average size under 20 μm. The shape of fly ash particles is represented by solid spheres and hollow cenospheres. The range of surface area is in the range of 300 to 500 m^2/kg. Finer fly ash material considerably improves the mechanical properties of concrete and increase heat of hydration without reducing workability.

Blending supplementary cementitious materials such as slag cement with portland cement, results in chemical activation and provides excellent long-term cementitious properties. Pozzolanic by-products (especially Class F fly ash) can react with $Ca(OH)_2$ released due to cement hydration, resulting in the formation of an additional C-S-H, the main binding component of hydrating matrix. Also, pozzolanic fly ash can combine with cement alkalis (K_2O and Na_2O), minimizing the risk of alkali-silica reaction.

Up to date, numerous researches have been conducted on using fly ash as pozzolanic material focusing on strength development and densified structure of cement-based composites. The most important parameters affecting the performance of fly ash are calcium content and particle size distribution. Ultra-fine particles can provide a nucleation effect initiating and accelerating hydration. Celik et. al reported that the finer particles of fly ash can be used to achieve higher compressive strength [72]. A relationship between the particle size distribution and compressive strength was established. Additionally, microstructural investigation was conducted for fly ash samples revealing the shape and size differences and thus the potential effects on the compressive strength. As a result, ASTM-grade fly ash products are specified as replacement of portland cement at up to 30%, however, higher substitution rates, the decrease of strength was observed.

Incorporation of fly ash affects the early strength development. The heat of hydration, strength development and setting times may be delayed, especially, at high volume replacements. Thongsanitgarn et. al [73] investigated the effect of fly ash on heat of hydration in blended cements and high calcium fly ash incorporated with limestone powder. Heat of hydration was accelerated vs. the reference blend of fly ash and portland cement and strength increased due to the contribution of finer limestone particles (the size of 5 μm). It was proposed that finer particles have greater surface area and so allow the increase of nucleation site density affecting the hydration. Additional results indicated the stabilization of ettringite at the age of 28 days when both limestone and fly ash were applied. To overcome poor early age strength development, the mechanical activation was proposed [26]. A new nano-cement concept with mechano-chemical activation, accelerated hydration and the formation of nano-cement and nano C-S-H was proposed by Sobolev et al [74]. It was concluded that the activated cement with mechano-chemical activation (MCA) can provide significantly improved strength at all ages hardening.

Fly ash mainly consists of amorphous material, and thus the activation carried out by mechanical milling can improve the reactivity. The main objective of using vibration milling is to reduce the size of cement and supplementary cementitious materials (SCM). The most of supplementary cementitious materials results in the reduction of heat of hydration and increase of the setting time of cement.

The mechanical activation can be realized using a conventional grinding process. Due to activation and dispersion process, fly ash products with high fineness can be achieved. Several studies proved that the activation of fly ash by grinding results in higher surface area and, consequently, in higher chemical reactivity. Additionally, milling of fly ash improves the

rheological properties. Smaller particles act as filler thus result in a higher strength and durability. Therefore, the strength improvement of cement composites can be achieved by wet milling of individual cementitious components such as fly ash [75]. Hela et.al [76] proposed several methods of mechanical activation of fly ash. To maximize the pozzolanic reactivity of fly ash, grinding process was utilized and was investigated the influence of milled material on workability, compressive strength and durability.

Li [19] explained that the addition nanosilica combined with high volumes of fly ash resulted in the refinement the pore size distribution and decreased the porosity of cement matrix at the early ages. The activated fly ash with higher fineness results in higher pozzolanic reactivity. By incorporating nanosilica that has high activity and larger specific surface area along with fly ash during the milling process, the pozzolanic activity can be significantly increased, as nanosilica can activate fly ash. Sobolev et al. [26] produced nano-engineered cement (NEC) with mechano-chemically activated cementitious component using liquid-state milling. Activated cement was applied at 10-30% cement replacing levels. The research results demonstrated that the cement hydration and mechanical performance were facilitated due to intensive activation.

Kawashima et.al [77] studied the effect of nanoparticles such as nano-SiO_2 and nano-$CaCO_3$ on strength development of fly ash- portland cement-based mortars [77].

2.3. CONCRETE MIXTURE OPTIMIZATION

Concrete mixture optimization is a broad term used for fine tuning of various types of concrete targeting for several performance aspects and desirable properties. More specifically, the optimization of concrete mixture proportions deals with the selection of the most efficient

quantities of aggregates, SCM, chemical admixtures, and the minimization of cementitious material content (*Figure 12*).

Concrete mixture proportioning was holistically represented by many researchers [7, 78-85]. The subject was further approached by performance based modeling [85], computer-aided modeling for a system of ingredient particles [86-88], sustainability concepts [69, 89, 90], chemical admixture optimization, aggregates optimization, including the effect of aggregates on concrete strength [7, 80, 91-97], and statistical design of concrete mixtures [98]. Furthermore, a mix proportioning for sustainable "green" concrete was realized by using by-products [99-101] and by improving the aggregate characteristics related to packing density [102].

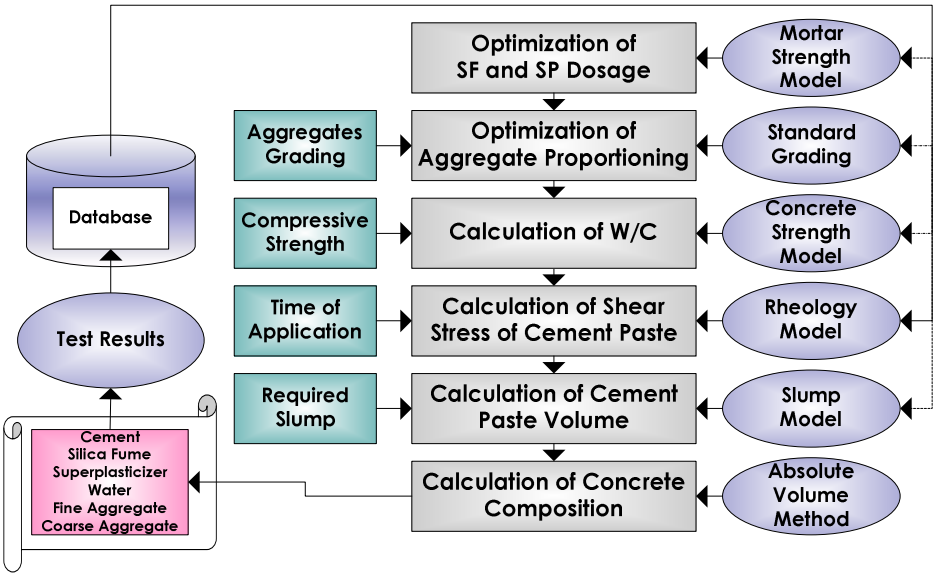

Figure 12. Mixture proportioning method for high-performance concrete [103]

2.4. DESIGN OF SELF-CONSOLIDATING CONCRETE (SCC)

Self-consolidating concrete (SCC) is a new type of concrete which is characterized by its ability to fill the formwork under its own weight without the use of vibration, while maintaining the homogeneity at a very low segregation. Self-consolidating concrete can flow easily under its own weight and is characterized by near zero yield value. Therefore, for measuring the

workability, the yield stress component becomes less pronounced than conventional concrete. To understand the workability and flow properties of developed SCC, this study investigated the rheological response shear stress and viscosity of cement pastes of the same composition as SCC.

For maintaining SCC workability it is essential to provide the adequate spacing between the aggregates in order to reduce the friction between the particles. This is achieved by using mixtures with higher volumes of cement paste and the optimization of aggregates spacing grading and proportions. The cement paste between the aggregates depends on the aggregate packing and is known as a compact paste (affected by aggregates packing), while the cement paste surrounding the aggregates is known as an excess paste. This excess paste allows concrete to flow and maintain a uniform dispersion [2].

In the reported study, the SCC was developed using nanoparticles such as nanosilica and the effect of nanomaterials on the fresh and hardened properties of nano-engineered SCC was investigated. Furthermore, the SCC mixtures were designed with different proportions of fly ash used as a cement replacement material along with nanosilica and superplasticizer. In addition, for selected SCC mixtures, the use of activated fly ash was investigated to enhance the fresh and mechanical performance.

3. MATERIALS AND METHODS

3.1. MATERIALS

3.1.1. Portland Cement

Four ASTM Type I portland cements from three different suppliers were used for the research. The chemical composition and physical properties of cements are presented in *Table 2* and *Table 3*, respectively, along with the requirements of ASTM C150 Standard Specification for Portland cement. The chemical composition of cements was tested using the X-Ray Fluorescence (XRF), Scanning Electron Microscope (SEM), Energy Dispersive X-ray Spectroscopy (EDS) techniques. SEM images and EDS spectrums of portland cement are shown in *Figures 13 and 14*.

Table 2. Chemical composition of portland cement

Parameter	ASTM C150 Limits	Test Result L1	L2	H1	S1
SiO_2	-	19.8	19.1	19.4	18.6
Al_2O_3	-	4.9	5.1	5.3	5.5
Fe_2O_3	-	2.8	2.5	3.0	2.6
CaO	-	63.2	63.3	63.2	61.1
MgO,	6.0 max	2.3	2.7	2.9	4.3
SO_3,	3.0 max	2.9	3.3	3.3	3.9
Na_2O,	-	0.2	0.3	0.3	0.3
K_2O	-	0.5	0.6	0.7	0.6
Others,	-	0.6	0.9	0.9	1.5
Ignition loss,	3.0 max	2.8	2.5	1.1	1.5
Potential Composition					
Al_2O_3 / Fe_2O_3		1.8	2.1	1.8	2.1
C_4AF,	-	8.5	7.5	9.1	8.0
C_3A,	-	8.2	9.3	8.9	10.1
C_2S,	-	10.3	4.9	9.9	11.3
C_3S,	-	61.6	65.8	60.7	55.8
Na_2O_{equi},	0.6 max	0.5	0.7	0.8	0.7

Table 3. Physical properties of portland cement

Parameter	ASTM C150 Limit	Test Results L1	L2	H1	S1
Specific Gravity	-	3.13	3.17	3.08	3.07
Time of setting, min					
Initial	45 min	103	74	88	93
Final	375 max	264	231	222	228
Compressive strength, MPa (psi) at the age of:					
1 day	-	12.1 (1731)	17.2 (2460)	18.1 (2589)	21.2 (3032)
3 days	12 (1716)	21.7 (3104)	28.5 (4077)	28.7 (4105)	26.2 (3748)
7 days	19 (2718)	28.3 (4048)	32.6 (4663)	34.3 (4906)	29.4 (4205)
28 days	28 (4005)	36.5 (5221)	40.4 (5779)	40.1 (5735)	34.6 (4949)

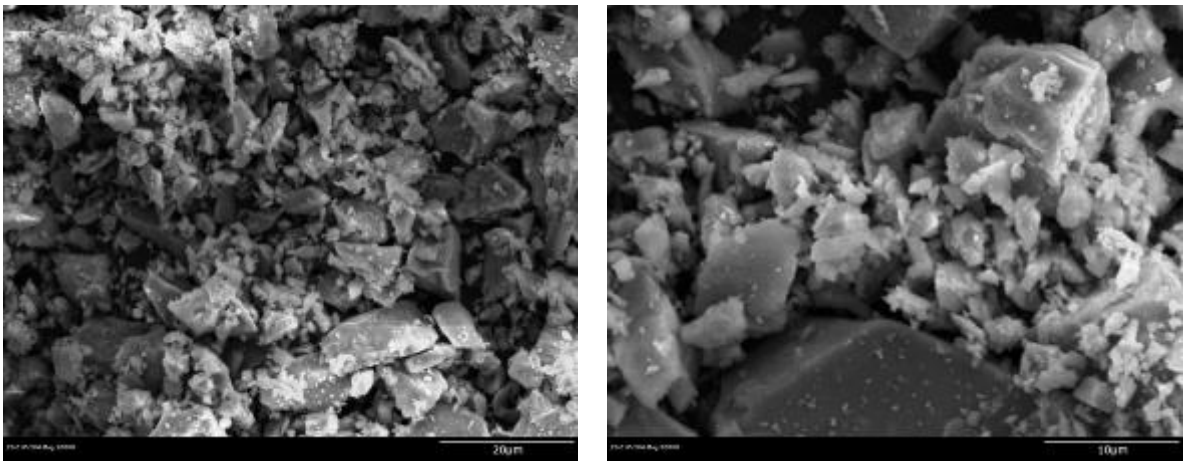

Figure 13. SEM images of portland cement at: a) 1000x magnification, and b) 2000x magnification

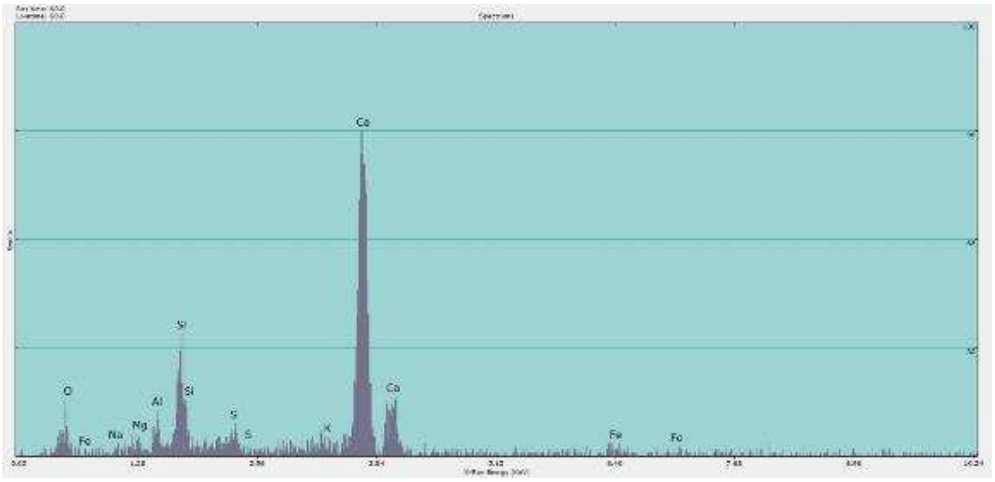

Figure 14. EDS spectrum of portland cement

3.1.2. Fly Ash

ASTM Class C and F fly ash from Wisconsin power stations were used in this research. The chemical composition and physical properties of two types of fly ash are summarized in *Table 4* and *Table 7*, respectively, along with the requirements of ASTM C618, "Standard Specification for Coal Fly Ash and Raw or Calcined Natural Pozzolan for Use in Concrete". SEM images and EDS spectrums of Class C and F Fly Ash are shown in *Figure 15* and *Figure 16*.

Table 4. Chemical composition of fly ash

Component	Chemical Composition %			
	Class F (AF)	Class C (AC)	ASTM C618 limits Class F	Class C
SiO_2	46.9	32.7	-	-
Al_2O_3	22.9	17.6	-	-
Fe_2O_3	19.2	5.9	-	-
Total, SiO_2+Al_2O_3+Fe_2O_3	89.0	56.2	70 min	50 min
SO_3	0.3	2.0	5.0 max	5.0 max
CaO	3.8	27.3	-	-
MgO	0.8	6.6	-	-
K_2O	1.7	0.4	-	-
Na_2O	0.6	2.2	-	-
Moisture Content, %	0.1	0.8	3.0 max	3.0 max
Loss on Ignition, %	2.3	0.3	6.0 max	6.0 max

Table 5. Physical properties of fly ash

Parameter	Class F (AF)	Class C (AC)	ASTM C618 limits: Class F	ASTM C618 limits: Class C
Specific Gravity	2.50	2.83	-	-
7-day Strength Activity Index, %	77.5	82.9	75 min	75 min
Water Requirement, %	102	91	105 max	105 max

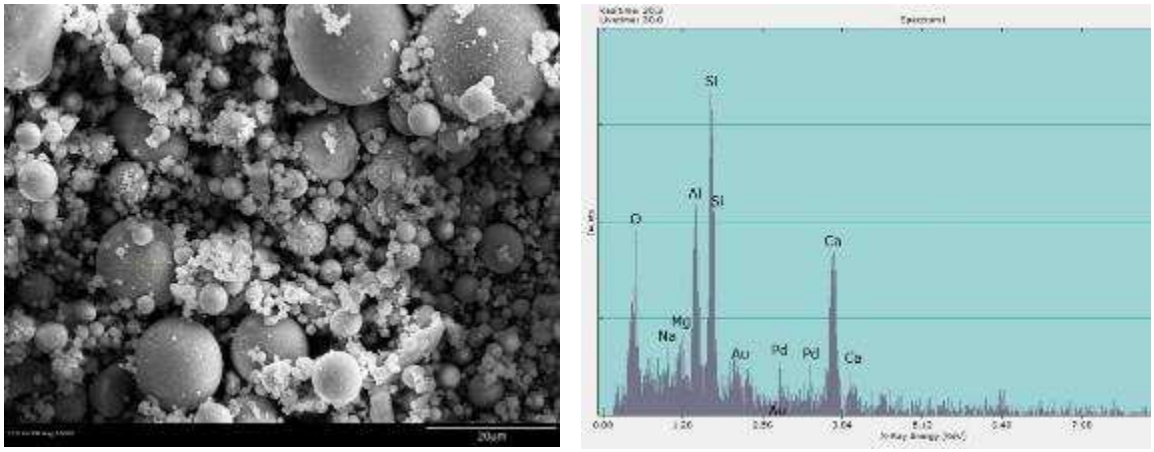

Figure 15. SEM images and EDS spectrum of ASTM Class C fly ash

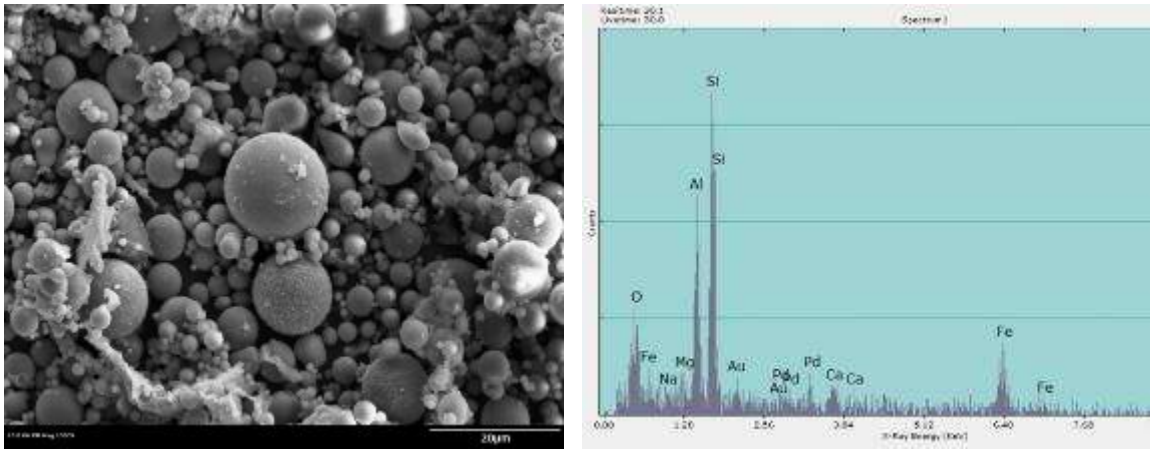

Figure 16. SEM images and EDS spectrum of ASTM Class F fly ash

To maximize the strength development of portland cement composites, the fineness fly ash was optimized. In addition, the water content in the mix proportion played an important role

in terms of fly ash utilization. The proportion of water should increase due to a bigger surface area in pulverized fly ash.

The chemical and physical properties of class F fly ash are defined by the requirements of ASTM Specification for Coal Fly Ash and Raw or Calcined Natural Pozzolan for use in concrete (C618). As a replacement of portland cement, up to 30% of fly ash can be used as an SCM. There are many advantages for using fly ash as a replacement of portland cement:

- Improved compressive strength
- Increased resistance to alkali silica reaction
- Increased resistance to sulfate attack
- Reduced heat of hydration
- Reduced porosity and permeability
- Reduced water demand
- Improved workability
- Reduced cost

3.1.3. Mechano-Chemical Activation

Mechanical activation is an effective method to improve the reactivity of blended cements. Fine grinding of cementitious materials creates a larger surface area available for hydration reaction. The test results indicated the potential for significant improvement in mechanical properties and also the possibility of acceleration of cement hydration due to presence of nano-sized and submicron phases.

In this research, the activated component (AC) was prepared from fly ash C (FAC) and F (FAF). Fly ash was used as a cement replacement material at the amount 20% and 30%. Two

approaches to realize the NEC concept were investigated. First, the mechano-chemical activation (MCA) was used to activate Class F fly ash which was used at a replacement level of 20% with 10% of additional (non-activated) fly ash and at W/CM of 0.36 as presented in *It can* be observed that the activation of fly ash in vibro mill considerably accelerates the heat of hydration of cementitious systems with fly ash (*Table 27*) vs. reference (*Figure 58).* The highest hydration peak associated with the C3S hydration was reached by the composition with fly ash activated for 3 hours.

Table 27. The activation of 20% of class F fly ash was realized with superplasticizer in a water solution and the remaining 10% of fly ash was added during mortar mixing stage. The SP was added to facilitate the dispersion of fly ash in liquid state during milling. Different milling times 1 hour, 2 hours, 3 hours and 4 hours were used. All the experimental results were compared with superplasticized mortars containing 30% fly ash (without activation). Therefore, all mortars had identical composition. The objective of this research phase was to determine the optimal activation time providing the best mechanical performance.

Second phase of activation research was conducted to compare the effects of fly ash type and used the optimal activation time of 3 hours for fly ash utilization rate of 20% replacement at W/CM of 0.3. To produce the activated component (AC), the required quantities (20% of total cementitious materials by weight) of fly ash were pre-mixed with tap water, superplasticizer and, optionally, nanosilica. The fly ash blend was activated by vibro-milling. Indeed, the activation of fly ash occurs at grinding media to material ratio of 10:1 and leads to the reduction of particle size and considerable change in particle size and shape, however provides little change in the mineral composition of the product.

Fine grinding and mechanical activation was used as a key method to enhance the reactivity of the blended cements. This study used 500 ml plastic containers with slurry placed into the frame of vibro-mill and milled for different activation times. Upon grinding, the AC slurry was immediately removed from the chamber and was placed into the mixing bowl the preparation of mortar by mixing with all the remaining materials (cement, sand and chemical admixtures).

Not only using the vibro-miling of water-based slurries, but also the use of grinding media was optimized. To achieve the effective milling, a specific set of grinding media is required to disperse the material, including the distribution, size and shape of media charge. In this research, two different types of grinding media: cylindrical (with diameter of 2 mm and length of 4 mm) and spherical (with diameter of 3 mm) were used to achieve the milling. *Figure 17* shows the characteristic shapes of grinding media used in this research.

Spherical Cylindrical

Figure 17. Characteristic shapes of grinding media

The grinding media was optimized based on the milling of reference sand. The mix of cylindrical and spherical media was prepared in 500 ml plastic container bottles. Each bottle contained a combination cylindrical and spherical media and also quartz sand at a weight ratio of

10 to 1. The 75:25 blend of cylindrical to spherical charges was found to be effective and used for activation of fly ash.

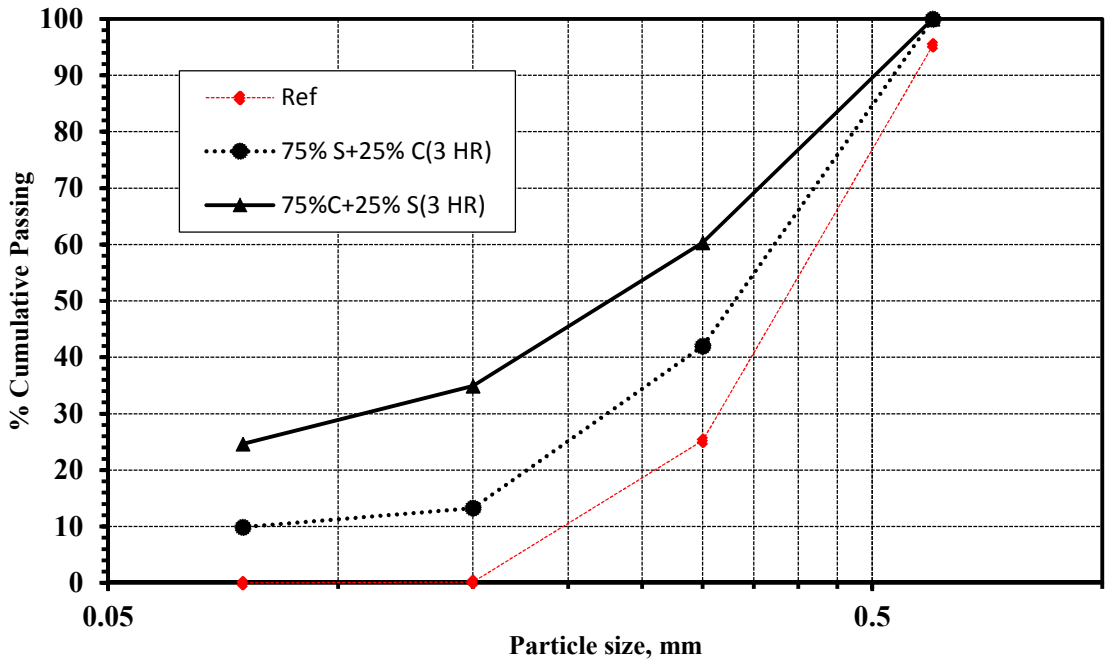

Figure 18.The optimization of grinding media for 3-hour activation

3.1.4. Nanosilica: Colloidal SiO_2 Nanoparticles

Commercial Products

For this study two commercial colloidal nanosilica products were used. The first is Cembinder 50 which has an average particle size of 5 nm and a solid concentration of 15%. The other is Cembinder 8 which has an average particle size of 10-100 nm and a solid concentration of 50%. The properties for Cembinder products are listed in Table 6.

Table 6. Properties of Nanosilica

Test Parameter	SiO_2 Cembinder Grade	
	50	8
Density, g/cm^3	1.1	1.4
SiO_2 ,%	15	50
pH	10.0	9.5
Viscosity, mPas	<10	<10
Average particle size, nm	5	10-100

The BET study confirmed that the colloidal nanosilica is meso-pore (2-50 nm, Cembinder 50) and macro-pore (Cembinder 8) materials with higher BET surface area corresponding to material with finer particle size, *Figure 19.* Therefore, due to very smaller particle size and large surface area, Cembinder acts both as microfiller reducing the porosity, and also as a pozzolan reacting with $Ca(OH)_2$ supplied from the hydration of portland cement.

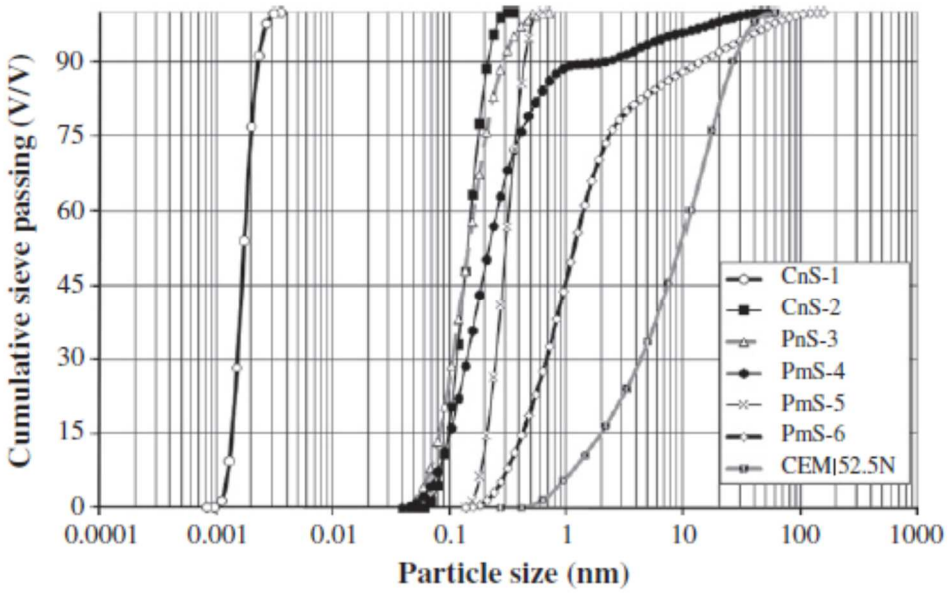

Figure 19 PSD of the collected nanosilica samples of Cembinder 50 and Cembinder 8 (samples CnS-1 and CnS-2, respectively) [104]

Cembinder is an amorphous surface modified colloidal silica (nanosilica) product which was designed for concrete applications. It is the key component of SCC affecting the flow,

density and heat of hydration. By partially replacing portland cement with a small amount of nanosilica material, workability, density, compressive strength and the rate of heat of hydration release can be tailored. Nanosilica as a super pozzolan which has been used to develop the beneficial microstructure and to improve cement based systems. The amount of nanosilica used in cement based systems is up to 2%.

The most important component in the cement hydration process is C-S-H. In the hydration of cement, the calcium silicates are dissolved and form C-S-H and calcium hydroxide (CaOH, CH) as per as reaction:

$$C_3S + 2H_2O \Rightarrow \text{C-S-H} + 2\ Ca(OH)_2 \quad (1)$$

The addition of nanoparticles results in the reaction of dissolved silica and calcium hydroxide, *Figure 20*. From the equation below, additional C-S-H is formed:

$$Ca(OH)_2 + SiO_2 \Rightarrow \text{C-S-H} \quad (2)$$

Björnström et al, has conducted the effect of colloidal nanosilica is capable of densifying cement. By adding nanosilica into cement, the new C-S-H binder improves the cement paste density which reinforces the structure between cement grains [53]

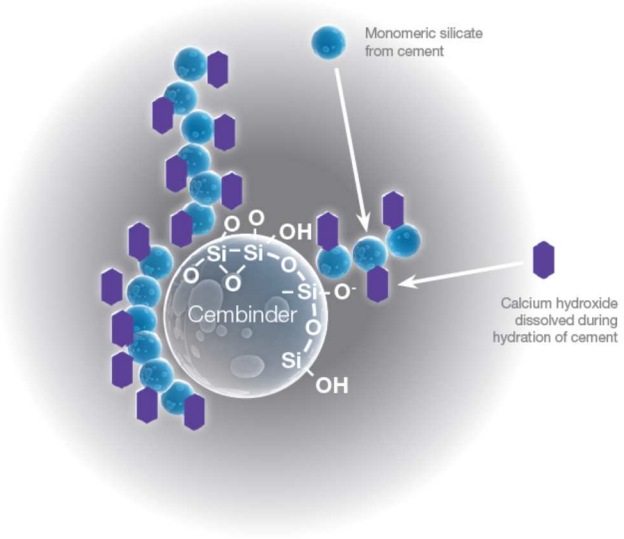

Figure 20. The formation of C-S-H gel from nanosilica [105]

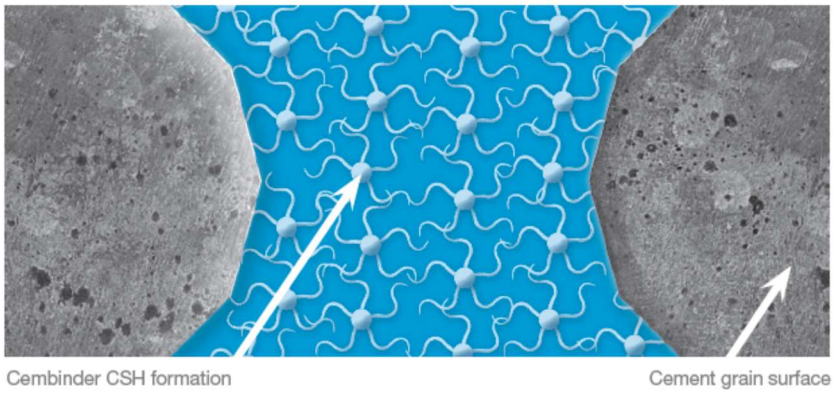

Figure 21. The effect of C-S-H formation on the surface of cement grain [105]

In order to characterize the size and morphology of commercial Cembinder 50 and Cembinder 8, Quercia et.al [104] analyzed these products by using the scanning electron microscope (SEM) to determine the characterization for different amorphous nanosilica samples with respect to application in cement paste. The research investigated the addition of 0.5% to 4% of nanosilica and it was concluded that nanosilica can reduce the water cement ratio (W/C) and the linear relationship between the deformation coefficients, and the specific surface area was established.

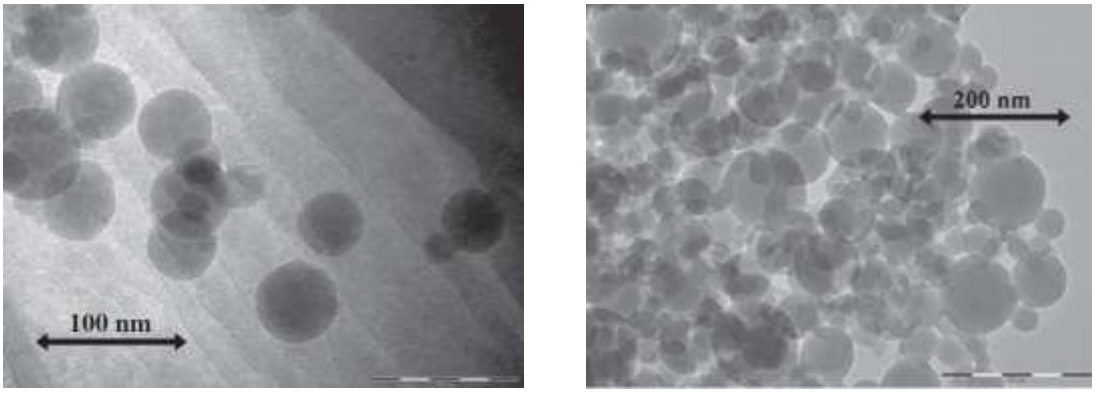

(a) Cembinder 50 (b) Cembinder 8

Figure 22. Particle shape of (a) Cembinder 50 and (b) Cembinder 8 [104]

Natural Silica Nanoparticles

Low cost silica nanoparticles were obtained from the hydrothermal solutions containing of silicic acid (H_4SiO_4). The initial solution also contained other components listed in *Table 7.* Nanodispersed powders were harvested from the solutions by removing the excess water by filtering through membranes and, for selected specimens, by a cryochemical vacuum sublimation drying (e.g.,with the use of liquid nitrogen) [106, 107]. For membrane filtering, polyether-sulfone and poly(acrylonitrile) capillary ultrafiltration membranes with pore sizes from 20 to 100 nm and tubular ceramic microfiltration membranes with an average pore diameter of 70 nm were used [10]. For sublimation drying, slightly aggregated nanodispersed powders were obtained from concentrated aqueous sols by treatment with liquid nitrogen at a pressure of 3 Pa and a temperature of -80°C. Commercially available nano-SiO_2 admixture Cembinder-8 (CB8, available in a form of 51.5% water suspension) from Eka Chemicals was used as a reference nano-SiO_2 product.

Table 7. The composition of the hydrothermal solutions [106]

Component	Na^+	K^+	Li^+	Ca^{2+}	Mg^{2+}	Fe^{x+}	Al^{3+}	Cl^-	SO_4^{2-}	HCO_3^-	CO_3^{2-}	H_3BO_3	SiO_2
Concentration, mg/l	282	48.1	1.5	2.8	4.7	<0.1	<0.1	251.8	220.9	45.2	61.8	91.8	780

Three types of nanoparticles were produced by ultrafiltration from the geothermal solutions in the form of a gel (specimen MB) and two dry powder specimens (TB and N2) by subsequent sublimation drying using liquid nitrogen. The temperature used for the formation of TB particles was higher than that used for N2 and so larger TB particles were characterized by reduced surface area.

Dry silica specimens were pulverized in a ceramic mortar with the addition of acetone. The test for BET specific surface area included three steps: sample preparation, degasification, and analysis. For each step, the weight of the sample was controlled. A maximum temperature of 200 °C and vacuuming for 2 hours were used for degasification. This procedure was used to remove any moisture or solvent residues from the samples. The XRD powder diffraction and scanning electron microscope (SEM) techniques were used to analyze the silica powders. The results of the BET investigation are reported in *Table 8*. In *Figure 23*, an X-ray diffractogram (left) and SEM image (right) reveals an amorphous structure of spherical silica nanoparticles.

Table 8. Characterization of Silica Nanoparticles

	Material	Solid Concentration, %	BET Surface Area, m^2/g
Reference	CB8	52	61
Sol	MB	35	352
Dry	TB	100	43
	N2	100	228

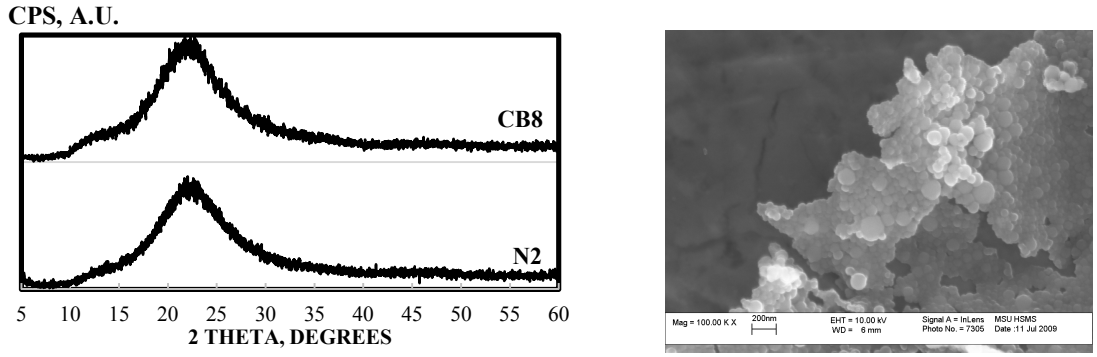

Figure 23. The X-ray Diffractogram (left) and Scanning Electron Microscope image (right) of the N2 silica powder

Fourier Transform Infrared (FTIR) spectroscopy was used to compare the molecular structure of silica nanoparticles as reported in *Figure 24*. The bonds corresponding to water molecules were observed in CB8 and MB samples at the wave length of 900 to 980 cm^{-1}. Stretching vibration characteristic for Si-(OH) bonds at 900 to 980 cm^{-1} and Si-O-Si bonds at approximately 800 cm^{-1} and 1000 to 1250 cm^{-1} were observed for investigated samples.

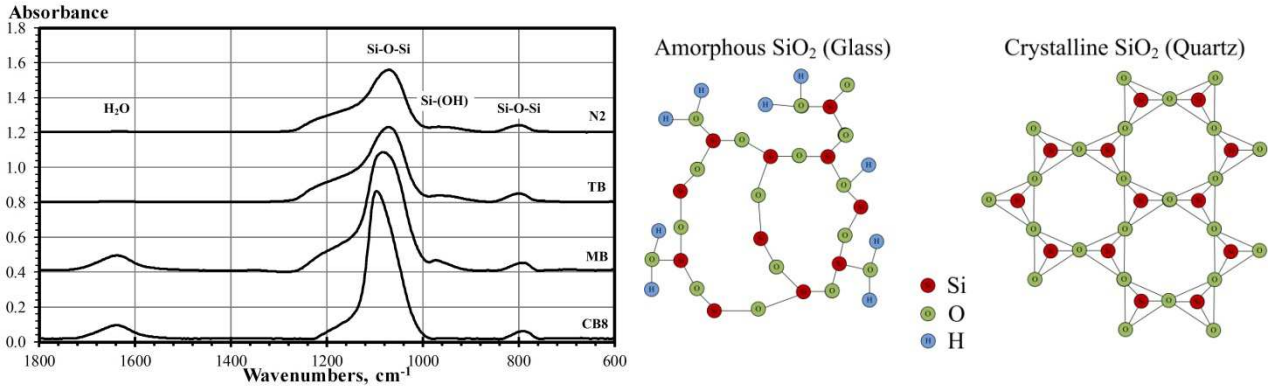

Figure 24. The FTIR spectroscopy of silica nanoparticles (left) and model of the corresponding amorphous structure (right).

The intensity of the stretching vibration peak corresponding to the Si-O-Si bond can be correlated to the number of bonds present in the material. The lack of Si-(OH) bonds in the CB8 specimen is a sign of very poor coordination between the silica and water (H-O-H) molecules (or OH^- groups). A higher crystallinity of SiO_2, or the presence of a surfactant (stabilizing agent)

attached to the silica particles, may be the reason for the absence of Si-(OH) bonds on the spectrum of CB8 sample. In this way, higher intensity corresponding to the Si-O-Si bond and the absence of Si-(OH) bonds can suggest that CB8 is a more ordered material. Therefore, more ordered molecular structure of CB8 can be expected (*Figure 24*). This can reduce the reactivity of CB8 in portland cement systems; however, due to very small particle size a seeding (nucleation) effect may still be very pronounced.

Lower intensity corresponding to the Si-O-Si bond observed at 1000 to 1250 cm^{-1} for nanosilica harvested from hydrothermal solutions suggests the formation of poorly ordered structures (*Figure 24*). The intensity of Si-O-Si bonds can be reduced due to the development of Si-(OH) bonds on synthesized nanoparticles. Lower intensity of the Si-O-Si bonds and the presence Si-(OH) bonds suggest that all hydrothermal silica nanoparticles are highly amorphous materials. This can potentially improve the reactivity of nanosilica in portland cement systems, indicating a high capacity for seeding (nucleation) and pozzolanic effects. Here, the FTIR study confirms the results of the XRD investigation.

Processing of Silica Nanoparticles

The dispersion of nanoparticles with PCE superplasticizer was achieved by an ultrasound processor (Hielscher UIP1000hd). The PCE was first mixed with water using a glass stick until the uniform dissolution was observed. The solution was further treated using the ultrasound (at 20 kHz) processor at 50% of the maximum power (750 W) for 30 seconds to ensure the effective dispersion. The nanoparticles were added to PCE solution and dispersed using the ultrasound processor at 75% of the maximum power for 6 minutes. A water bath filled with ice and cool water was used to control the temperature during the process (<30 ºC).

3.1.5. Chemical Admixtures

Locally available air-entraining, mid-range and high-range water-reducing (superplasticizing) admixtures were used in this study. After preliminary evaluation and screening, one plasticizing (mid-range) and four superplasticizing products combined with AE admixture (AMA) were selected for the research program as summarized by *Table 9*. After evaluation of chemical admixtures, two commercially available polycarboxylate superplasticizers (PCE/SP) supplied by Handy Chemicals Megapol 40 DF and GUSR-AC with solid concentration of 38.9 and 38.5%, respectively were used in the experimental program related to nanosilica and SCC. The study of DOT concrete used HG7 superplasticizer, midrange water reducing admixture RP8 and air entraining admixture from BASF (*Table 9*)

Table 9. Properties of chemical admixtures

Designation	Admixture Type	Composition	Specific gravity	Solid Content, %	Manufacturer recommended dosage *
AMA	Air-Entraining	Tall Oil, Fatty acids, Polyethylene Glycol	1.007	12.3	8-98 mL (0.13-1.5 fl oz)
RP8	Water-Reducing Admixture	4-chloro-3-methyl phenol	1.200	40.3	195-650 mL (3-10 fl oz)
HG7	High Range Water-Reducing	Polycarboxylate Ether	1.062	34.0	325-520 mL (5-8 fl oz)
HR1		Naphthalene Sulphonate	1.193	40.3	650-1600 mL (10-25 fl oz)
HAC		Polyacrylate Aqueous Solution	1.072	36.7	650-1040 mL (10-16 fl oz)
HD1		Naphthalenesulfonic acid, polymer with formaldehyde, calcium	1.193	39.8	650-1040 mL (10-16 fl oz)
MP G		Polycarboxylate ether	1.082	38.5	200-1000 mL
MP 40		Polycarboxylate ether	1.079	38.9	65-650 mL

* *The dosage of chemical admixtures is expressed by 100 kg (100 lbs) of cementitious material*

3.1.6. Aggregates

Coarse, intermediate and fine (natural sand) aggregates from Southern WI were used in this project. *Table 10* provides a summary of the aggregate types and sources. Physical characteristics of aggregates are summarized in *Table 11*. Bulk density and void content for loose and compacted aggregates are listed in *Table 12*. The sieve analysis of aggregates is provided by *Tables 13 - 15* and *Figure 25*.

Table 10. Designation and sources of aggregates

Designation	Type	Location
C1	1”Limestone	Sussex Pit - Sussex, WI
I1	5/8”Limestone	Lannon Quarry - Lannon, WI
F1	Torpedo Sand	Sussex Pit - Sussex, WI

Table 11. Physical characteristics of aggregates in oven dry (OD) and saturated surface dry (SSD) conditions

Aggregate Type	Specific Gravity			Density, kg/m^3			Water Absorption, %	Fines <75µm, %
	OD	SSD	Apparent	OD	SSD	Apparent		
C1	2.730	2.765	2.829	2723	2758	2822	1.29	0.78
I1	2.684	2.734	2.824	2678	2727	2817	1.84	0.79
F1	2.566	2.637	2.762	2559	2630	2755	2.77	1.19

Table 12. Bulk density and void content of aggregates in loose and compacted state

Aggregate Type	Loose			Compacted		
	OD Bulk Density kg/m^3	SSD Bulk Density kg/m^3	Void Content, %	OD Bulk Density kg/m^3	SSD Bulk Density kg/m^3	Void Content, %
C1	1562	1582	42.7	1638	1659	39.9
I1	1466	1493	45.3	1605	1635	40.1
F1	1782	1831	30.4	1868	1920	27.0

It can be observed that the aggregate gradings were within the limits set by ASTM C33. Slight access of 300 µm fraction in sand F1 can be considered acceptable.

Table 13. Grading of coarse aggregates

Aggregate Types	Amount Finer than Sieve (mass %)				
	25 mm (1 in)	19 mm (3/4 in)	9.5 mm (3/8 in)	4.75 mm (No. 4)	2.36 mm (No. 8)
No. 67: 3/4 - No.4 (ASTM C33)	100	90-100	40-70	0-15	0-5
C1	100	97.4	23.4	1.1	0.2

Table 14. Grading of intermediate aggregates

Aggregate Types	Amount finer than Sieve (mass %)						
	19 mm (3/4 in)	12.5 mm (1/2 in)	9.5 mm (3/8 in)	4.75 mm (N. 4)	2.4 mm (N. 8)	1.2 mm (N. 16)	0.3 mm (N.50)
No. 7: 1/2 - No.4 (ASTM C33)	100	90-100	40-70	0-15	0-5	-	-
I1	100.0	87.6	58.5	12.8	2.5	-	-

Table 15. Grading of fine aggregates (sand)

Aggregate Types	Fineness Modulus	Amount Finer than Sieve (mass %)						
		9.5 mm (3/8 in)	4.7 mm (N. 4)	2.4 mm (N. 8)	1.2 mm (N. 16)	0.6 mm (N. 30)	0.3 mm (N. 50)	0.15 mm (N. 100)
Sand (ASTM 33)	2.3-3.1	100	95-100	80-100	50-85	25-60	3-50	0-10
F1	2.43	100	99	83	70	58	35	13

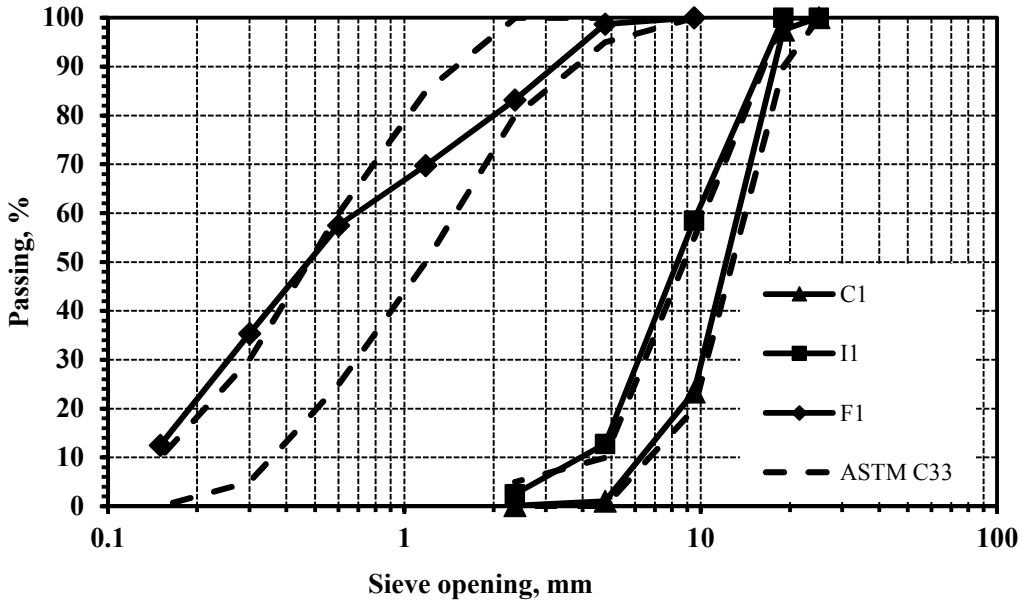

(i)

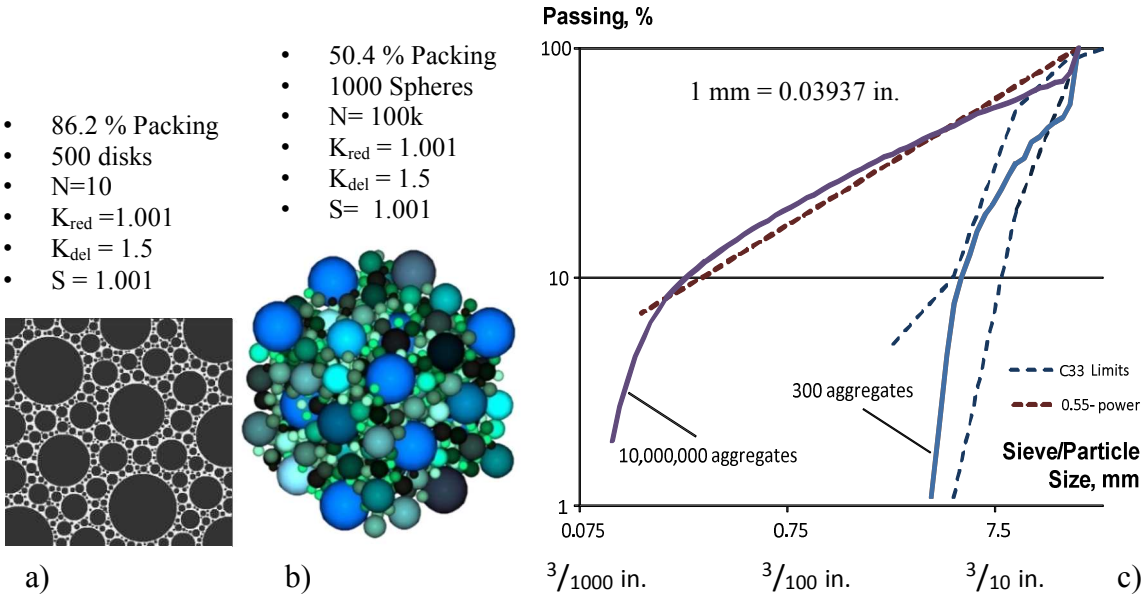

(ii)

Figure 25. Particle size analysis of southern aggregates C1, F1, I1 (i) and optimization of aggregates proportions using 0.55 power curve and packing simulations (ii) [108]

3.2. EXPERIMENTAL PROGRAM

Following the approach stated above, the experimental program was designed and executed. The performance of blended system with supplementary cementitious materials (SCMs) and superplasticizers can be used to evaluate concrete using express methods and computer models *(Figure 12)*. The properties of supplementary cementitious materials such as slag cement and fly ash are tested according to corresponding ASTM standards [109, 110], and, therefore, such information is readily available at the stage of concrete mixture design. The results of a mortar test (ASTM C109) can be effectively used for predicting the behavior of concrete manufactured with supplementary cementitious materials (e.g., slag cement, fly ash, silica fume) and chemical admixtures [69, 111]. A similar method was postulated by DIN and effectively used for concrete mixture proportioning in the case of blended cements or cements with different compressive strength. It was proved that the strength of mortars with different quantities of SCMs is proportional to the strength of concrete based on the same binder [111]. This approach was also used by P. Tikalsky et al. for evaluating the performance of ternary cementitious mixes [112, 113]. The main idea of this method is to use the specific performance characteristics (i.e., compressive/flexural strength) of binder materials rather than testing each particular source (since each particular source can demonstrate the variability in the performance over the time) and combination in concrete. This method can be effectively used in practice as SCM and chemical admixtures quality control, screening and acceptance tool.

The advantage of such multi-scale method is that it can effectively accommodate the contribution of virtually any cementitious material, mineral additive, and chemical admixture and, with sufficient accuracy, predict the performance of concrete (including strength development, flexural/splitting tensile strength, and the effect of admixtures).

The rheological behavior of cement paste corresponding to SCC mixtures was evaluated to determine the yield stress and viscosity parameter. Prior to preparation of concrete mixture, SCC mortars with and without activated class C fly ash were compared for fresh and hardened properties.

The experimental matrix for concrete study involved mixing and testing of 20 optimized mixtures containing a total of 280 kg/m^3 (reference DOT concrete) and also SCC with 400 kg/m^3 and 500 kg/m^3 of cementitious materials. The aggregate blend was selected using 40% of coarse aggregates, 10% of intermediate aggregates and 50% of fine aggregates which meets the optimized gradation and best packing. All concrete mixtures were proportioned according to the ACI 211 concrete specification. The reference portland cement mixtures were compared with fly ash based concrete.

Therfore, two approaches were investigated. The first approach consisted of making a conventional concrete mixtures as per as (DOT – specification) using two types of chemical admixtures (mid-range plasticizer and high-range water reducer), AE admixture and SCM. This study consisted of 10 concrete mixtures. The resulting concrete was evaluated for fresh properties, slump, air content, density, and temperature. The hardened properties such as the compressive strength at 1, 3, 7, and 28 days were tested.

The second approach consisted of testing SCC concrete based on supplementary cementitious material (with replacements up to 50%), nanosilica and high range water reducer (HRWR). This study also consisted of 10 concrete mixtures. The SCC was evaluated for fresh properties using v-funnel test, slump flow and J-ring flow (passing ability and stability). The hardened properties such as compressive strength at 1, 3, 7 and 28 days were also evaluated.

3.3. TEST METHODS

Paste, mortar and concrete mixtures were batched, mixed, and the concrete specimens were cast, cured, and tested according to the corresponding ASTM and AASTHO standards..

3.3.1. Mini-Slump of Cement Pastes

For the cement paste study, the water to cementitious material (W/C) ratio of 0.45 was selected. Lower W/C ratio vs. that specified by the ASTM Standard for mortars (W/C=0.485, ASTM C109) was used for the evaluation of water-reducing admixtures. In addition, similar W/C was used in concrete tests. The mixing procedure for pastes was performed as specified by ASTM C305.

A mini-slump cone (with a bottom diameter of 38 mm, a top diameter of 19 mm, and a height of 57 mm) was used in this research to determine the effect of supplementary cementitious materials and chemical admixtures. To determine the mini slump, the cone was filled with paste, lifted, and, when the cement paste stopped spreading, four flow diameters were recorded and the average value was reported.

3.3.2. Rheological Investigation of Cement Pastes

Rheology determines the flow deformation and the relationships between the stress, strain, rate of strain and time. Rheology testing is important to characterize the behavior of concrete and its individual phases in fresh state [114]. The range of rheological parameters of paste, mortar and different types of mortars are presented in the *Table 16.* Concrete uses up to 80% of aggregates by volume. As the particle sizes increases, the plastic viscosity of the paste and mortar becomes higher.

Table 16. Rheological parameters of cement based materials [115]

Material	Paste	Mortar	Self-compacting concrete	Flowing concrete	Pavement concrete
Yield Stress (Pa)	10-100	80-400	50-200	400	500-2000
Plastic Viscosity (Pa.s)	0.01-1	1-3	20-100	20	50-100

3.3.3. Mortars Tests

For mortar specimens, the water to cementitious material (W/C) ratio of 0.45 was selected, and the sand to cement (S/CM) ratio was set to 1. The W/C ratio was reduced from that specified by the ASTM Standard (W/C=0.485, ASTM C109) due to the use of water-reducing admixtures in the mix. Also, the W/C is selected to provide a reasonable workability for all tested compositions and enabling to compare the effects of WR and HRWR admixtures at different dosages without poor compaction or segregation. The mixing of mortars was performed as specified by ASTM C109 and ASTM C305. The workability and density of fresh mortars was evaluated as specified by ASTM C 1437 and ASTM C 138, respectively.

For the compressive strength investigation, cube mortar specimens with the dimensions of 50 × 50 × 50 mm (2 × 2 × 2 in.) were cast and cured in accordance with ASTM C 109. Test samples were removed from the molds after 24 hours of curing, immersed in a lime water, cured at a temperature of 23±2C^{o}, and then tested at the age of 3, 7 and 28 days. The compressive strength of the mortar specimens was determined using a pace rate of 1.4 kN (315 lb). The reported values represent a mean of at least two specimens tested for each age.

3.3.4. Heat of Hydration

An isothermal calorimeter measures the rate of heat release from hydrating mixture due to ongoing chemical reactions. In this study, an isothermal calorimeter TAM Air (TA Instruments) was used to evaluate the hydration kinetics at a constant temperature of 25 °C during the early 48-hour period. The output of the calorimeter was evaluated by graphical and mathematical means to evaluate the effect of different combinations of components. The isothermal curves or hydration profiles indicate setting characteristics, compatibility of different materials, early strength development, and the effect of chemical admixtures on the cement hydration.

3.3.5. Preparation, Mixing, and Curing of Concrete

Concrete batching, mixing, casting and curing procedures were conducted according to ASTM C192 "Standard Practice for Making and Curing Concrete Test Specimens in the Laboratory". The mixing procedure included mixing of aggregates with 20% of total water for 30 seconds using a drum mixer suitable for the volume of the batch. Next, cement was added to the mix, and then SCM (if any component) was added. The rest of the water with chemical admixtures was added upon the addition of cementitious materials. Finally, sand was added to the mixer. The mixing was resumed for an additional 3 minutes. The mix was left in the drum mixer at rest for a period of 3 minutes and was then mixed for another 2 minutes.

3.3.6. Slump

A concrete slump test was performed according to ASTM C143 to measure the workability of fresh concrete. This test is widely used in the field to determine the suitability of concrete pavement mixtures for slip-forming; however, there may be other characteristics such as finishability that are not accounted for by this test. The test was repeated for the time

corresponding to 30 minutes after the initial contact of water and cement in order to measure the slump loss.

3.3.7. Fresh Properties of SCC

V-Funnel Test

The V-funnel test is used to determine the filling and flow ability of an SCC mixture. The test included pouring SCC into the funnel and recording the time required for the mixture to completely flow through the funnel. Depending on the flow of the mixture, the time can vary; however, the average benchmark time for a SCC mixture to flow through the funnel is 9 seconds.

Slump Flow Test

The slump flow test helps to determine the free flow of the SCC mixture without any obstructions. The test is completed using ASTM C1611 standard. The process of this test included pouring SCC into a cone mold with the larger opening facing upwards. Once the SCC was poured into the mold, it is lifted straight up in a steady motion. The diameter of the concrete at rest was then measured twice and the average of the two was recorded. It is important to make sure the surface of where the test is taking place and the mold are sprayed down with water. In order to avoid moisture less and eliminate friction at the base.

Spread J-Ring Test

The spread J-Ring test is very similar to the slump flow test and helps to determine the flow through obstruction such as rebar. The test included the mold used in the slump flow test and a J-ring. The J-ring is a metal ring with bars attached to the ring. The cone mold is placed inside the J-ring and is filled with SCC. Again the mold is pulled straight up as in flow test at a steady rate and the diameter of the flow is measured twice with the average of the two recorded.

3.3.8. Density of Fresh Concrete

The density of fresh concrete was tested per ASTM C34. All the mixtures, regardless of the slump, were consolidated using rodding and tapping the side of the container with a rubber mallet repeated for 3 layers. The top of the container was leveled off and the weight was measured using a scale per ASTM C34.

3.3.9. Air Content of Fresh Concrete

Concrete air content was tested in the fresh state using pressure method with an air meter as per as ASTM C231. Optimized DOT-grade mixtures were designed to reach air content of 6±1.5%; however, some changes occurred due to the variation in type of HRWRA and SCM. No AE admixture was used in SCC mixtures.

3.3.10. Temperature

Fresh concrete temperature was tested according to ASTM C164 to monitor the potential effect of temperature. The temperature can be used to track any potential variation in different batches due to moisture loss, as well as heat of hydration.

3.3.11. Compressive Strength

Compressive strength tests were performed on cylinders with a diameter of 102 mm (4-in.) and height of 203 mm (8-in) according to ASTM C39. These specimens were tested with an ADR-Auto ELE compression machine at a loading rate of 2.4 kN/s (540 lb/s). The maximum load and maximum compressive stress were recorded. The test was performed at different ages including 1, 3, 7 and 28 days of normal curing.

4. DESIGN OF NANO-MODIFIED COMPOSITES

4.1. OPTIMIZATION OF SUPERPLASTICIZERS

The mini-slump of paste specimens corresponding to several water-to-cement ratios (W/C) was tested and reported in *Table 17*. The W/C of 0.45 resulting in a flow of ≈ 60 mm was selected for subsequent testing of admixtures. The selected W/C provides a good balance to compare plain pastes with different dosages of chemical admixtures with the range of 50 – 200 mm (2 – 8 in.).

Different portland cements (L1, L2, H1 and S1) combined with supplementary cementitious materials such as slag (SL), Class F fly ash (AF) and Class C fly ash (AC), and selected chemical admixtures were tested in pastes to determine the mini-slump at a specific dosage (RP8-0.15%, HR1-0.4% and HG7-0.15%). Other admixtures were evaluated and screened out; and, because of the best performance, HG7 was selected to investigate the effect of SCM. The results of these tests are reported in *Figure 26* and *Figure 27*.

Table 17. Mini-slump of cement pastes based on L1 at different W/C ratios

W/C	0.4	0.45	0.5	0.6	0.8	1.0
Flow, mm (in.)	38 (1.5)	59 (2.3)	65 (2.6)	98 (3.8)	138 (5.4)	189 (7.4)

Mini-slump tests had demonstrated that L1 and H1 cements are perfectly compatible with SNF (HR1) and PCE (HG7) superplasticizers; however, L2 and S1 cements designed for rapid strength development had a reduced compatibility with superplasticizers (*Figure 26*). The H1 cement had an excellent compatibility with all tested admixtures and demonstrated the best flow properties. The S1 cement had the worst compatibility with admixtures tested. The mini slump

test of pastes with SCM demonstrated that the addition of SCM (especially Class C fly ash and slag cement) was beneficial to improving the workability of cement pastes and portland cement systems with SCM (*Figure 27*).

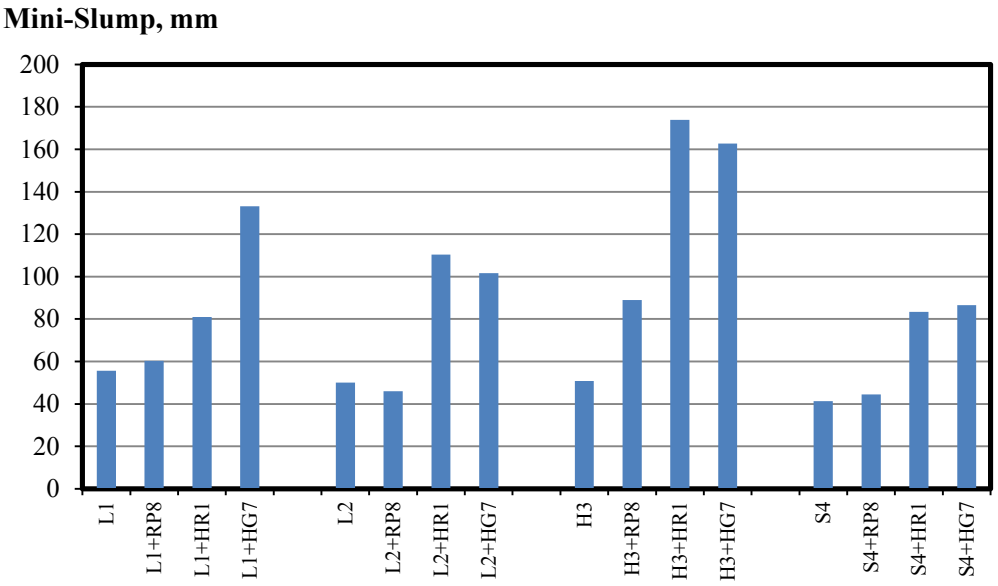

Figure 26. The effect of portland cement and admixture type on mini-slump

It can be observed that the addition of SCM improves the flow of blended cement pastes as demonstrated by *Figure 27*. Class C fly ash based mixtures had excellent flow properties in systems with plasticizing or superplasticizing admixtures. Slag cement had the best compatibility with PCE superplasticizer.

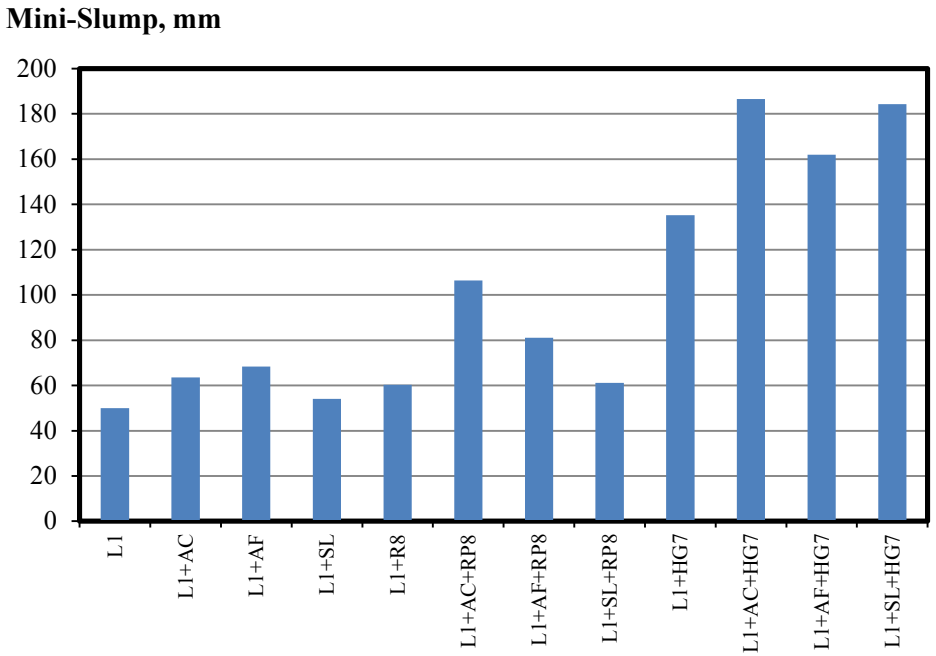

(a)

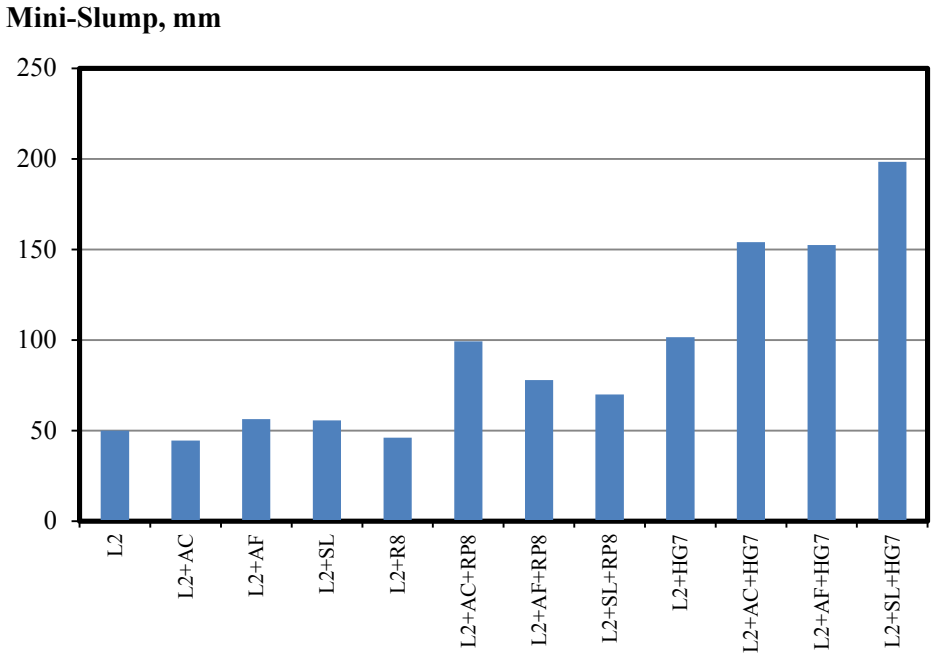

(b)

Figure 27. The effect of SCM and type of admixture on mini-slump of pastes based on cements L1 (a) and L2 (b)

4.2. RHEOLOGICAL BEHAVIOR OF CEMENT PASTES

Rheological behavior of cement pastes is affected by factors such W/CM ratio, chemical admixtures, mixing procedure and type of cement. To evaluate the workability behavior of cement based materials at different W/CM ratios, rheological tests were conducted using dynamic shear rheometer (DSR). This technique can perform the "classical" rheological tests by measuring shear stress (and viscosity) at a particular shear rate. The test was performed by the acceleration of shear rate from 0.1 s^{-1} to 10 s^{-1} in 5 minutes, followed by deceleration from 10 s^{-1} to 0.1 s^{-1} during an additional 5 minutes. To assess the contribution of ongoing hydration, the cement pastes were tested at two different periods, 10 and 30 minutes. During the test, the temperature was kept constant at a level 22° C.

This experiment considered testing the cement pastes with fly ash at replacement levels of up to 50%, superplasticizer and nanosilica at W/CM ratio of 0.3 and 0.375. For comparison, the fly ash pastes were compared with response of superplasticized (cement with nanosilica). The mixture proportion of all investigated pastes is presented in

Table 18.

Table 18. Mixture proportions of cement pastes

Mix ID	W/CM	Composition of Cement Paste , %		
		Fly Ash	SP	Nanosilica
0.3_R	0.3	0	0.25	0.15
0.3_30C	0.3	30	0.2	0.15
0.3_50C	0.3	50	0.15	0.15
0.375_R	0.375	0	0.25	0.15
0.375_30C	0.375	30	0.2	0.15
0.375_50C	0.375	50	0.15	0.15

The rheological response (shear stress) was analyzed at W/CM of 0.3 and 0.375 for each hydration time (10 and 30 minutes) as presented on *Figure 28* and *Figure 29*.

It was determined that the required shear stress is reduced with the addition of fly ash. However, for some mixtures (especially at W/C = 0.3) considerable increase of viscosity of the paste occurred at low shear rates (0.1 to 1 s^{-1}); this range can be difficult for the modeling of the composite materials response at free flow (for SCC). At shear rates higher than 1 s^{-1}, shear stress was increased with increased of the shear rate, but viscosity remained nearly constant. For modeling of concrete workability, the cement paste shear stress can be taken at the shearing rate of 1 s^{-1} which may correspond to the free flow of concrete with high workability.

Overall, the effective viscosity was reduced as the shear rate increased for each hydration time level as presented on *Figure 30* and *Figure 31*. This behavior is due to the structure build up induced by nanosilica corresponds to the thixotropic response of the suspension.

The addition of SP with nanosilica and fly ash creates well dispersed cement pastes, facilitating flow, and provides ultimate fluidization of cement pastes. This results in the considerable reduction of the shear stress vs. reference paste when tested at the same W/CM ratio.

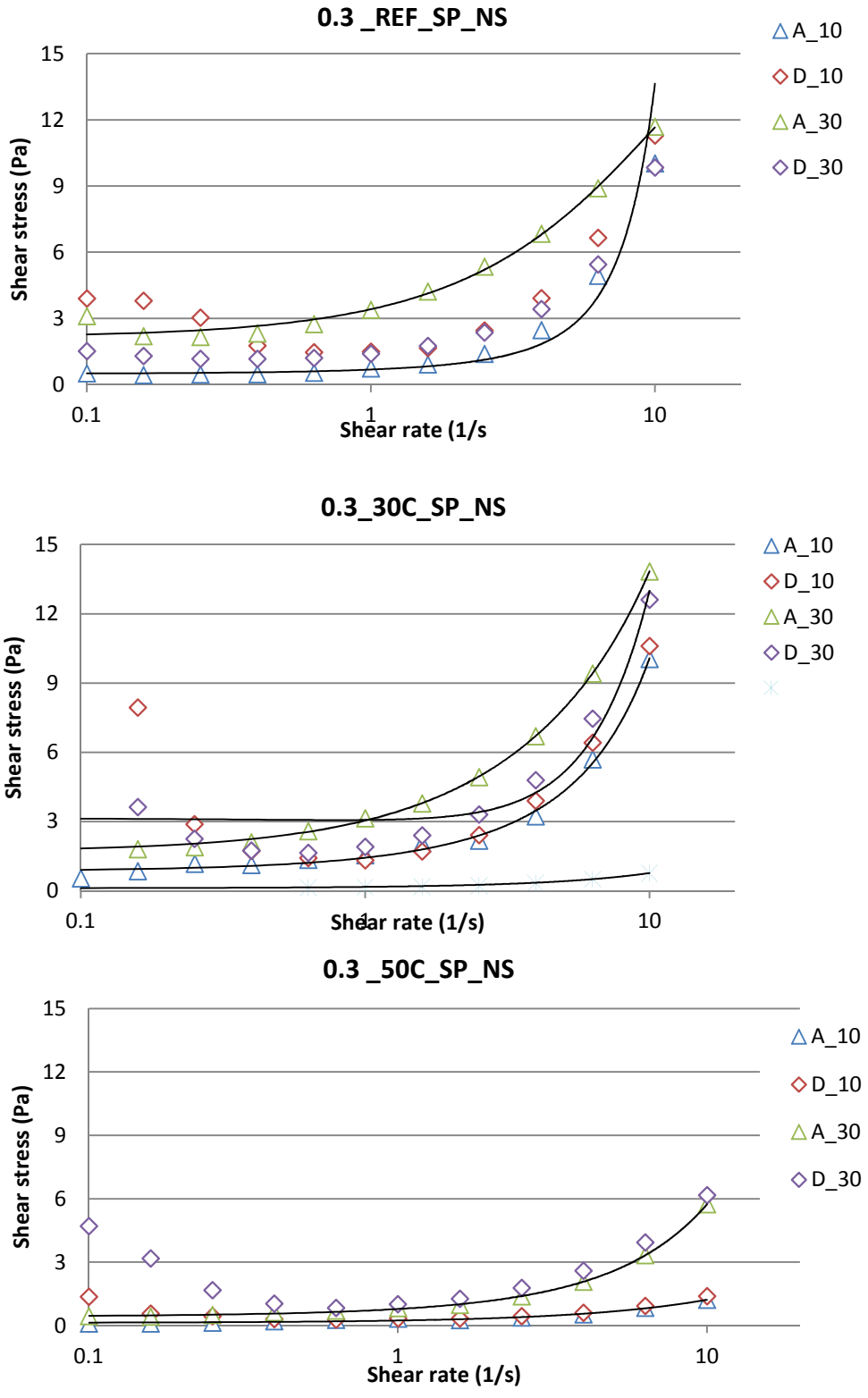

Figure 28. Shear stress vs. shear rate in cement paste W/CM = 0.3

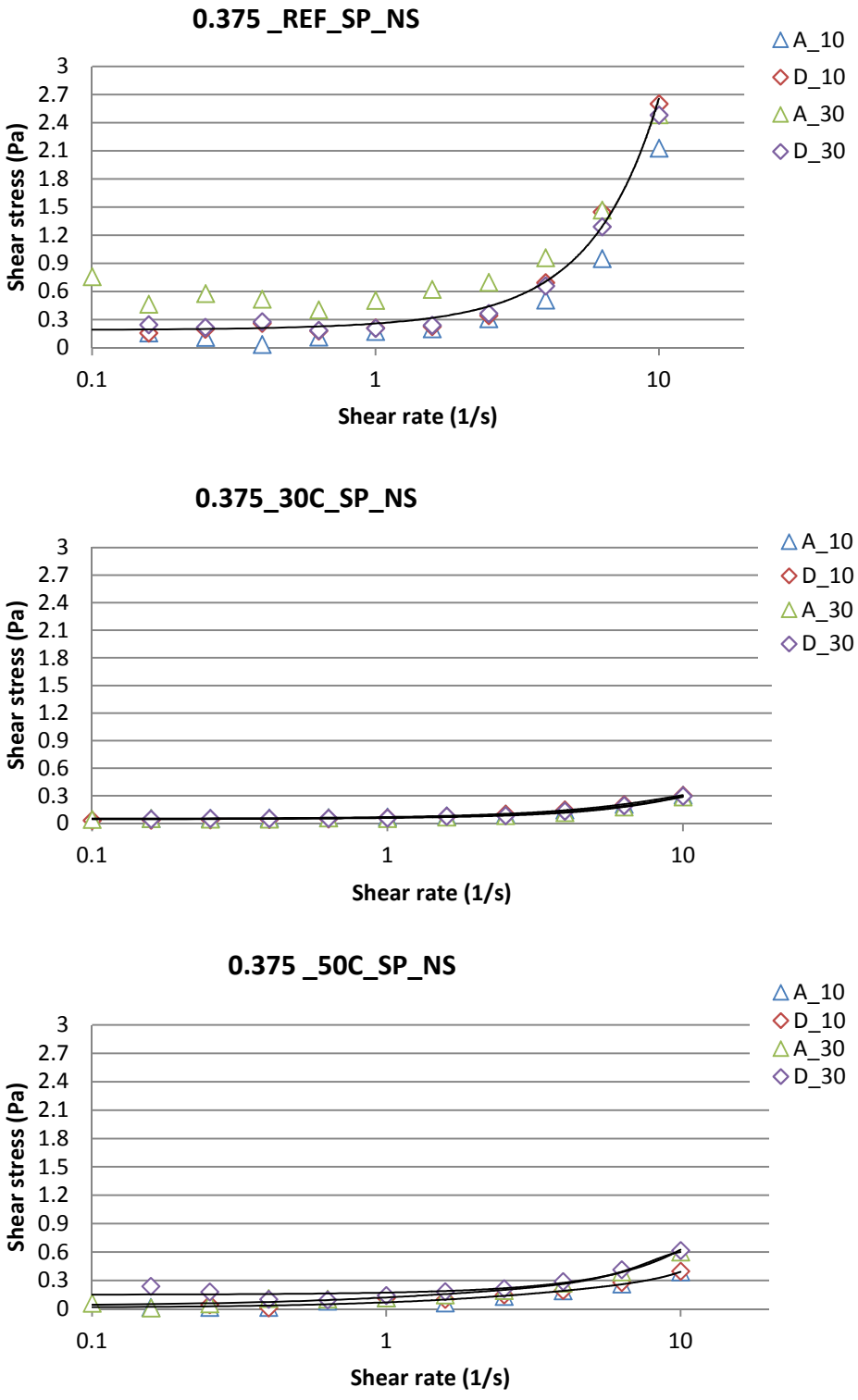

Figure 29. Shear stress vs. shear rate in cement paste W/CM=0.375

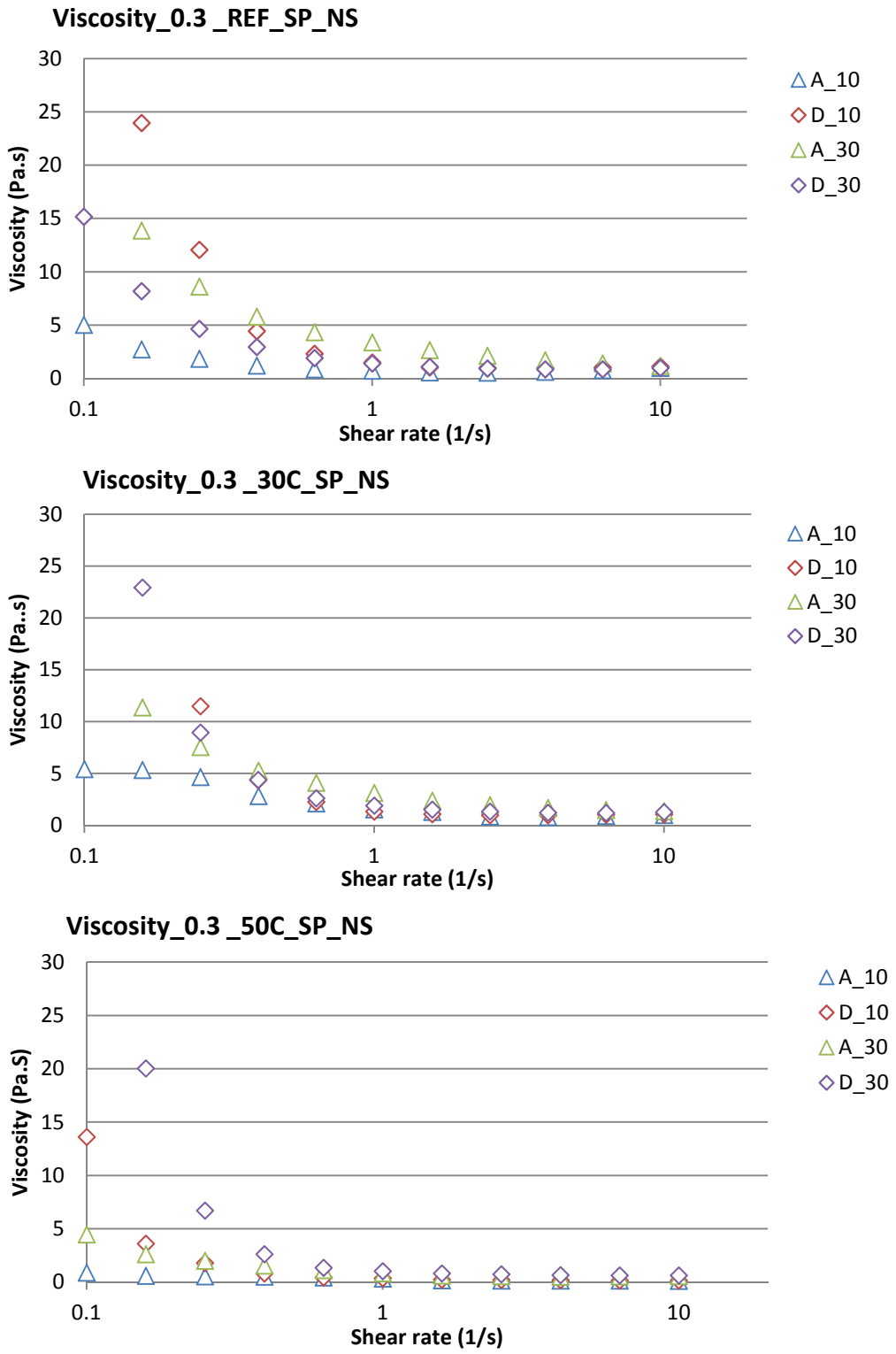

Figure 30. Viscosity vs. shear rate in cement paste W/CM = 0.3

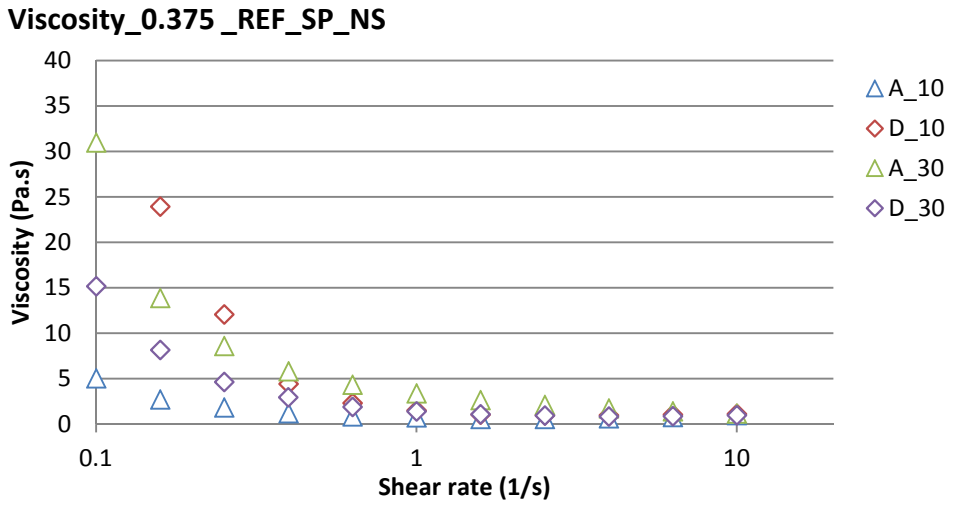

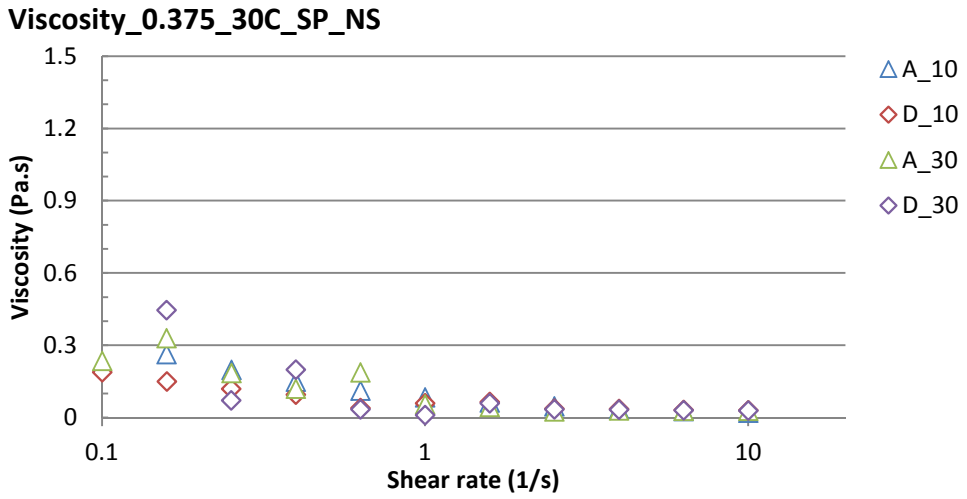

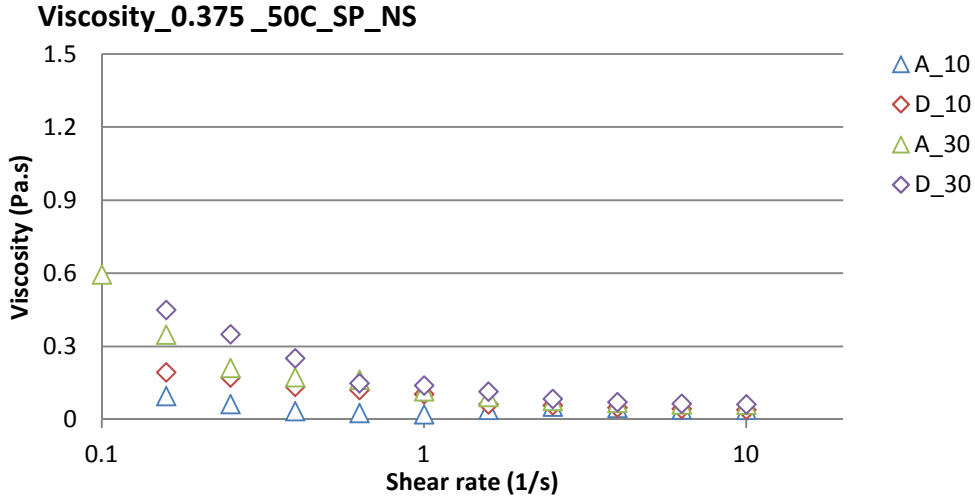

(b)

Figure 31. Viscosity vs. shear rate in cement paste W/CM=0.375

4.3. MORTARS: THE EFFECT OF SUPERPLASTICIZERS

4.3.1. Fresh Properties

Tests for flow and fresh density of mortars were used to determine the optimal dosage of chemical admixtures (expressed as a solid or "active" content, by the weight of the binder). The performance of chemical admixtures was compared with the properties of a reference mortar (Ref L1). Relevant ASTM standards were used for the evaluation of mortar flow (ASTM C 1437) and fresh density (ASTM C 138). The research results are reported in *Table 19* and *Table 20* and plotted in *Figure 32* and *Figure 33*. The superplasticizers were selected and recommended based on their flow and density performance in pastes and mortars. The HG7 (SNF) and HR1 (PCE) superplasticizers were selected for the use the DOT-grade concrete experiment due to their higher flow at lower dosage levels. The effect of reference RP8 plasticizer was similar to the performance of the superplasticizers, but, due to excessive air entrainment, at higher dosages the addition of RP8 drastically reduced the density of the mortar (*Table 20).*

Table 19. Effect of admixtures on flow of mortars

Chemical Admixtures	Flow, % at Admixture Dosage, %							
	0	0.05	0.1	0.15	0.2	0.3	0.4	0.5
Ref L1	26.5	-	-	-	-	-	-	-
HD1		-	-	45.5	54.0	57.4	61.8	62.9
HAC		-	52.4	60.4	66.3	71.0	-	-
HG7		56.1	68.9	73.4	-	-	-	-
HR1		-	-	49.6	55.8	65.9	70.5	-
RP8		-	38.2	60.6	76.7	-	-	-

Table 20. Effect of admixtures on fresh density of mortars (limiting value are selected)

Chemical Admixtures	Density, g/cm^3 at Admixture Dosage, %							
	0	0.05	0.1	0.15	0.2	0.3	0.4	0.5
Ref L1	2.297	-	-	-	-	-	-	-
HD1		-	-	2.202	2.129	2.076	2.071	2.061
HAC		-	2.153	2.142	2.121	2.070	-	-
HG7		2.155	2.128	2.092	-	-	-	-
HR1		-	-	2.202	2.160	2.129	2.106	-
RP8		-	1.990	1.974	1.971	-	-	-

Therefore, mortar tests can be effectively used to select or verify the optimal dosage of superplasticizers (e.g., 0.15% and 0.4% for HG7 and HR1, respectively). The dosage of mid-range plasticizing admixture must be limited to 0.15%, as a higher dosage may result in excessive air entrainment and the reduction in strength.

For the range of investigated compositions, there is a good correlation between the flow properties of pastes (mini-slump) and the flow of mortars (*Figure 34*). This indicates that using the mini slump test, the flow of mortars based on different cements and compatibility with admixtures can be predicted.

Mortars of the same compositions , but based on cements L1, L2 and H1 had a similar flow, and the use of cement S1 induced a reduced flow (possibly to higher fineness and higher C_3A content), as demonstrated by *Figure 35*. *S*imilarly to mini-slump performance, the flow of mortars was improved with the addition of SCM as reported in *Figure 36*.

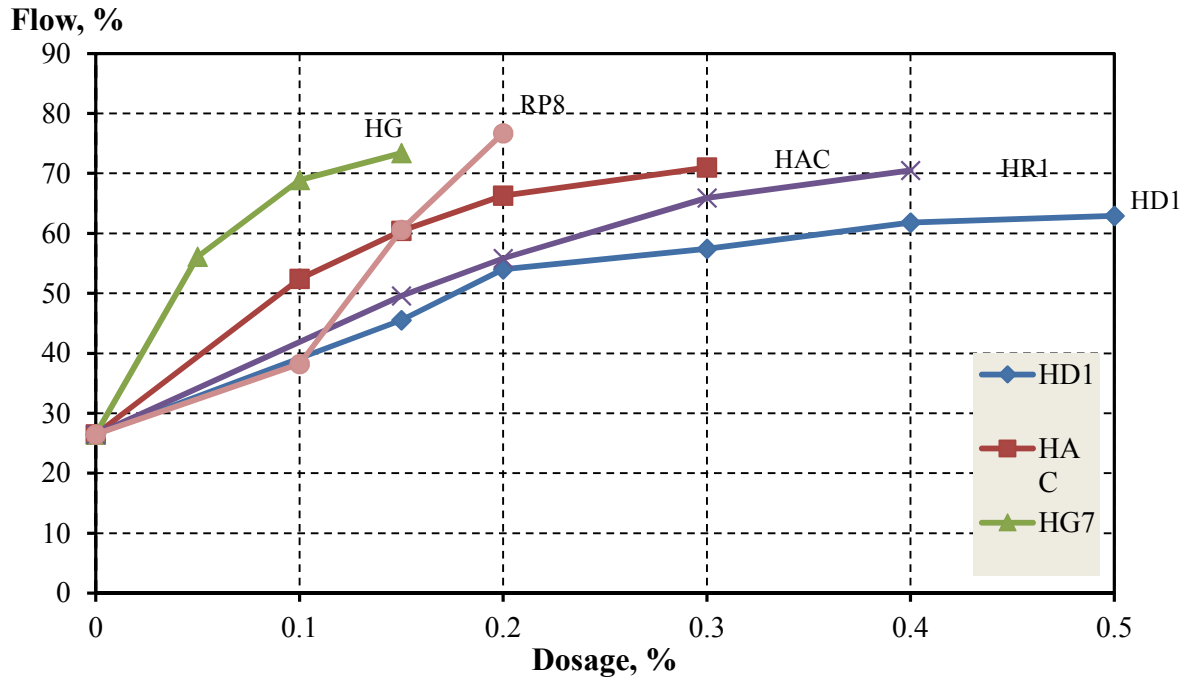

Figure 32. The effect of SNF (HR1 / HD1) and PCE (HAC / HG7) superplasticizers and mid-range water-reducer (RP8) on the flow of mortars

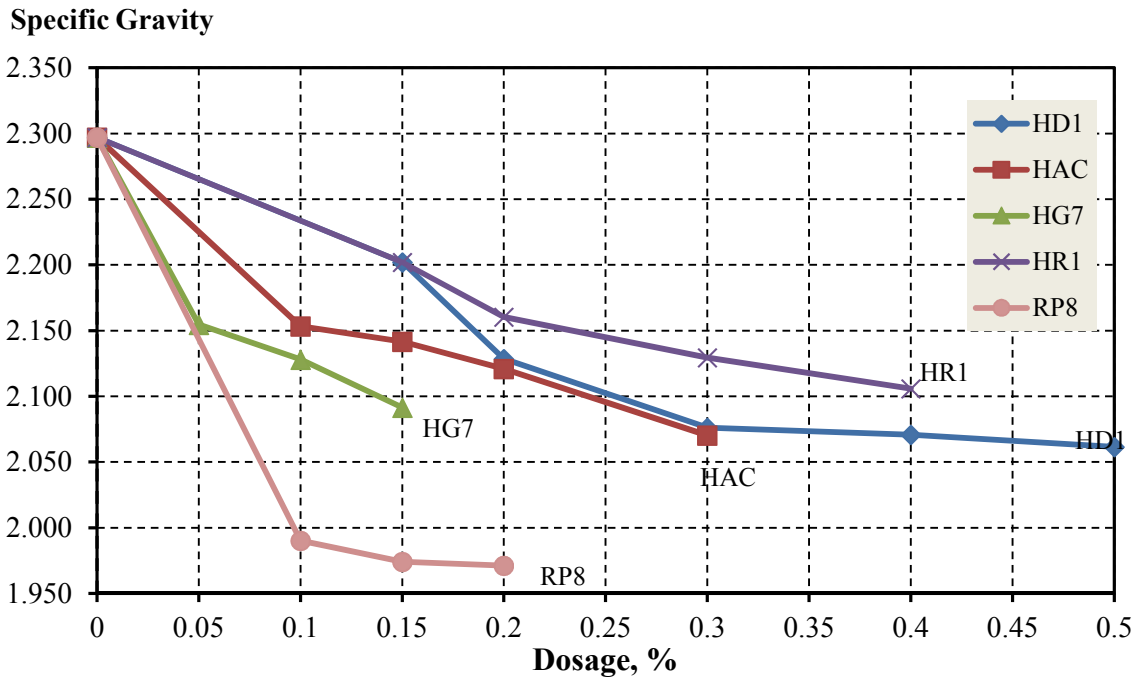

Figure 33. The effect of SNF (HR1 / HD1) and PCE (HAC / HG7) superplasticizers on the fresh density of mortars vs. mid-range water-reducer (RP8)

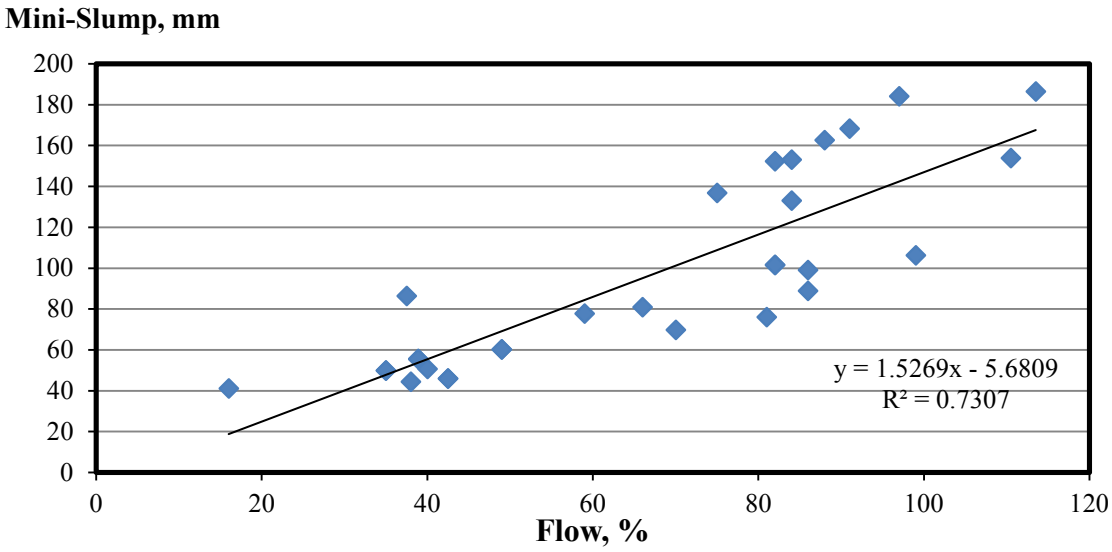

Figure 34. The correlation between the mini-slump of pastes and mortar flow

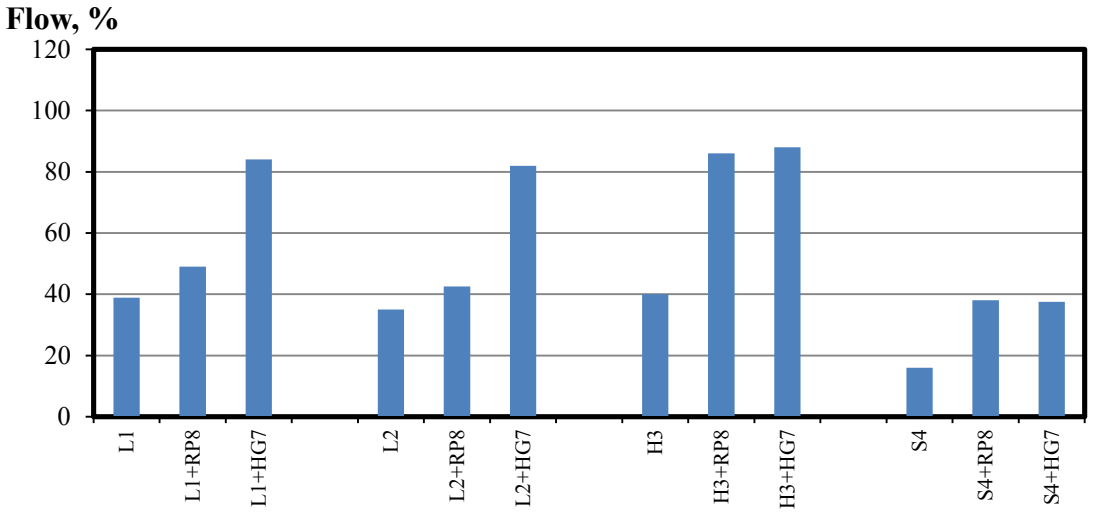

Figure 35. The effect of chemical admixtures on mortar flow

The best improvement was achieved in the systems with Class C fly ash, especially when combined with PCE (HG7) superplasticizers. The response of portland cement mortars with slag cement was very similar to reference portland cement systems modified with the corresponding admixture.

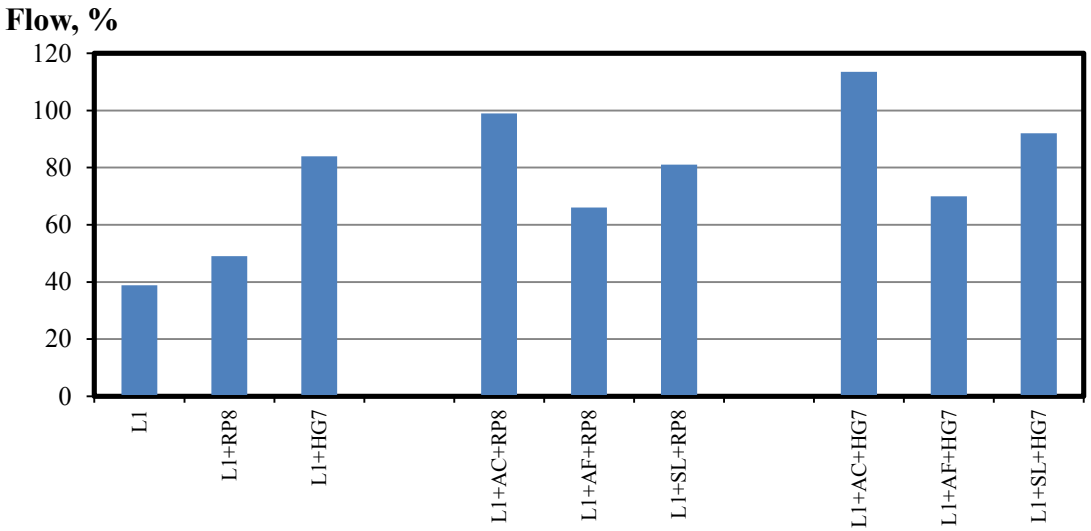

(a)

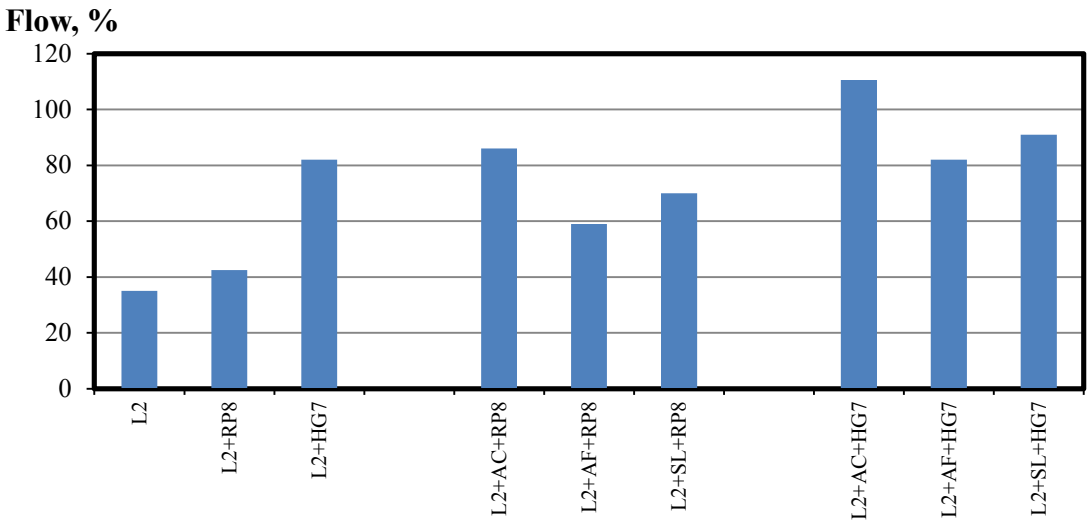

(b)

Figure 36. The effect of admixtures and SCMs on flow of mortars (based on cement L1 (a) and L2 (b)

In the systems with SCM, the relative flow enhancement was more significant when mid-range plasticizers were used. This can be explained by different absorption capacities of cements and SCM; therefore, cement replacement with SCM, which absorbs lower quantities of surfactants is equal to a relative increase in admixture dosage. In respect to this, in the systems

with SCM, the dosage of admixture can be reduced to avoid the overdose and potential delay in strength development (especially in the case of WR).

At the same time, in the case of synergy between the superplasticizer and SCM, no delay in the early strength is observed; and so, improved workability can be used to boost the strength of concrete (by reducing w/cm ratio) or to reduce the cementitious material content (at a constant w/cm ratio).

4.3.2. Mechanical Performance

The effect of chemical admixtures was evaluated by testing the compressive strength of mortars at different stages of hardening. The performance of selected admixtures is summarized in *Table 21* and further demonstrated by *Figure 37, Figure 38* and *Figure 39*.

Table 21. The effect of admixtures on the compressive strength of mortars (w/c=0.45)

Mix ID	Dosage, %	Compressive Strength, MPa (psi) at the Age of		
		3 days	7 days	28 days
Ref (L1)	-	18.4 (2669)	32.9 (4772)	36.8 (5337)
RP8 (0.1%)	0.1	18.0 (2611)	22.3 (3234)	26.7 (3873)
RP8 (0.15%)	0.15	18.9 (2741)	25.7 (3727)	30.6 (4438)
RP8 (0.2%)	0.2	14.8 (2147)	22.9 (3321)	31.7 (4598)
HR1 (0.15%)	0.15	28.5 (4134)	31.1 (4511)	39.5 (5729)
HR1 (0.2%)	0.2	24.0 (3481)	29.3 (4250)	34.9 (5062)
HR1 (0.3%)	0.3	20.7 (3002)	29.9 (4337)	39.5 (5729)
HR1 (0.4%)	0.4	20.8 (3017)	29.6 (4293)	38.3 (5555)
HG7 (0.05%)	0.05	20.8 (3017)	29.3 (4250)	38.7 (5613)
HG7 (0.1%)	0.1	27.0 (3916)	37.8 (5482)	44.8 (6498)
HG7 (0.15%)	0.15	33.1 (4801)	37.1 (5381)	41.2 (5976)
HG7 (0.2%)	0.2	23.6 (3423)	30.4 (4409)	36.2 (5221)

It can be observed that the use of plasticizing admixture RP8 results in a reduction of strength at 7 and 28 days of hardening. Surprisingly, the 3-day strength of these mortars was very similar to the strength of the reference L1, as reported by *Figure 37*. The plasticizing effect of RP8 was very impressive, especially at increased dosages; however, due to early-age strength reduction, the effective dosage of RP8 must be kept to the lowest tested. The 28-day strength of mortars with RP8 was 20% lower than reference (*Table 21*).

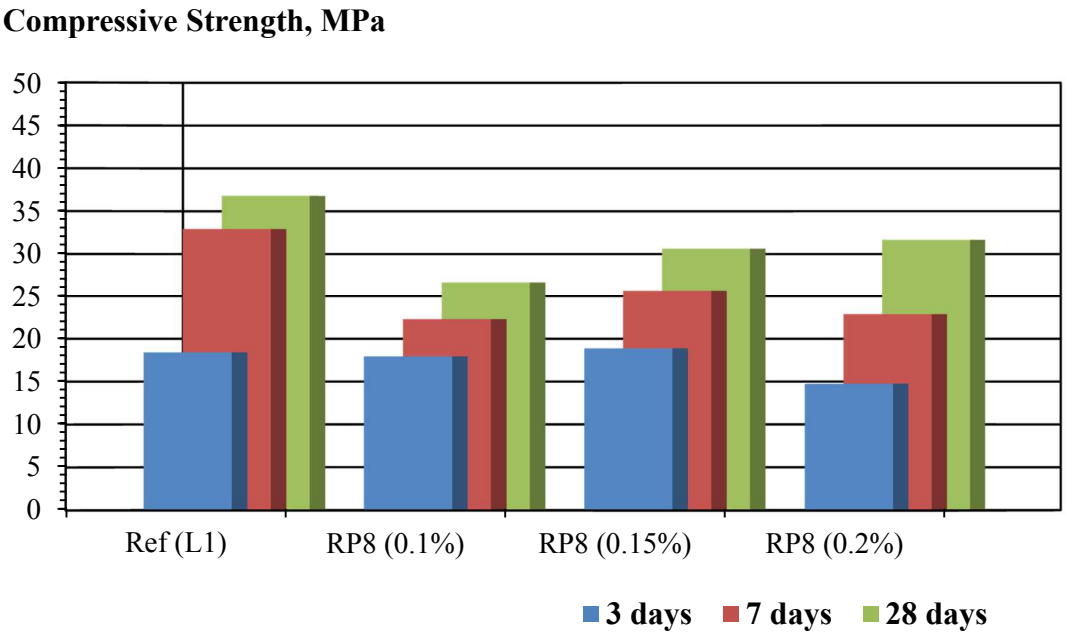

Figure 37. Compressive strength of mortars with mid-range water-reducer (RP8)

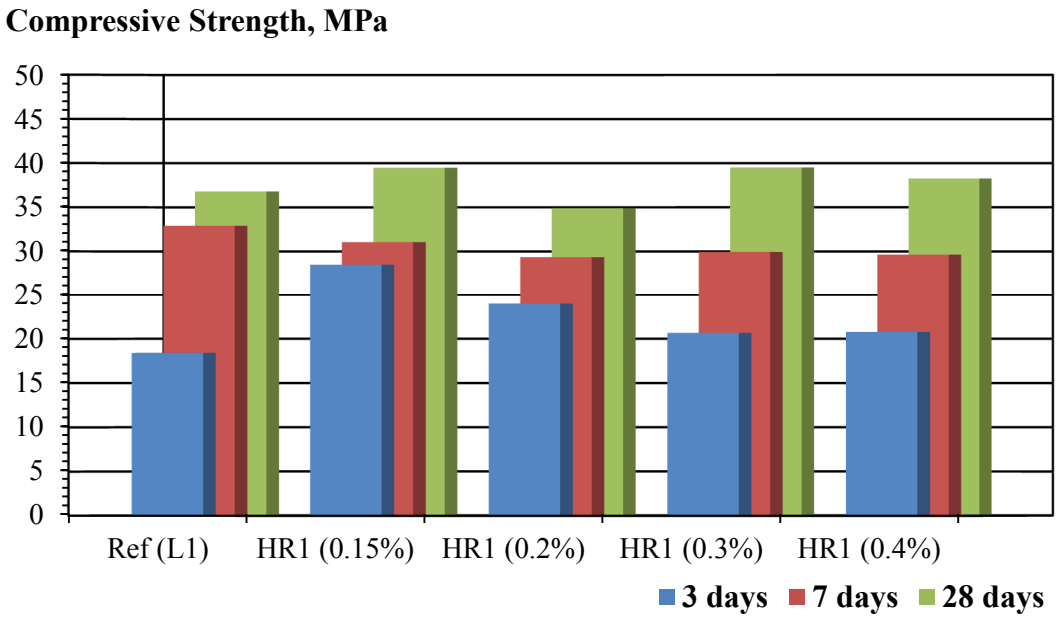

Figure 38. Compressive strength of mortars with SNF superplasticizer (HR1)

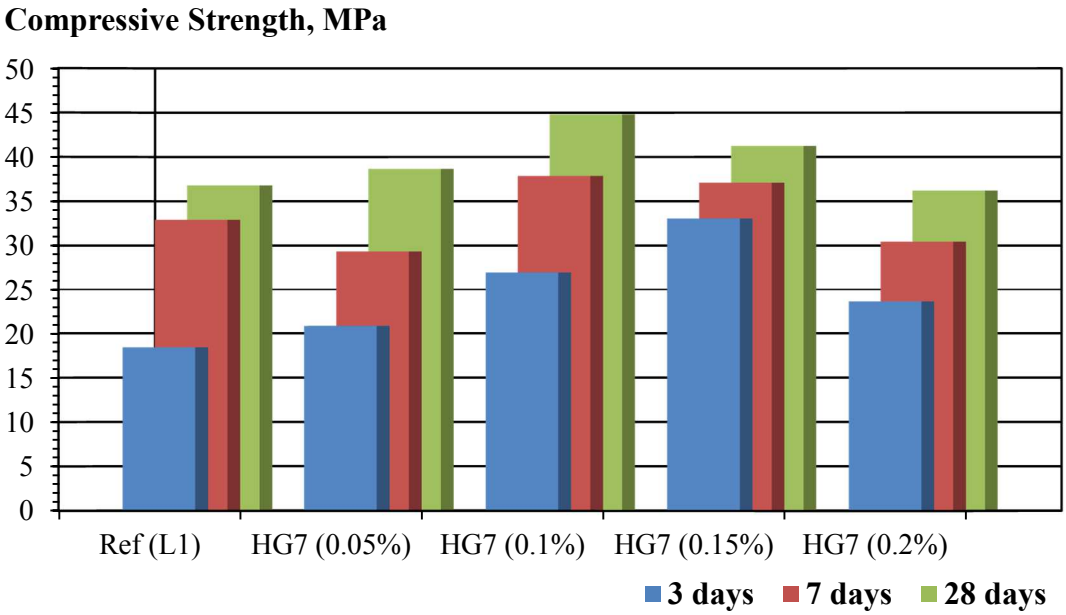

Figure 39. Compressive strength of mortars with PCE superplasticizer (HG7)

At the age of 7 and 28 days, the strength of SNF modified mortars was similar to that of reference mortars, suggesting that tested admixture dosage range of 0.15% to 0.4% was robust

and applicable for investigated binding systems. A significant increase of 3-day strength was observed at the SNF dosage of 0.15%: 28.5 MPa vs. 18.4 MPa for reference plain mortar. This effect diminished at higher SNF dosages (up to 0.4%). In this way, SP can be used in the portland cement systems to achieve the desired response. Practically, a higher SP dosage can be used for reduction of W/C and, therefore, to boost the strength at all ages of hardening.

The PCE superplasticizer demonstrated very exceptional performance in mortars based on L1 cement (*Figure 39*): at the same W/C ratio, the mortars with HG7 had a 28-day compressive strength of 44.8 MPa vs. 36.8 MPa observed for reference plain mortar. The 3-day compressive strength of mortars with 0.15% of HG7 was 33.1 MPa vs. 18.4 MPa of reference plain mortar. This beneficial response can be correlated to observations on accelerated hydration and higher released heat of these systems (*Figure 43*).

4.3.3. The Effect of SCM

The test results related to the effects of SCM and strength of mortars based on L1 and L2 cements are reported in *Table 22* and *Figure 40*. It can be observed that the use of SCM results in a reduction of 3- and 7- day compressive strength, which was considerable for Class F fly ash and slag cement mortars produced using cement L1 and plasticizer RP8 . However, L2 cement provided a better compatibility with SCM and chemical admixtures used.

Table 22. Compressive strength of mortars designed with different SCM

Mortar Mix ID	Flow, %	Compressive Strength, MPa (psi) at the Age of		
		3 days	7 days	28 days
L1	39	19.1 (2770)	21.9 (3176)	25.9 (3756)
L1+RP8	49	20.3 (2944)	23.9 (3466)	28.4 (4119)
L1+HG7	84	26.3 (3814)	32.9 (4772)	38.7 (5613)
L1+AC+RP8	99	10.3 (1494)	21.2 (3075)	27.9 (4308)
L1+AF+RP8	66	10.4 (1508)	15.6 (2263)	24.7 (3582)
L1+SL+RP8	81	7.5 (1088)	12.7 (1842)	19.1 (2770)
L1+AC+HG7	114	14.5 (2103)	20.4 (2959)	31.5 (4569)
L1+AF+HG7	70	13.5 (1958)	15.4 (2234)	25.4 (3684)
L1+SL+HG7	92	15.2 (2205)	24.0 (3481)	32.6 (4728)
L2	35	20.6 (2988)	26.2 (3800)	28.1 (4075)
L2+RP8	47	23.2 (3365)	31.2 (4525)	34.4 (4989)
L2+HG7	81	27.9 (4046)	32.1 (4656)	42.3 (6135)
L2+AC+RP8	86	17.2 (2495)	23.3 (3379)	37.7 (5468)
L2+AF+RP8	59	16.0 (2321)	18.4 (2669)	30.4 (4409)
L2+SL+RP8	70	13.9 (2016)	24.9 (3611)	38.2 (5540)
L2+AC+HG7	111	20.4 (2959)	26.3 (3814)	35.9 (5207)
L2+AF+HG7	82	18.3 (2654)	22.2 (3219)	29.6 (4293)
L2+SL+HG7	91	24.1 (3495)	23.5 (3408)	39.0 (5656)

At the age of 28 days, the compressive strength of mortars with SCM was comparable to the properties of corresponding portland cement mortar. However, considerable reduction of 28-day strength was observed for L1-SCM based mortars combined with plasticizer RP8; in this group (with RP8), only Class C fly ash mortars had demonstrated the strength levels comparable to portland cement systems. The performance of RP8 in L2-SCM based mortars was better (vs. L1-SCM mortars), resulting in a 28-day strength comparable to that of the reference portland cement mortars with RP8 (*Figure 40*).

The use of Class C fly ash and slag cement in mortars with plasticizing or superplasticizing admixtures was very effective, as supported by 28-day strength results. Class F fly ash resulted in a considerable reduction of early strength and, actually, reduced the strength at

all ages of up to 28 days. Due to ongoing pozzolanic reactions, the strength of mortars with Class F fly ash can potentially be improved longer periods of hardening.

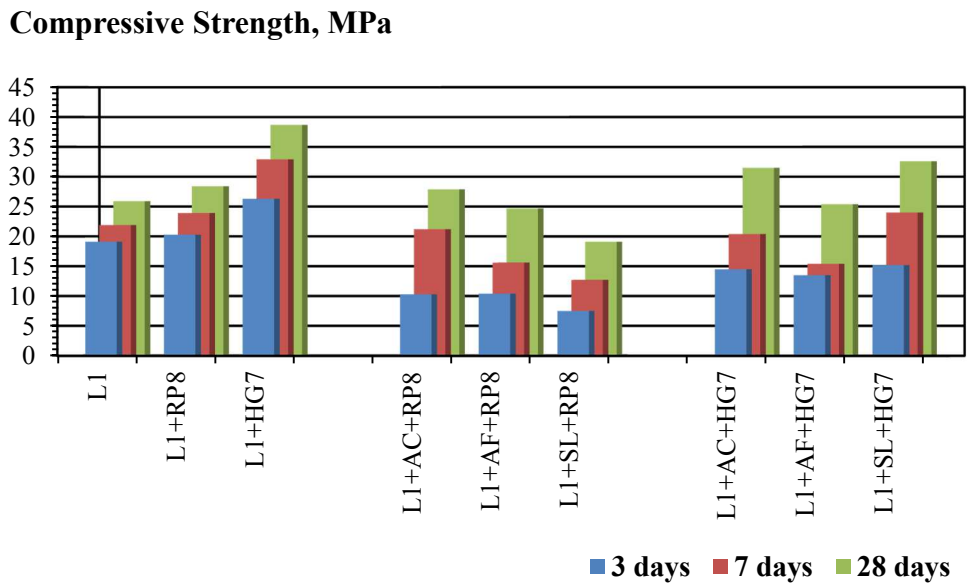

(a)

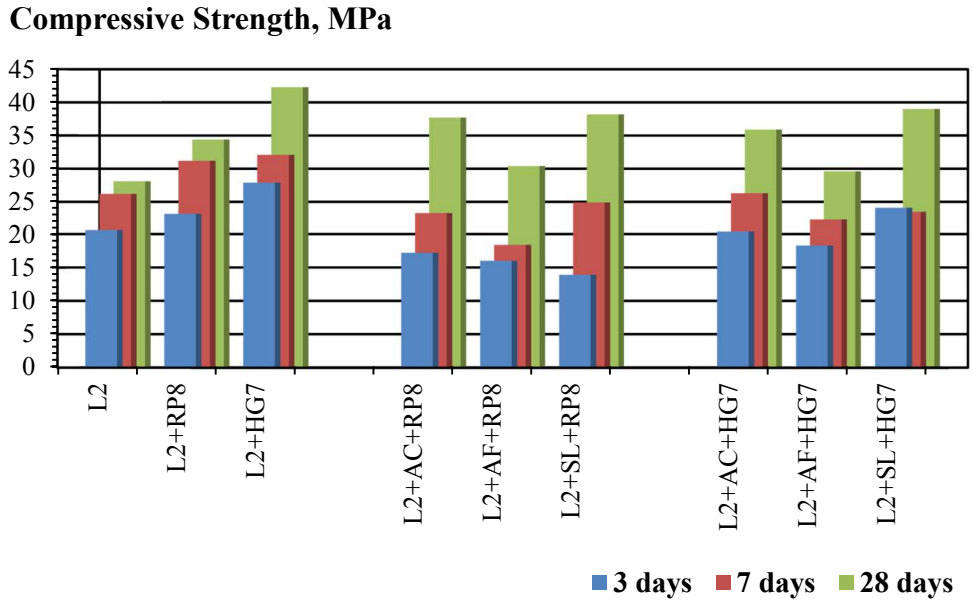

(b)

Figure 40. The effect of SCM on strength of mortars based on cement L1 (a) and L2 (b)

4.3.4. Heat of Hydration

The performance of selected plasticizing (RP8) and superplasticizing (HR1/ HG7) admixtures was investigated and compared to a reference mortar using the parameters of the hydration process detected by isothermal calorimeter. For this study, mortars based on portland cement L1 were monitored for the early hydration period of 48 hours. The observed effects are represented by *Figure 41*, *Figure 42* and *Figure 43* reporting on the of RP8, HR1 and HG7 admixtures, respectively.

It can be observed that all admixtures slightly delay the hydration as demonstrated by the 3- to 3.5- hour shift of the C_3S hydration peak and about 2- hour extension of the dormant period. Still these minor delays can be considered as positive, reducing slump loss and enabling to preserve the workability while in transit to the jobsite. With the addition of admixtures, the intensity of the main exothermal peak was reduced, possibly because of selective action of the admixtures, delaying the hydration of C_3A by about 7.5 hours, so the 2nd peak (corresponding to C_3A) appears at the heat flow curves.

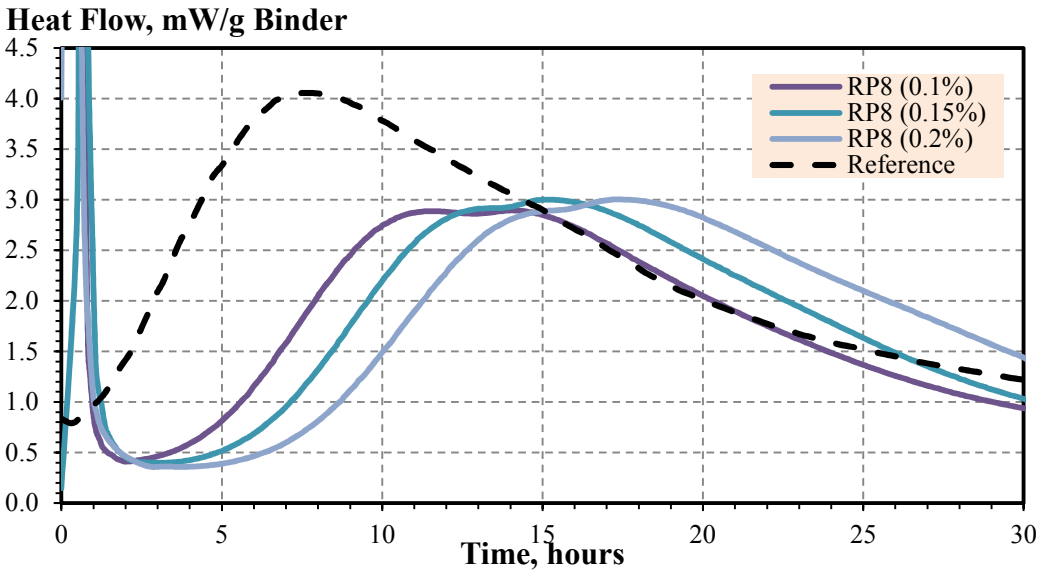

Figure 41. The effect of mid-range water-reducing admixture (RP8) on cement hydration

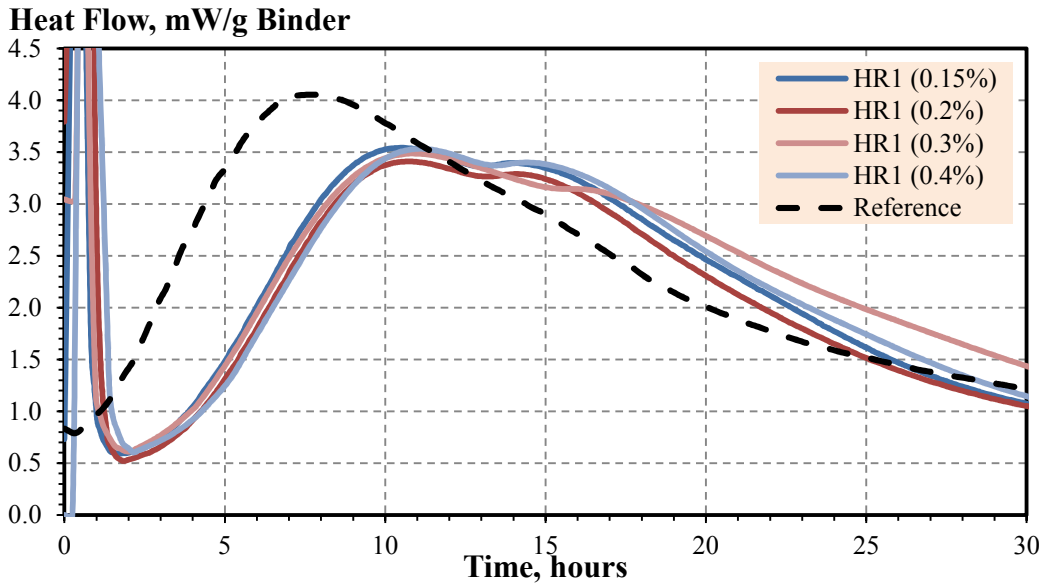

Figure 42. The effect of SNF (HR1) admixture on cement hydration

The heat flow curves can be used to confirm the decision on optimal dosage of admixture. It can be observed that an increment of RP8 as small as 0.05% (by weight of cement), e.g., from 0.1% to 0.15%, can result in a significant delay of cement hydration associated with a potential reduction of strength, especially, at the early age of 1 to 3 days.

It can be confirmed that the addition of SNF superplasticizer (HR1) at the dosage from 0.15% to 0.4% has no significant effect on the heat of hydration. Therefore, this admixture can be used within this entire tested range.

The addition of PCE superplasticizer (HG7) at a dosage of 0.15% (of cement weight) results in a considerable increase of the heat responses associated with C_3A and C_3S, suggesting that 0.15% dosage intensifies the hydration. However, a further increase of SP to 0.2% results in a reduction of the heat flow, suggesting a delay in hydration (due to overdose). Therefore, 0.15% was suggested to be the optimal dosage of HG7 in cement systems based on L1 cement. These observations are commonly verified by strength testing.

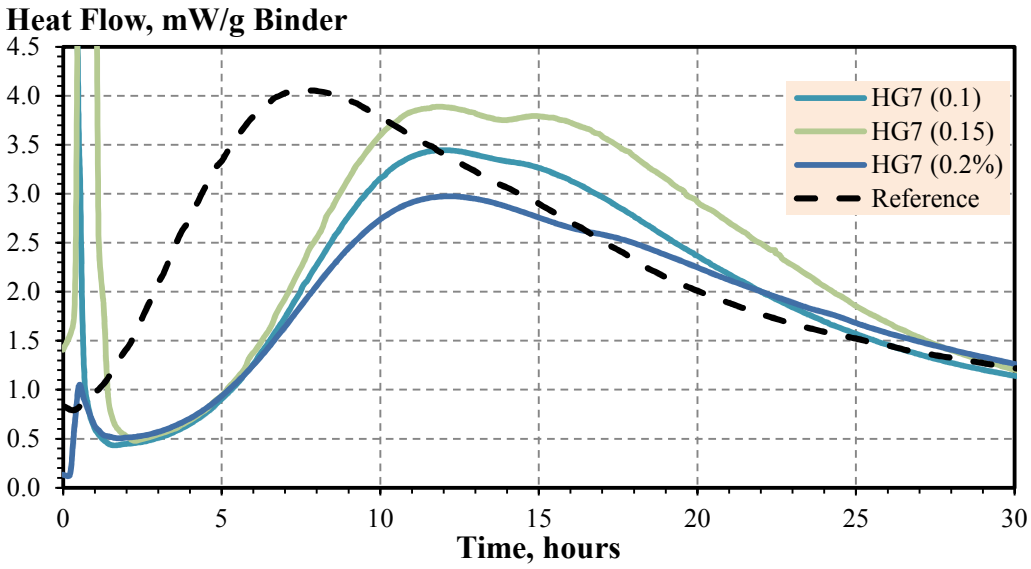

Figure 43. The effect of PCE (HG7) admixture on cement hydration

4.4. INCORPORATION OF NANOSILICA

4.4.1. Use of Cembinder Grade Nanosilica

The main purpose of research was to investigate the effect of nanosilica materials such as Cembinder 8 and Cembinder 50 on the properties of concrete. Nanosilica is the key component of HPC/SCC which can affect the flow, density, heat of hydration and compressive strength of portland cement systems.

Heat of Hydration

The Cembinder additives were used at different dosages and properties of nano-engineering mortars were compared with the performance of reference portland cement mixtures. Cembinder additives were added to mortar as cement replacement to determine the heat of hydration, flow and compressive strength. The effect of Cembinder can be determined by monitoring the isothermal hydration during early periods of hardening. The heat of hydration was measured by monitoring the rate of heat realized as plotted in *Figure 44* and *Figure 45*.

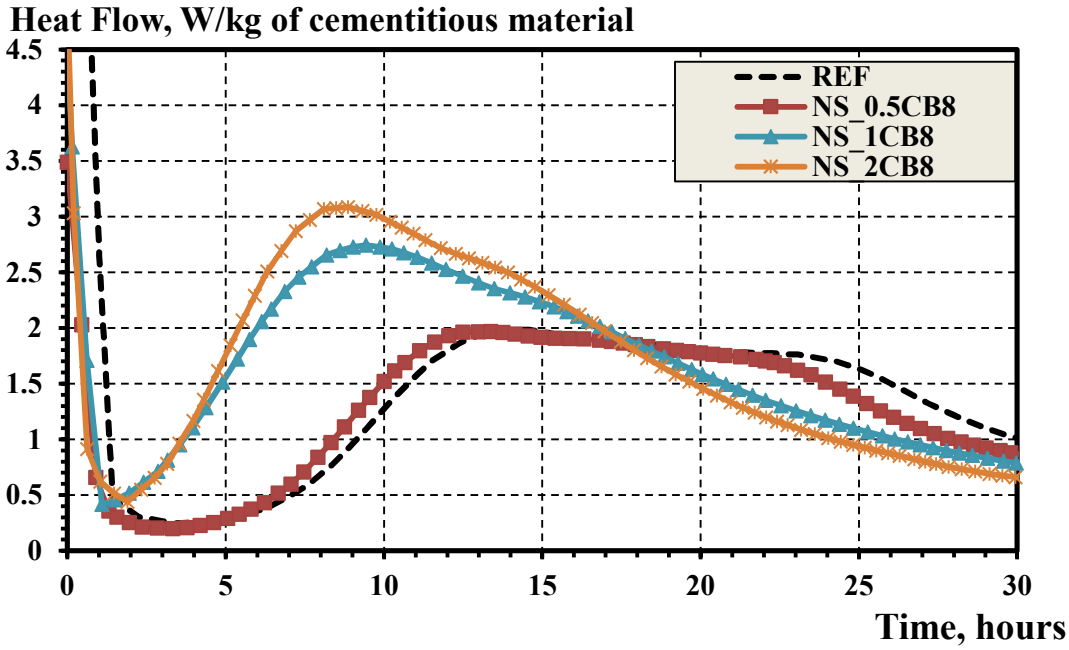

Figure 44. Effect of cembinder 8 on heat of hydration of cement mortars

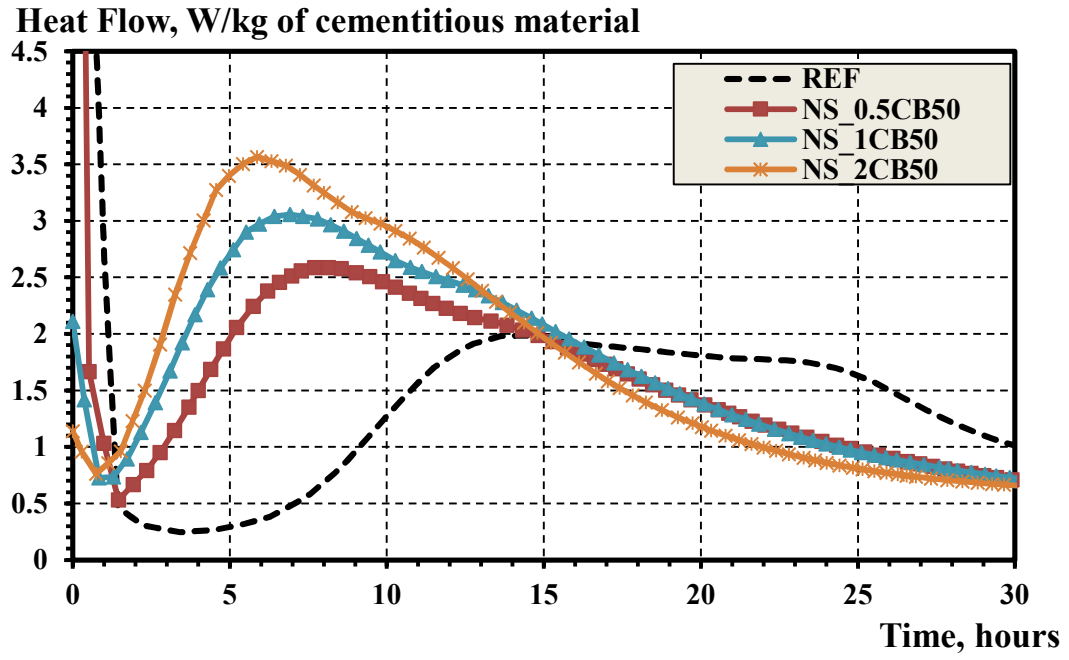

Figure 45. Effect of cembinder 50 on heat of hydration of cement mortars

It can be observed that the addition of Cembinder 8 at a dosage of 0.5%, 1% and 2% (by weight), reduces the setting time by 4-5 hours and increases the hydration heat by 1.0 W/kg flow

compared with the reference. The use of Cembinder 50 at a dosage of up to 2% (by weight) decrease the setting time by 6-10 hours and increases the heat flow by 1.5 W/kg.

Table 23. Properties of investigated binders

ID	Setting Time					Maximal Heat Flow			
	Initial		Final		Diff	C_3S		C_3A	
	hours	min	hours	min	min	Heat, W/kg	Time, hours	Heat, W/kg	Time, hours
REF	3.5	210	8.2	492	282	1.9	11.7	1.7	24
NS_0.5CB8	3	180	7.5	450	270	1.7	23	1.6	22
NS_1CB8	1.1	66	5.5	330	264	2.7	9.4	2.1	16
NS_2CB8	1.8	108	4.9	294	186	3.1	8.5	2.5	14.3
NS_0.5CB50	1.5	90	4	240	150	2.6	8.1	2	14.3
NS_1BCB50	0.75	45	3.3	198	153	3	6.4	2.1	14
NS_2CB50	0.74	44.4	3.1	186	141.6	3.5	6.3	2.8	10.7

Increasing the dosage of colloidal nanosilica (Cembinder 8 and Cembinder 50), leads to acceleration of the hydration process in cement systems. Fresh mortars based on Cembinder 8 had increased flow compared to the reference. However, further increase in the dosage of Cembinder 50 results in the decreased flow (*Figure 46*).

From the above results, it can be concluded that combining Cembinder and SP can improve the mechanical performance. The distribution of nanosilica particles within the cement matrix has an important role and is a key factor to enhance the performance. For Cembinder 50, with higher surface area (179.4 m^2/g vs. 61.2 m^2/g for Cembinder 8), the addition of nanosilica reduces the free flow and flow due to enhanced cohesion between the particles.

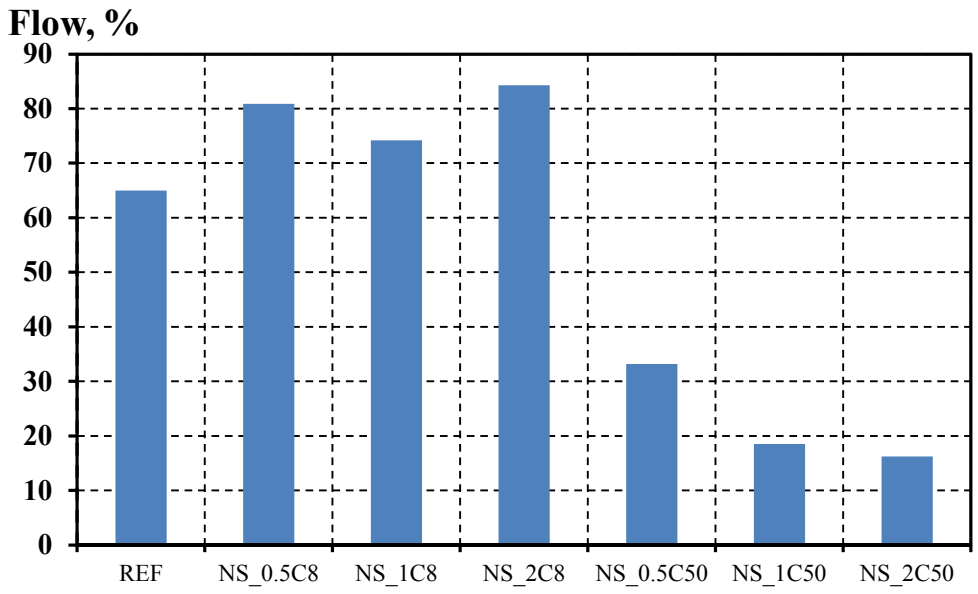

Figure 46. The dosage and type of nanoparticles on mortar flow

Compressive Strength

Figure 47 reports on the compressive strength of mortars with Cembinder as compared to the reference.

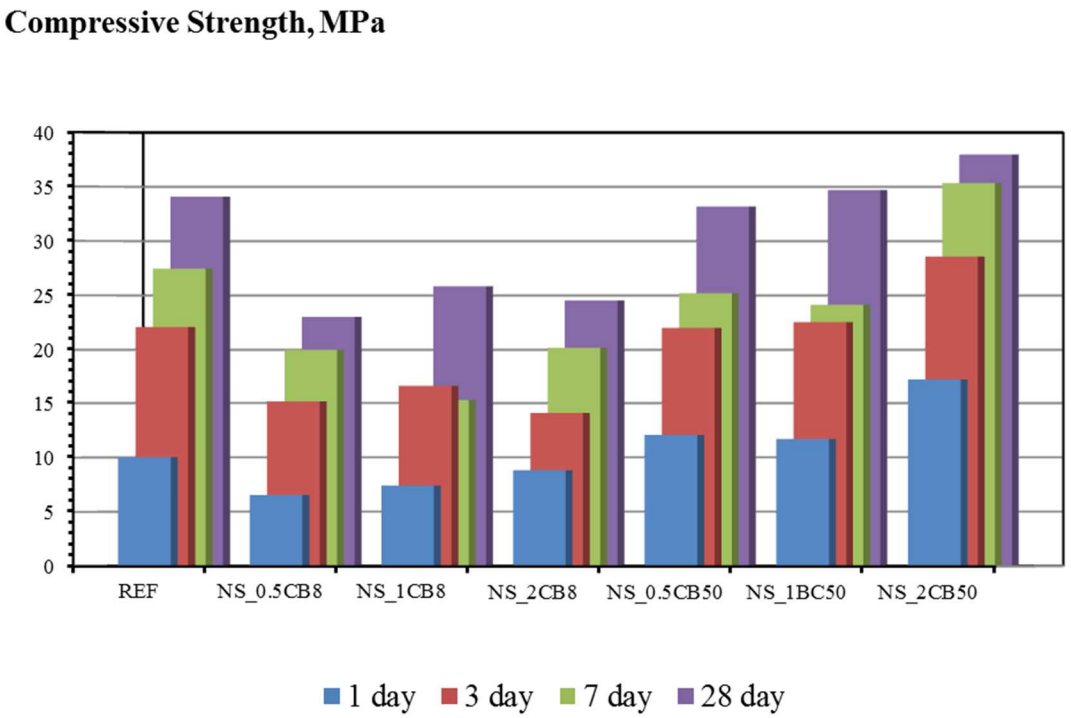

Figure 47. Dosage and type of nanoparticles in mortar compressive strength

It can be observed that increasing the dosage of Cembinder 8 resulted in the reduction of compressive strength at different ages of hardening compared to reference**.** In the case when Cembinder 50 was used, the acceleration of early-age strength development was observed, and considerable improvement of performance was found at the dosage of 2%. However, due to high cost, the optimal nanosilica dosage must be less than 1%. Therefore, lower dosage of nanosilica must be used in mortars with activated fly ash.

4.4.2. The Effect of SP on Hydration and Strength of Mortars with SCM

The effect of superplasticizer (PCE MP40, high range water reducer) on the performance of portland cement and blended (30% of fly ash) mortars with 0.25% of nanosilica was evaluated. The composition and performance of investigated blends are reported in *Table 24.*

Table 24. The effect of PCE MP40 superplasticizer on performance of mortars with nanosilica

Mix ID	Fly Ash, %	W/CM	S/CM	SP,%	Nano SiO_2, %	Flow, %	Setting Time, minutes		Compressive Strength (MPa)		
							Initial	Final	1-day	7-day	28-day
R_0.1%SP	0	0.3	1	0.15	0.25	77	38	142	42.6	77.9	92.0
R_0.15%SP	0	0.3	1	0.15	0.25	131	42	165	47.2	86.7	99.9
R_0.2%SP	0	0.3	1	0.2	0.25	139	60	195	55.7	89.7	102.6
R_0.25%SP	0	0.3	1	0.25	0.25	>140	70	233	47.4	74.4	76,0
0.1%SP	30	0.3	1	0.15	0.25	>140	126	255	22.2	43.9	83.7
0.15%SP	30	0.3	1	0.15	0.25	>140	156	321	32.6	63.4	79.8
0.2%SP	30	0.3	1	0.2	0.25	>140	180	378	34.9	73.9	100.4
0.25%SP	30	0.3	1	0.25	0.25	>140	216	355	29.7	63.4	87.2

Based on the preliminary experimental results, it is obvious that the dosage of superplasticizer must be limited to 0.2%, as a higher dosage may provide a delay in hydration and overall reduction in strength. However, higher SP dosage maybe required for effective dispersion of nanosilica with high surface area. Notably, the flow of mortars was improved with

the addition of fly ash as presented in the *Table 24*. Superplasticized mortars with 30% of class C fly ash had a considerable increase of flow to >140% (exceeding the diameter of flow table) which may suggest excellent workability in concrete and, especially, applicability in SCC. At the same time, due to the synergy between the superplasticizer and SCM, no delay in strength development was observed; and so, improved workability can be used to boost the strength of concrete (by reducing W/C ratio) or to reduce the cementitious material content (at a constant W/C ratio). Because of this effect, the W/CM in concrete with fly ash can be reduced.

The use of increased dosages of superplasticizer (SP) results in the retardation of cement hydration and the reduction of released heat. The use of significant amounts of SP, more than 0.2% (of cement by weight) may result in slight extension of the dormant period and the delay of acceleration phase for few hours. However, the heat of hydration of cement systems with SP dosage of 0.25% was found to be higher than for mortars with 0.15% and 0.2% of SP, possibly due to incorporation of nanosilica and better dispersion of cement grains, *Figure 48*.

The hydration kinetics of blended cement with class C fly ash and nanosilica at various SP dosages is analyzed in *Figure 49*. It can be observed that at low SP dosage (0.1%) the addition of fly ash reduces the total heat in proportion to the fly ash content as no pozzolanic activity of fly ash during the first hours of hydration is expected.

The extension of dormant period was proportional to the dosage of SP and the slop of the heat flow curve was reduced due to the use of fly ash. The increased dosage of superplasticizer (SP) results in the retardation of cement hydration and the reduction of the heat released. However, the heat of hydration for system with 0.25% of SP was higher when compared to blends with lower SP, possibly due to better dispersion.

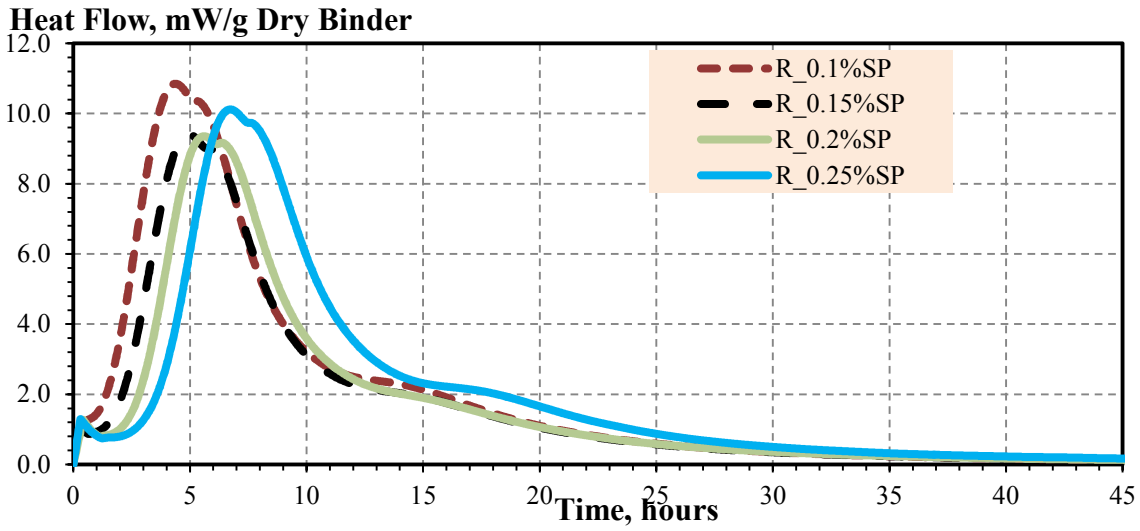

(a)

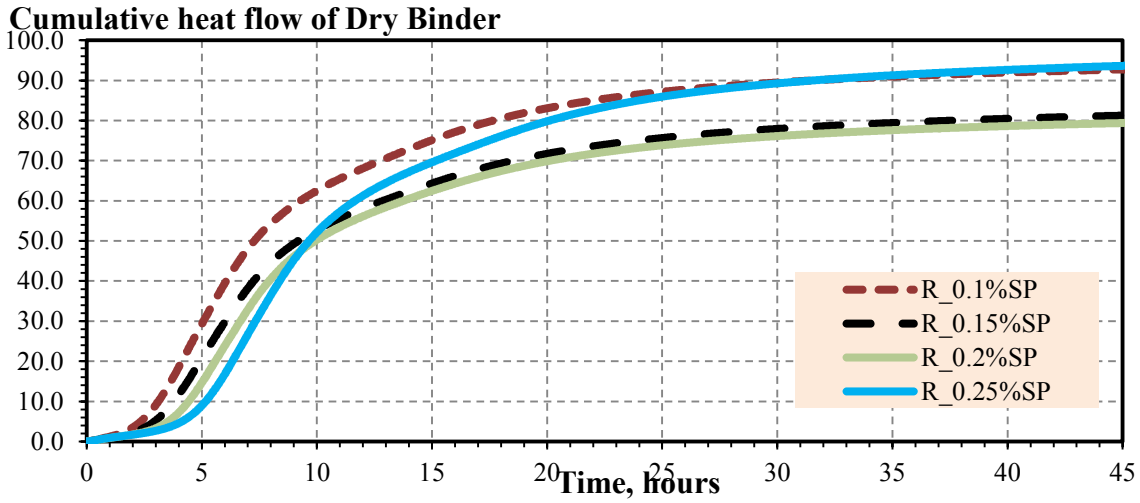

(b)

Figure 48. The effect of SP dosage on cement hydration a) heat flow, b) cumulative heat

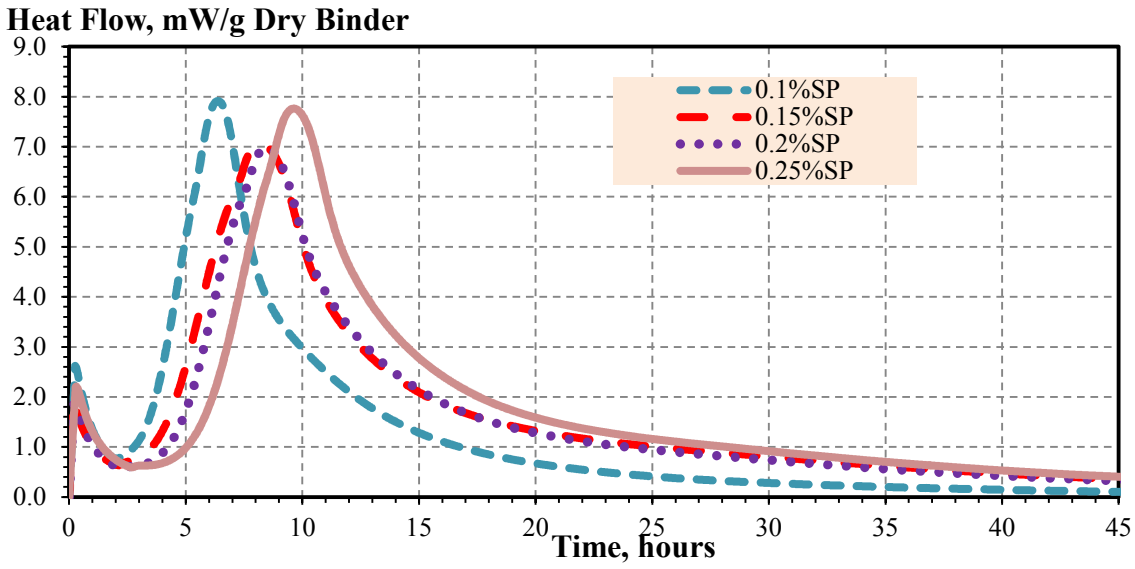

(a)

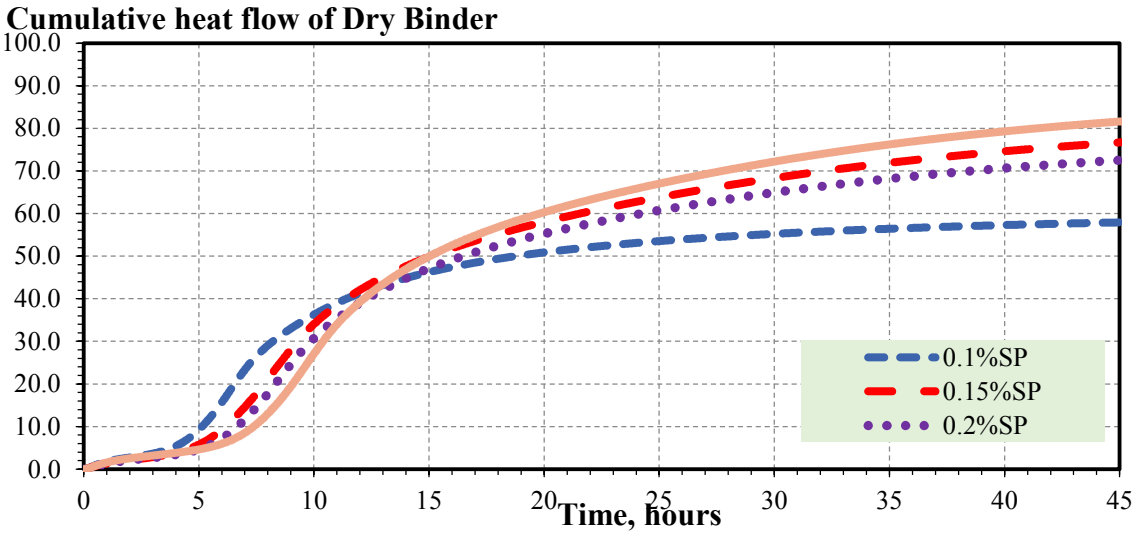

(b)

Figure 49. The effect of SP dosage on the hydration of blended cement with class C fly ash and nanosilica. a) heat flow, b) cumulative heat

The compressive strength of mortars with different SP dosages is reported in *Figure 50*. For all ages the highest compressive strength was achieved at a SP dosage of 0.2%. Incorporation of fly ash at 30% and the use of optimal SP dosage resulted in the mortars of

similar 28-day strength of 100.4 MPa vs. 102.6 MPa, the strength of reference mortar. However, the use of fly ash resulted in the reduction of 1- and 7-day strength, *Table 24.*

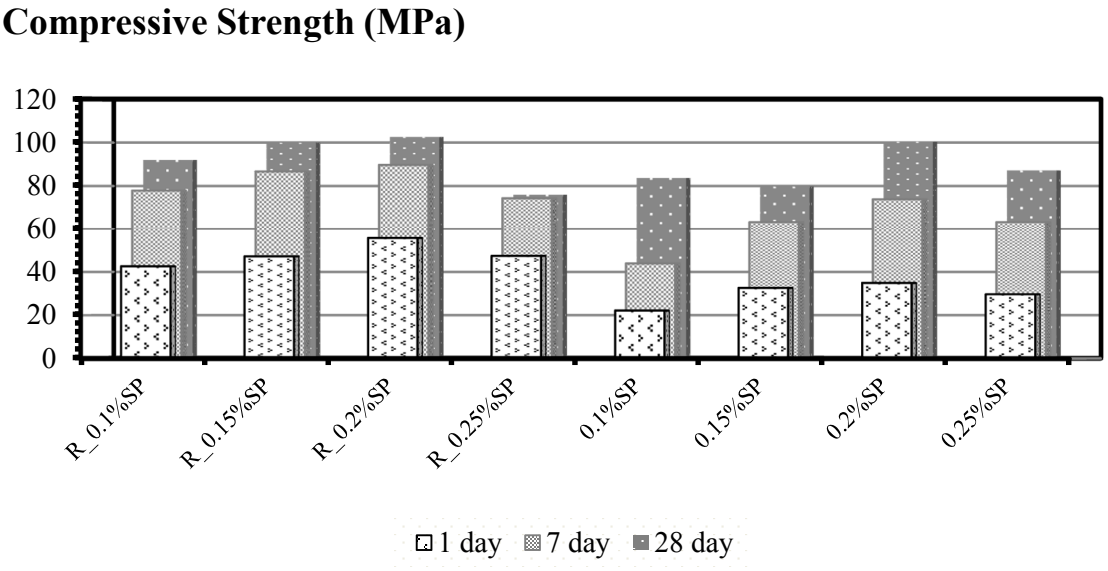

Figure 50. The effect of SP dosage on the compressive strength of mortars

4.4.3. The Effect of Nanosilica Derived from Hydrothermal Solutions

Properties of Fresh Mortars

The flow of mortars was determined for all mixtures and reported in Table 4. The reference material (Ref) had the highest flow among all tested mortars. The addition of well dispersed nano-SiO_2 at low dosage (0.25%) had a significant impact on the rheological response of fresh mortars. Commercially available nano-SiO_2 (CB8), which is commonly used as a viscosity modifying agent, had the lowest surface area (*Table 8).* However, the nanoparticles of CB8 are well dispersed and demand higher volumes of water to achieve the required levels of workability. Therefore, at the same W/C, the addition of CB8 reduces the flow of mortar.

Powder particles TB had the least impact on the flow, most probably due to the lowest surface area. The N2 had the highest flow reduction compared with the rest of the nanosilica

products. The high surface area and a higher degree of agglomeration as well as insufficient dispersion may be the causes for the flow reduction in N2 based mortars. A moderate effect was observed in the case of nanosilica sol (MB) material. It was expected that MB would have the highest impact on the flow due to its highest surface area.

The research results indicate that the addition of nano-SiO_2 increases the cohesiveness and reduces the bleeding and segregation in portland cement based systems. The source type, the impurities, crystallinity and agglomeration of nanosilica particles are the possible causes affecting the rheological properties and flow of mortars. Therefore, to keep the specified workability levels in the systems with nano-SiO_2, the dosage of superplasticizer can be increased.

Hydration of Mortars

The effects of hydrothermal nanosilica products such as TB, N2 and MB on the hydration of mortars was analyzed by monitoring the heat of hydration with an isothermal calorimeter using a reference mix for comparison (*Figure 51*). The isothermal calorimetry responses were used to determine the setting times and heat released during the hydration (*Table 25*).

The first (C_3S) and second (C_3A) peaks for the reference system and mortars with CB8 were observed at 10.5 and 14 hours after mixing, respectively with C_3A characterized by a lower heat flow.

Table 25. The Effect of Nano-SiO_2 on Hydration of Mortars

Mix ID	Flow %	Setting Time , min		Max Heat Flow				Hydration Energy, J/g	
				C_3S		C_3A			
		Initial	Final	Heat, mW/g	Time, hours	Heat, mW/g	Time, hours	24 h	Total
Ref	95	102	408	3.90	10.5	3.43	13.7	126	170
CB8	79	132	420	3.90	10.7	3.33	14.4	130	170
MB	83	102	396	3.77	10.8	4.14	12.9	132	175
TB	93	150	420	3.66	11.3	3.36	14.8	126	166
N2	71	132	384	4.12	10.3	3.75	13.8	142	178

The addition of powder nano-SiO_2 products (such as N2 and TB) had a considerable effect on the heat of hydration. Specifically, N2 nanoparticles had a profound increase of heat of hydration (HOH).

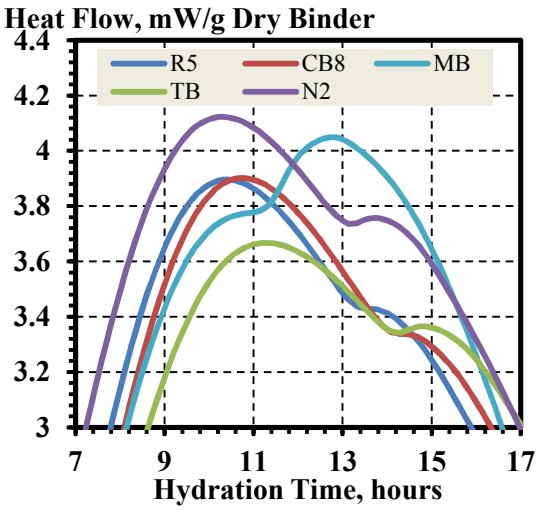

Figure 51. The effect of SiO_2 nanoparticles on the heat flow of mortars

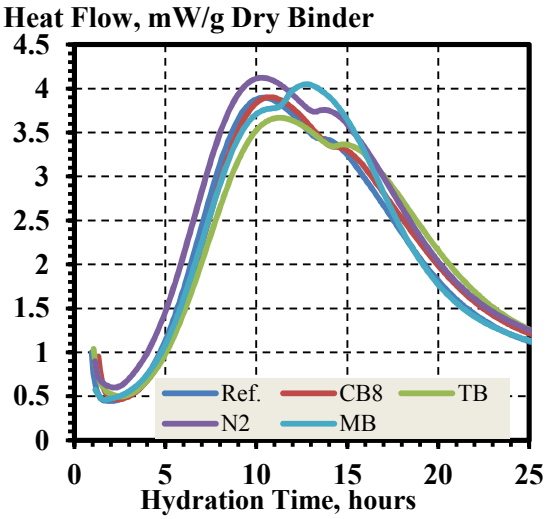

Figure 52. The shift of C_3S and C_3A peaks due to the addition of nanosilica (left) and hydration energy of investigated systems (right)

The increased rates of C_3S hydration can be correlated with the BET surface area, as higher surface area (SSA) must lead to the acceleration of C-S-H gel formation due to the seed

effect. With the addition N2 particles, the first peak corresponding to C_3S hydration was observed after 10 hours followed by second peak at 14 hours (from mixing with water). For this composition, the rate of hydration heat was about 5% higher compared with the reference and CB8 based mortars (*Table 25*).

For TB mortars, the first peak (C_3S) was observed after 11.3 hours and the second peak (corresponding to C_3A) was identified at 15 hours at the rate of hydration of about 5% lower compared with the reference and CB8 based mortars. With the addition of nano-SiO_2 the hydration of C_3S was accelerated due to a heterogeneous nucleation effect. Heterogeneous nucleation is typically the dominant acceleration mechanism when well dispersed seed component with a size smaller than cement particles is incorporated.

The extension of initial setting time was due to the addition of TB and N2 as reported in *Figure 53*. However, the final setting time for TB and N2 mortars was shortened by 36 minutes and 54 minutes, respectively as compared with the reference. This effect was expected as nanoparticles with higher specific area accelerate the cement hydration process and reduce the setting time. Mortars with powder nano-SiO_2 (e.g., N2 with the highest SSA) were characterized by the highest heat of hydration followed by CB8 and TB products. In addition to pozzolanic activity, the use of nano-SiO_2 particles with higher SSA increase the wettable surface area and so provide the bulk of the nucleation sites required for the formation of hydration products at very early stages of hydration. However, for MB, the sol based nano-SiO_2 product, the hydration of C_3S was hindered and C_3A hydration was accelerated [116]. In addition to these effects, the MB additive provided a shorter setting time compared with the reference.

The C-S-H is the main product of cement hydration and a primary binding phase in portland cement. When superfine particles with higher surface area (such as nanoparticles) are added, a denser matrix is created due to the formation of uniformly distributed C-S-H gel structure. As a result, the mechanical performance and durability in cement systems with nanosilica is improved. The increased hydration rates of C_3S can be correlated to BET surface area as the materials with higher surface area accelerate the formation of C-S-H gel *(Figure 53*).

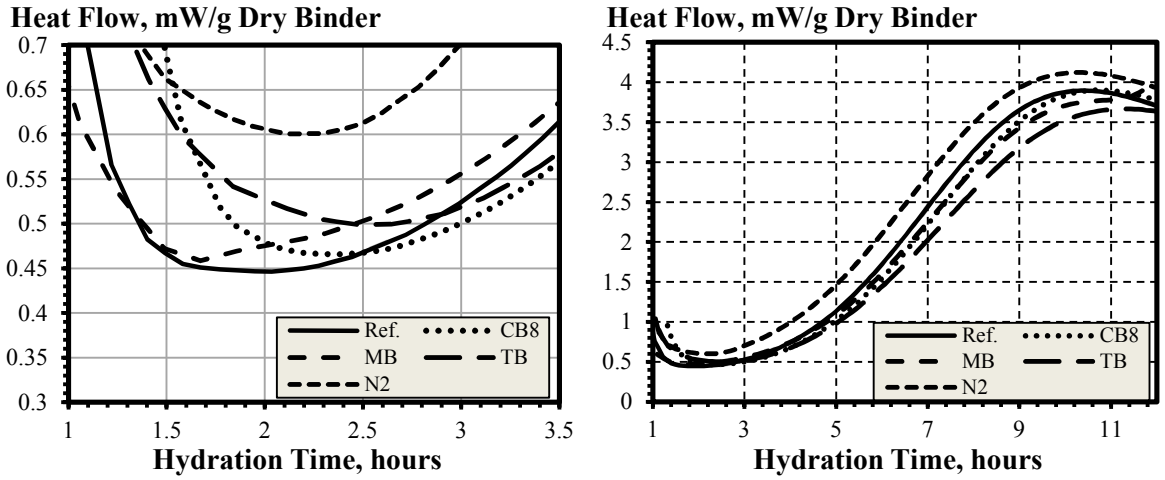

Figure 53. The determination of setting time of nano-SiO_2 based mortars

Mechanical Performance

The compressive and splitting tensile strengths of mortars with nano-SiO_2 at different curing ages are reported in *Figure 54*. At the age of 28 days the specimens containing MB type of nano-SiO_2 had the highest compressive strength of 110 MPa. There was a slight increase of 1-day strength in mortars with MB and N2, which corresponds to about 12% and 19% improvement as compared to the reference.

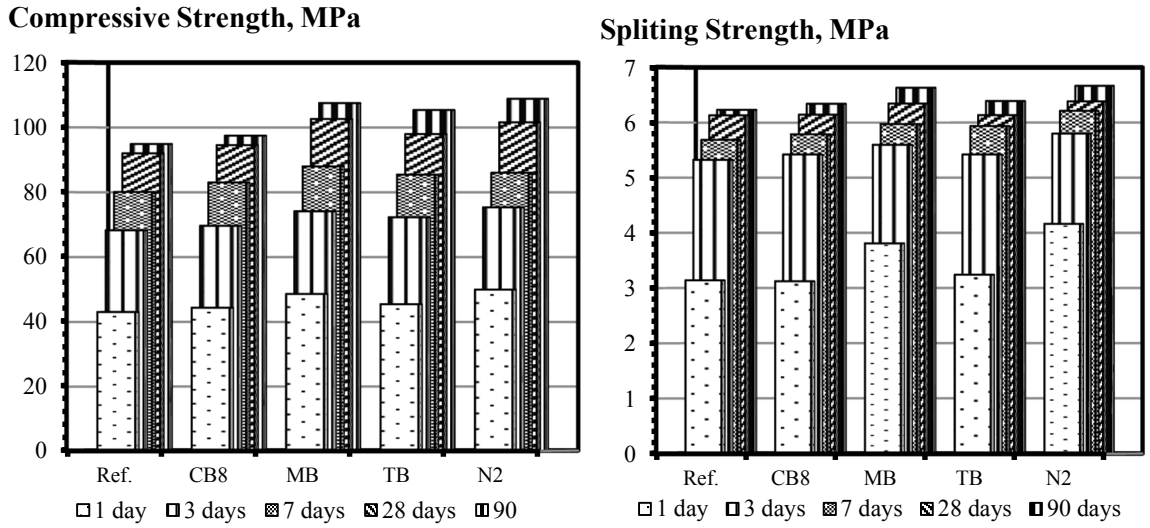

Figure 54. The compressive strength of mortars with nano-SiO_2 particles

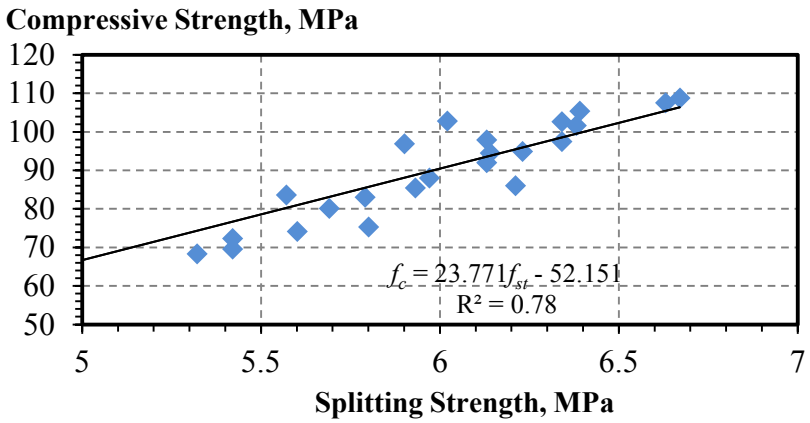

Figure 55. The correlation of compressive and splitting tensile strength for mortars with nano-SiO_2

The splitting tensile strength of investigated mortars followed similar trends and, therefore, can be correlated to the compressive strength, especially at the age of 3 days and afterwards (*Figure 55*). As a results, it can be observed that the use of some nano-SiO_2 products obtained from hydrothermal solutions at a very small dosage of 0.25% (by weight of cementitious materials) can provide a considerable enhancement of strength.

Table 26. Compressive and splitting tensile strength of mortars with nano-SiO_2

Mix ID	Compressive Strength, MPa, at the age of, days					Splitting Strength, MPa, at the age of, days				
	1	3	7	28	90	1	3	7	28	90
Ref	43.1	68.3	80.1	92.0	94.9	3.1	5.3	5.7	6.1	6.2
CB8	44.4	69.6	83.0	94.5	97.5	3.1	5.4	5.8	6.1	6.3
MB	48.6	74.1	88.0	102.6	107.5	3.8	5.6	6.0	6.3	6.6
TB	45.5	72.3	81.2	97.9	105.4	3.2	5.4	5.9	6.1	6.4
N2	50.0	75.3	82.3	101.6	108.8	4.2	5.8	6.2	6.4	6.7

Based on the results of reported investigation, it can be concluded that the use of nano-SiO_2 particles obtained from the hydrothermal solutions can improve the overall performance of portland cement.

The hydration of portland cement systems can be accelerated by nano-SiO_2 due to higher surface area and adequate dispersion of nanoparticles. The C_3S hydration rate can be correlated with the BET surface area of nano-SiO_2 particles, as the higher surface area accelerated the formation of C-S-H gel due to seeding effect. As detected by FTIR, the powder nano-SiO_2 products had a lower intensity of Si-O-Si bonds compared with nano-SiO_2 sol products. The degree of disorder (as opposite to crystallinity) of nano-SiO_2 structure can play a role in the reactivity and strength development of mortars with nanomaterials.

Typically, finer particles with higher surface area react more vigorously than the larger particles. With the addition of nano-SiO_2 the setting time is shortened due to accelerated hydration. The powder nano-SiO_2 products with higher surface area can accelerate the hydration of cement and provide enhancement of early-age strength. Due to ongoing pozzolanic reactions, nano-SiO_2 additives can modify the structure and morphology of C-S-H products resulting in denser matrix structure and improved mechanical performance of mortars. The addition of very small dosage of nano-SiO_2 such as 0.25% by the weight of cementitious materials combined with

0.15% of PCE superplasticizer (partially used for the dispersion of nano-SiO_2) can provide consistent, up to 10% improvement of mortar strength in all ages of hardening.

4.5. EFFECT OF MECHANO-CHEMICAL ACTIVATION

4.5.1. Microstructure of activated fly ash

The microstructure of activated fly ash was investigated to quantify the process of mechano-chemical activation. The activated class F fly ash was characterized using scanning electron microscopy (SEM) of specimens activated for 1 hour, 2 hours, 3 hours and 24 hours (*Figure 57*). The SP and nanosilica were added to facilitate the dispersion of fly ash in liquid state during the milling.

It can be observed that longer activation results in the formation of smaller particles. However, the activation for 3 hours can be considered as sufficient in terms of reduction of particle size.

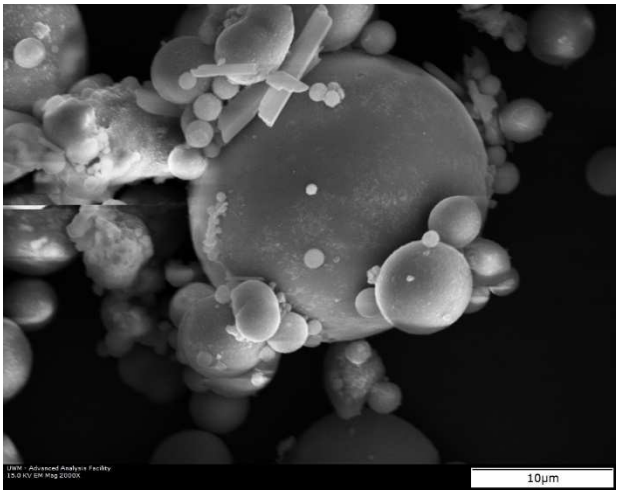

FA_Ref

Figure 56. Reference fly ash with large cenospheres

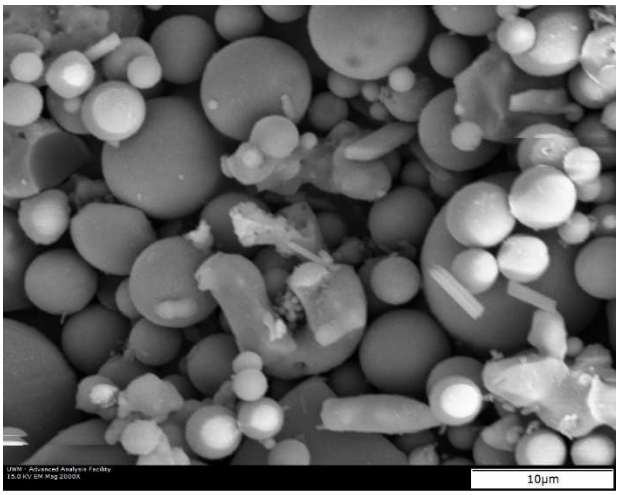

FA_1-hour activation

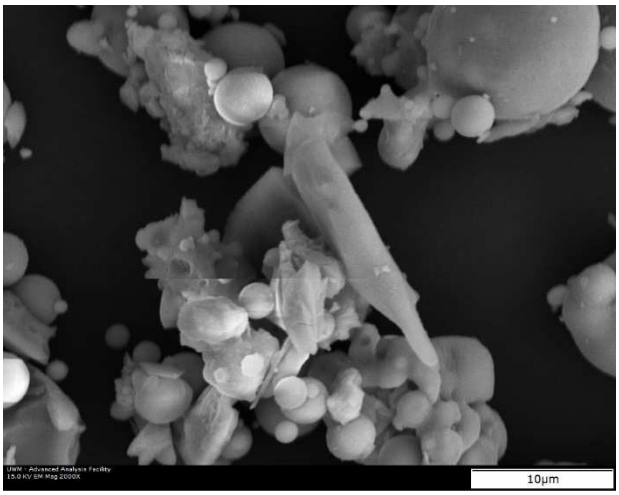

FA_2-hour activation

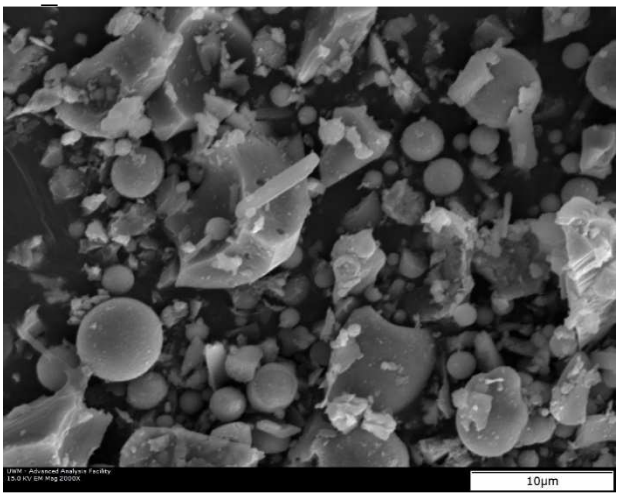

FA_3-hour activation

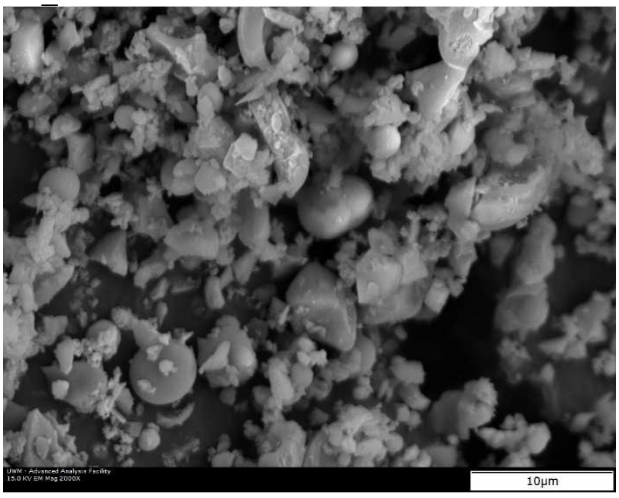

FA_24-hour activation

Figure 57. The SEM image for fly ash activated for different times, about 30% of small cenospheres are still present after 3-hour activation, 2000X magnification

4.5.2. Hydration Process

It can be observed that the activation of fly ash in vibro mill considerably accelerates the heat of hydration of cementitious systems with fly ash (*Table 27*) vs. reference (*Figure 58).* The highest hydration peak associated with the C_3S hydration was reached by the composition with fly ash activated for 3 hours.

Table 27. Experimental matrix and performance characteristics of mortar

Mix ID	Cement Replacement with Fly Ash, %	Activation Time, hours	W/CM	Composition of Activated Component, %				Flow, %	Setting time, minutes	
				Fly Ash		SP	Nano silica		Initial	Final
				Class F	Class C					
R1	30	-	0.36	20	-	0.15	-	82	210	450
30AFAF-1	30	1	0.36	20	-	0.15	-	83	210	435
30AFAF-2	30	2	0.36	20	-	0.15	-	94	180	372
30AFAF-3	30	3	0.36	20	-	0.15	-	108	165	332
30AFAF-4	30	4	0.36	20	-	0.15	-	>140	150	306
R2	-	-	0.3	-	-	0.15	-	47	84	420
20FAC-R	20	3	0.3	-	20	0.15	-	42	228	582
20AFAC-3	20	3	0.3	-	20	0.15	-	105	54	240
20AFAC-NS-3	20	3	0.3	-	20	0.15	0.1	90	60	258
20FAF-R	20	3	0.3	20	-	0.15	-	>140	108	324
20AFAF-3	20	3	0.3	20	-	0.15	-	>140	108	300
20AFAF-NS-3	20	3	0.3	20	-	0.15	0.1	130	108	348

The mechano-chemical activation can reduce the dormant period, setting times and enhance early strength properties of blended cementitious composites with up to 30% of fly ash. It appears that the activation for 3 hours results in optimal performance of blended cement systems. Mortars with 20% of activated class F and class C fly ash, superplasticizer and nanosilica were produced at W/CM of 0.3 and S/CM of 1. Combined application of activated fly ash and nanosilica enables the acceleration of hydration of portland cement-fly ash system vs. reference portland cement mortar (R2) as demonstrated by *Figure 59.*

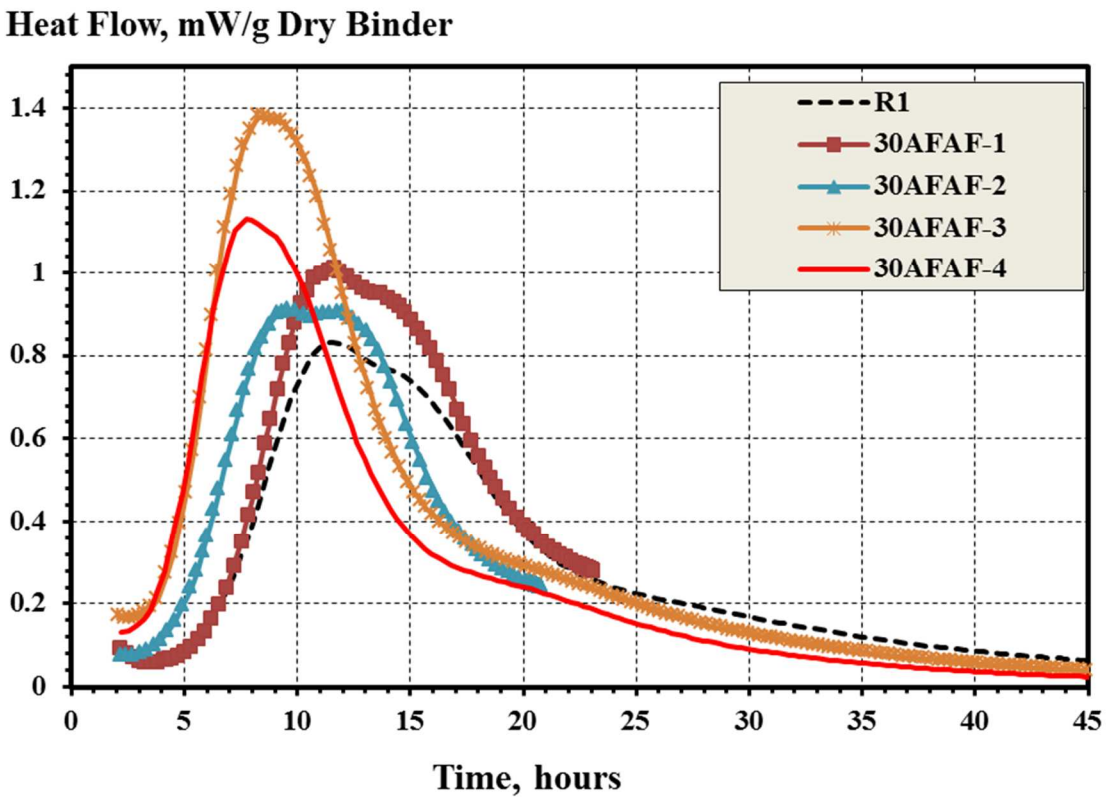

Figure 58. The effect of activation on hydration of cement with fly ash

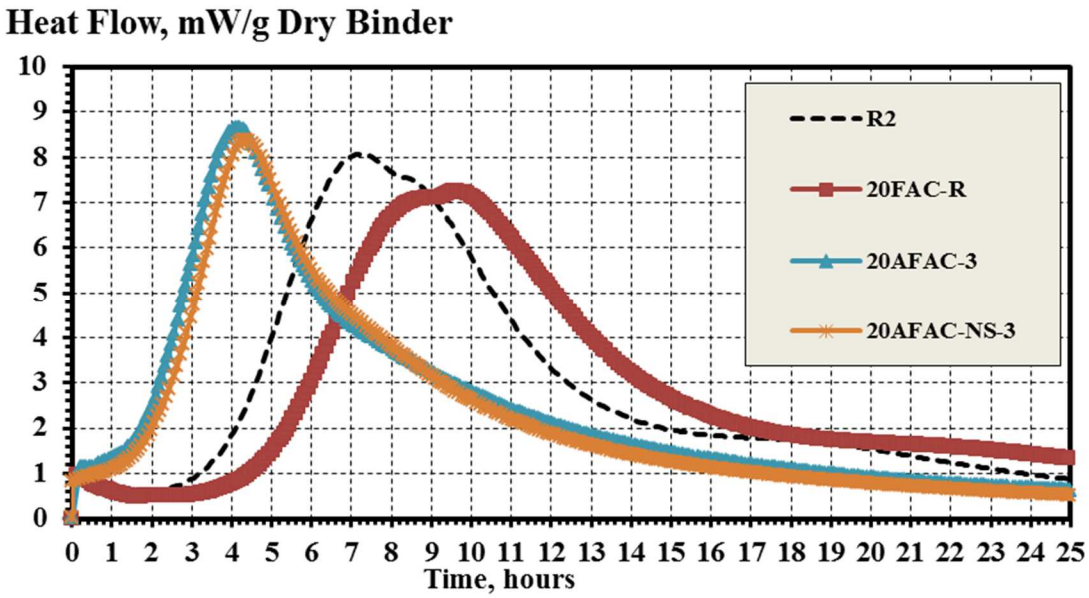

(a)

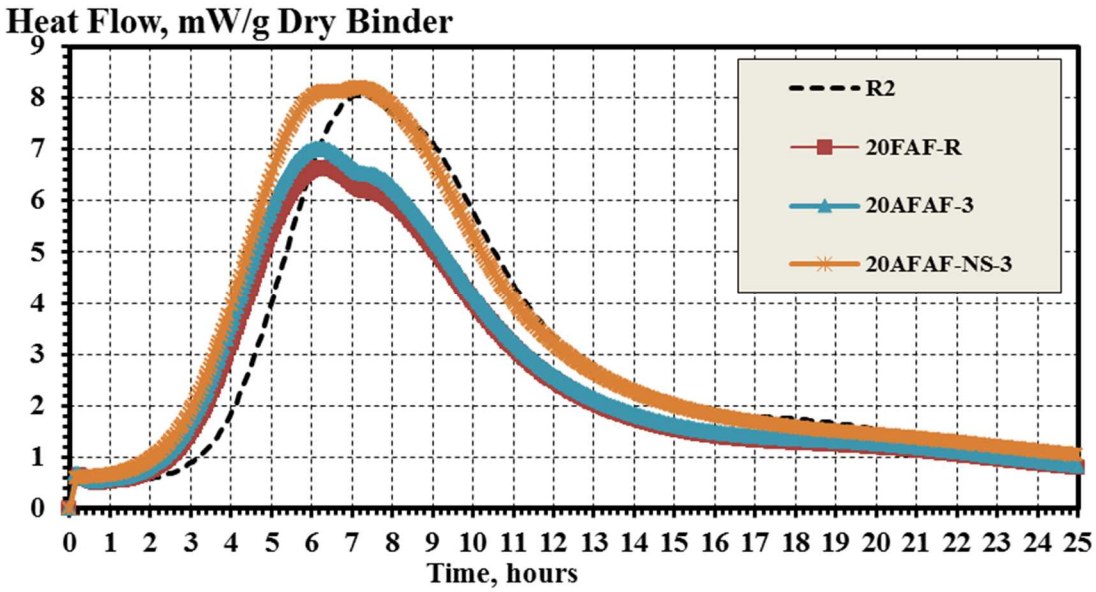

(b)

Figure 59. The effect of activated fly ash on cement hydration; a) class C fly ash; b) class F fly ash

4.5.3. Compressive Strength

The use of activated fly ash in combination with plain (non-activated fly ash) as 20% +10% blend enables to improve the strength of blended cement mortars in all ages of hardening.

Specifically, 1-day and 7-day compressive strength of mortars with activated class F fly ash were considerably improved. The best results were achieved by the systems with fly ash activated for 3 hours (*Figure 60*).

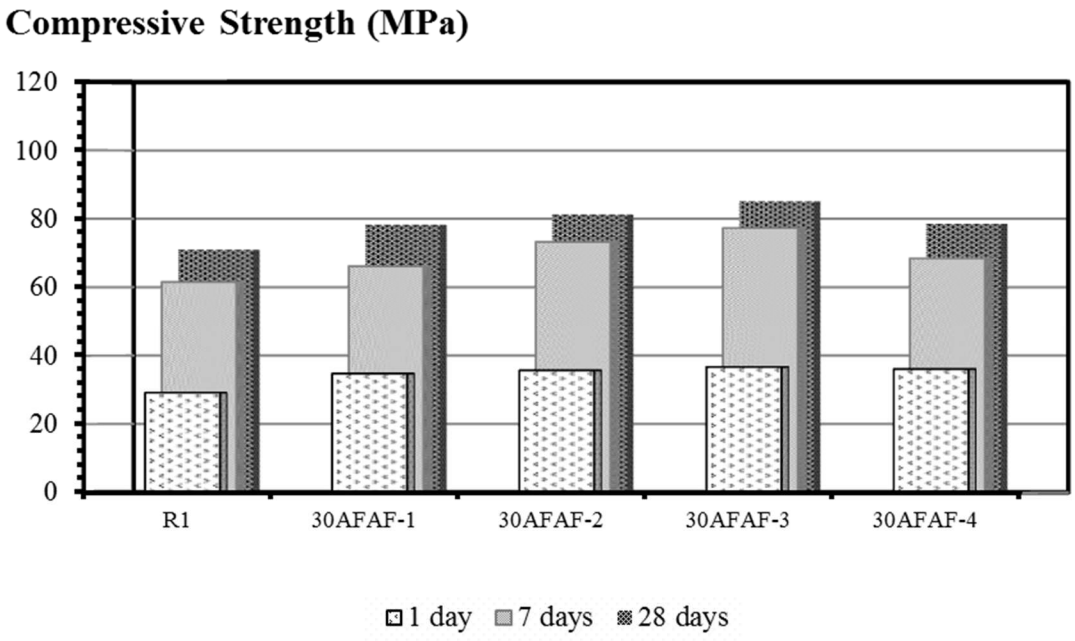

Figure 60. The effect of activation time on compressive strength of cement systems with 30% of fly ash.

Furthermore, nanosilica can be effectively used to boost the performance of systems with activated fly ash. It can be observed that the use of 20% activated class F fly ash and class C fly ash result in the 28-day compressive strength comparable to the strength of reference portland cement. The effect of activation can be seen in the improvement of early, 1- and 7-day strength (*Figure 61*). Overall, mortars based on activated class C fly ash had a better performance than

reference portland cement in all ages of hardening. This is achieved due to ultrafine milling and activation of fly ash. While systems with 20% of activated class F fly ash had 7- and 28-day compressive strength comparable to reference portland cement mortar, 1-day strength was about 50% lower vs. the reference.

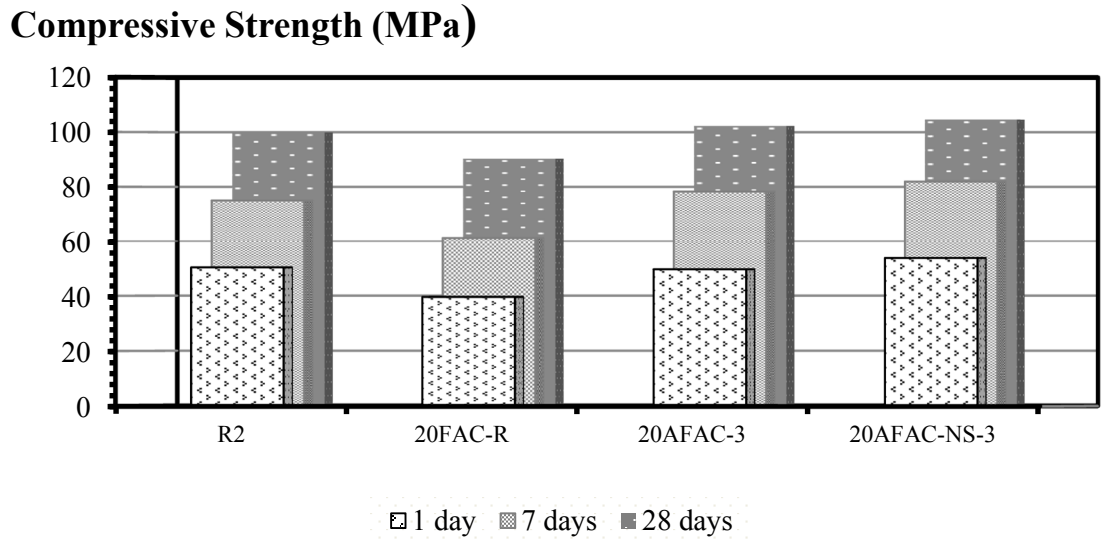

(a)

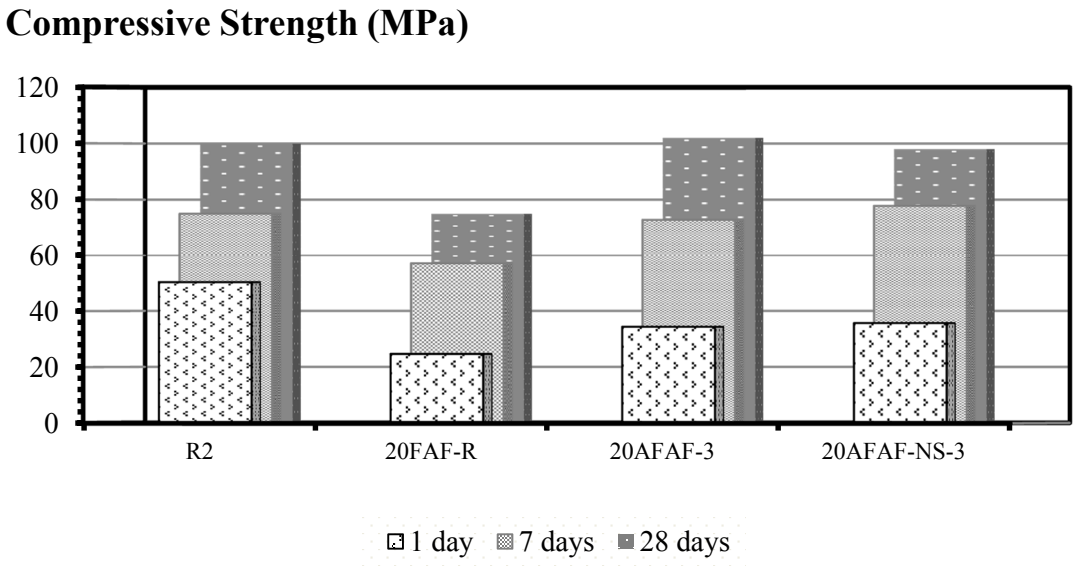

(b)

Figure 61. The effect of activated fly ash and nanosilica on compressive strength of mortars with 20% of fly ash a) Class C fly ash b) Class F fly ash

5. OPTIMIZATION OF CONCRETE MIXTURES

The rheological behavior of cement paste corresponding to SCC mixtures was evaluated to determine the yield stress and viscosity. Prior to the design of concrete mixtures, SCC mortars with and without activated class C fly ash were compared for fresh and hardened properties.

This chapter reports on the performance of optimized eco-friendly fly ash concrete mixtures designed using two different approaches: a) conventional concrete mixtures containing 280 kg/m^3 of cementitious materials and b) SCC containing 400 kg/m^3 and 500 kg/m^3 of cementitious materials.

Conventional concrete mixtures were optimized based on two types of chemical admixtures (mid-range plasticizer and high-range water reducer), AE admixture and SCM. The fresh properties in terms of slump, air content, and fresh density were analyzed. The SCC concrete mixtures were produced at various dosages (up to 50%) of supplementary cementitious materials and with nanosilica and superplasticizer (high range water reducer, HRWR). The use of nanosilica improves the cohesiveness and reduces the bleeding and segregation of the SCC mixtures. For this research phase, the cementitious material content used in SCC was 400 kg/m^3 and 500 kg/m^3. For fresh properties, v-funnel test, slump flow and J-ring flow were investigated. For hardened properties, the compressive strength was investigated at different ages of hardening.

5.1. CONCRETE FOR PAVING APPLICATIONS

5.1.1. Target Properties

The mixture proportions of concrete with 280 kg/m^3 are reported in *Table 28.* The fresh and hardened properties of concrete are presented in *Table 29*. To optimize the dosage of

admixtures, the lowest desirable W/C ratio that results in the slump of 50 - 100 mm (2 - 4 in.) was selected. Other target parameters were air content of 7 ±1.5% and early (7-day) compressive strength of 20 MPa (3,000 psi).

5.1.2. Fresh Properties

Workability of the concrete mixtures was evaluated using the slump test. Concrete slump depends on various parameters, including W/C ratio, water and cement content (the volume of cement paste), the type of chemical admixtures (WR vs. HRWR), and the volume of air. The constant dosage of WR and HRWR admixtures (RP8 and HG7, respectively) was used at 0.15%. In this study, proportioning of aggregates was held constant for each level of cement content and composition; therefore, this parameter did not affect the slump results. The workability of fresh concrete was evaluated right after the mixing and also at one hour after the contact of cement with water (in the mixer) as reported by *Table 29.*

Comparing the reference concrete produced with a W/CM ratio of 0.45 (FF1, FF2) indicates that PCE admixture (HG7) perform better than the mid-range plasticizer (RP8) in terms of workability. The use of PCE admixture (FF2) provided a higher slump of 40 mm than the mixture with the mid-range water reducing admixture (FF1).

Concrete with fly ash (class C and class F) produced at the same W/C ratio of 0.45 and mid-range plasticizers (FF3, FF7) had a similar slump within the range of 10-60 mm as corresponding concrete with superplasticizer at W/C ratio of 0.4 which was characterized by the slump of 5- 64 mm. When using class F fly ash though, concrete mixtures may require the use of higher water content to achieve the same levels of workability as attained in class C mixtures. This correlates with increased water demand of class F fly ash mortars. The air content of all fly ash based concrete was within the limits of 4.7 – 8%.

The air content of mixtures can be correlated to fresh density as illustrated in *Figure 62*. Although the air contents for concrete with less than 6% are scattered, the mixtures with air content that is greater than 6% have a strong linear relationship with fresh density. To extend the durability performance of concrete, the dosage of AE admixture may need to be adjusted to ensure the required air void structure and spacing factor.

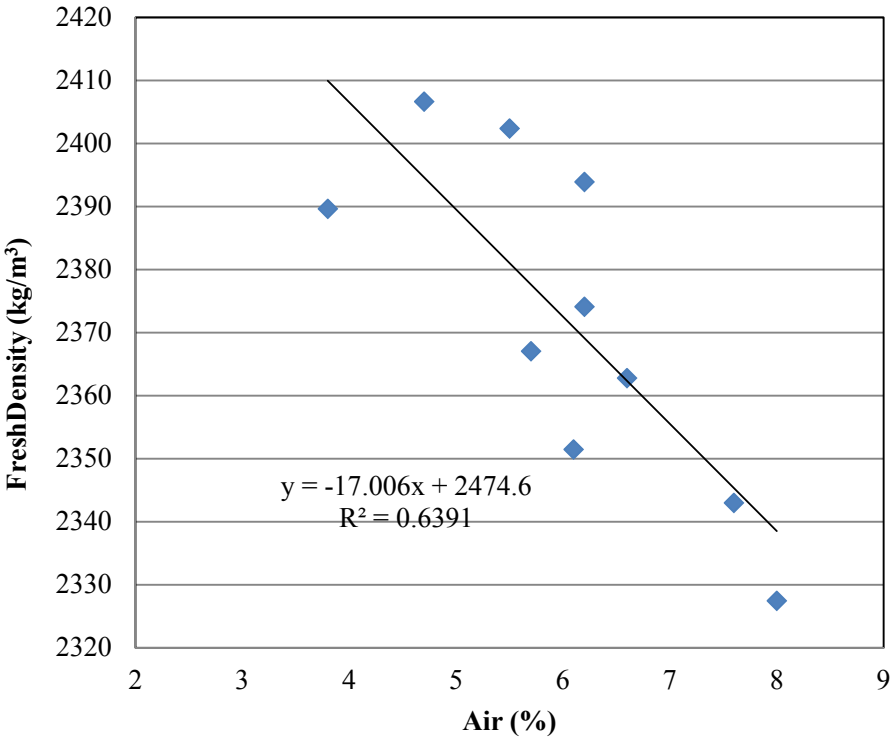

Figure 62. The relationship between the air content and fresh density of concrete mixtures

5.1.3. Strength Development

Superplasticizing admixtures were used to achieve the required air and slump parameters at the lowest W/C ratio with the goal of obtaining optimal mechanical performance. Here, the higher compressive strength can be achieved at a lower W/C ratio; however, a lower W/C ratio may result in impractical workability levels and poor compaction. The mechanical performance was evaluated for early (1-7 days) and long-term (28 days) periods.

As demonstrated by *Figure 63* below, the highest compressive strength was achieved by concrete with a 30% of Class C fly ash and PCE superplasticizer; this concrete had the 7-day strength of 33 MPa and 28-day strength of 44 MPa. This proves that the use of PCE admixtures in concrete with Class C fly ash can provide superior performance in terms of workability and strength development.

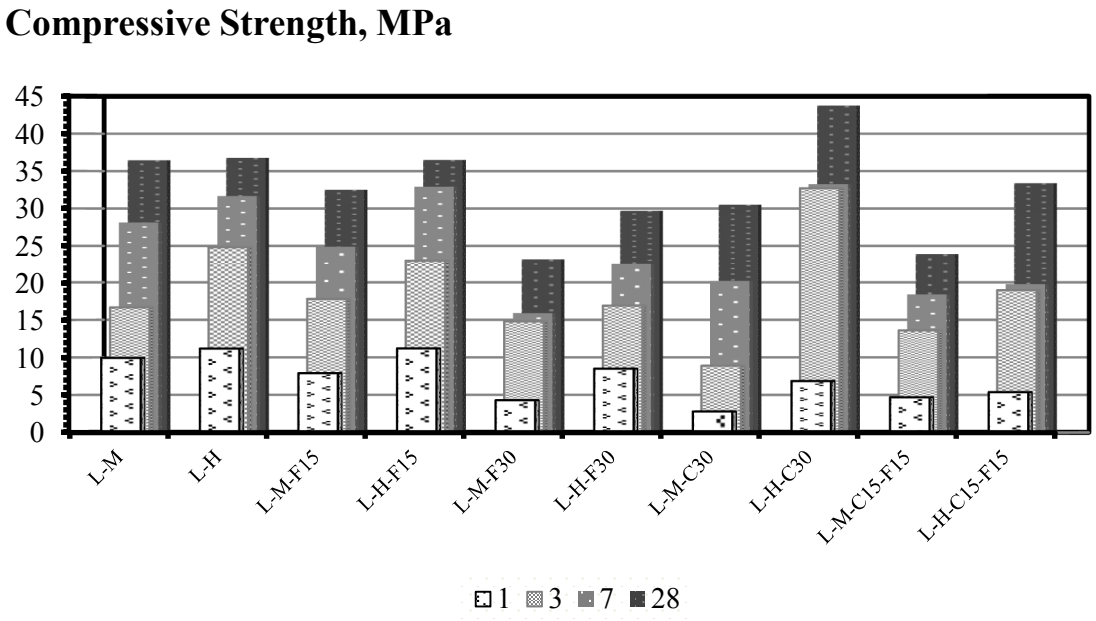

Figure 63. Strength development of concrete produced at cementitious material content of 280 kg/m^3

.

Table 28. Mixture proportions used for concrete with cementitious material content of 280 kg/m^3

Cement Factor	Mix ID		Dosage of Admixtures, %			Mixture Proportions, kg/m^3									
						Cement	SCM		Aggregate (SSD)				Admixtures		Total Water
			PCE	Mid-Range	AE		FAF	FAC	CA	IA	FA	Total	WR / HRWHA	Air Entraining	
280 kg/m^3, 470(lb/yd^3)	L-M	FF1		0.150	0.010	280	0	0	793	195	932	1920	0.620	0.199	158
	L-H	FF2	0.150		0.010	280	0	0	793	195	932	1920	0.812	0.199	157
	L-M-F15	FF5		0.150	0.010	238	42	0	789	194	928	1911	0.620	0.199	157
	L-H-F15	FF6	0.150		0.010	238	42	0	804	198	945	1947	0.812	0.199	144
	L-M-F30	FF7		0.150	0.015	196	84	0	785	193	922	1900	0.620	0.298	158
	L-H-F30	FF8	0.150		0.015	196	84	0	800	197	940	1937	0.812	0.298	144
	L-M-C30	FF3		0.150	0.005	238	0	42	790	194	928	1912	0.620	0.099	158
	L-H-C30	FF4	0.150		0.010	196	0	84	805	198	946	1949	0.812	0.199	144
	L-M-C15-F15	FF9		0.150	0.010	196	42	42	787	193	925	1906	0.620	0.199	158
	L-H-C15-F15	FF10	0.150		0.010	196	42	42	802	197	943	1942	0.812	0.199	144

Table 29. Fresh and hardened properties of concrete with cementitious material content of 280 kg/m³

Cement Factor	Mix ID		W/CM	Vol. of AGG	Yield	Air, %	Temp., F	Fresh Density, kg/m³	Slump, mm		Compressive Strength, MPa at the Age of			
									15 minutes	1 hour	1 day	3 days	7 days	28 days
280 kg/m³, 470(lb/yd³)	L-M	FF1	0.45	0.726	0.99	3.8	69	2390	18	0	9.9	16.7	28.1	36.4
	L-H	FF2	0.45	0.726	1.00	5.7	69	2367	40	2	11.2	24.8	31.7	36.8
	L-M-F15	FF5	0.45	0.722	0.98	4.7	70.5	2407	10	2	7.9	17.8	24.9	32.5
	L-H-F15	FF6	0.40	0.736	0.99	5.5	68	2402	5	0	11.2	23.0	32.9	36.5
	L-M-F30	FF7	0.45	0.718	0.99	6.1	68	2351	11	0	4.3	14.8	15.9	23.2
	L-H-F30	FF8	0.40	0.732	1.00	6.6	69	2363	9	0	8.5	16.9	22.6	29.7
	L-M-C30	FF3	0.45	0.723	0.99	6.2	68.7	2374	60	5	2.8	8.9	20.2	30.5
	L-H-C30	FF4	0.40	0.736	0.99	6.2	67.8	2394	23	0	9.9	16.7	28.1	36.4
	L-M-C15-F15	FF9	0.45	0.720	1.01	8.0	68	2327	50	15	11.2	24.8	31.7	36.8
	L-H-C15-F15	FF10	0.40	0.734	1.01	7.6	68.4	2343	64	0	7.9	17.8	24.9	32.5

At the age of 7-days almost all concrete types exceeded the standard level of 20 MPa, except for the concrete mixtures with mid-range plasticizer containing 30% of class F fly ash and also combination of 15% class F and 15% class C. This is due to the retardation effect of class F fly ash.

5.2. OPTIMIZATION OF SELF CONSOLIDATING CONCRETE

5.2.1. The Evaluation of SCC

The mixture proportions of concrete are reported in *Table 30.*The fresh and hardened properties of concrete mixtures are presented in *Table 31*. The fresh properties, rheological properties, and compressive strength were investigated for SCC produced with class C fly ash, nanosilica, and superplasticizing (high-range water-reducing, HRWR) admixtures. The SCC mixtures were designed at a fly ash content of 0%, 30% and 50%. In addition, mixtures with 30% of activated fly ash (AC-FAC) and various SP dosages were tested in order to evaluate the improvement on early strength development. The flowability and stability are two most important properties of SCC. A high flowability of SCC can be achieved without changing the W/C ratio by using effective SP/HRWR admixtures such as PCE. The improved stability can be achieved by increasing the total quantity of fine aggregates which is affecting viscosity and reducing segregation. In this study, stability of SCC mixtures was achieved by using fly ash and nanosilica.

5.2.2. Fresh Properties

The flow time of the SCC mixtures was investigated using V-funnel test. The V-funnel times were in the range of 3.9 to 15 seconds. The SCC with 50% FA content had the lowest flow times and reference SCC without fly ash had the highest times. It was determined that due to

spherical shape of fly ash particles, the replacement of portland cement with fly ash improves the flow times as well as the overall workability of SCC mixtures. The flow performance of SCC depends on the volume of cementitious materials and the volume of cement paste (and air). Due to higher viscosity (induced by low W/C), the flow time for SCC with 500 kg/m^3 was longer than that of the 400 kg/m^3 mixtures. It was observed that the use of activated fly ash in SCC with higher cement content provided more cohesive and viscous concrete mix.

The slump flow performance of investigated SCC was in a range of diameters changing between 430 mm and 1015 mm. Based on ASTM C1611, the typical SCC slump flow ranges from 450 mm to 810 mm. For SCC with cementitious content of 400 kg/m^3 all the mixtures were within the range of the required standard except for SCC with activated fly ash produced with 0.25% of superplasticizer, *Figure 64*. These results prove that incorporating of activated fly ash and nanosilica dispersion can provide concrete with significantly enhanced slump flow. The SCC mixtures with 500 kg/m^3 of cementitious materials content were within the specified flow range except for SCC mixtures with high fly ash content of 50%, *Figure 64b*.

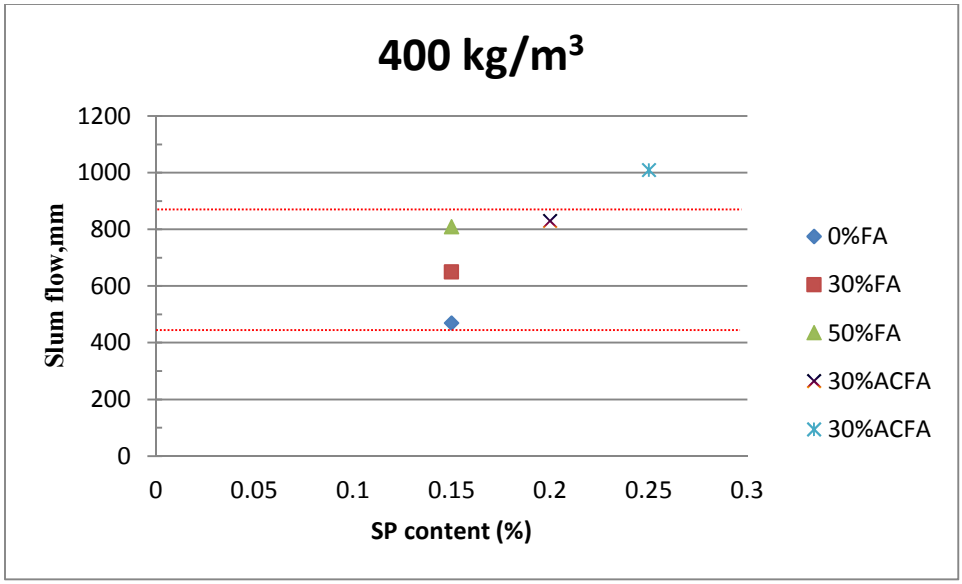

(a)

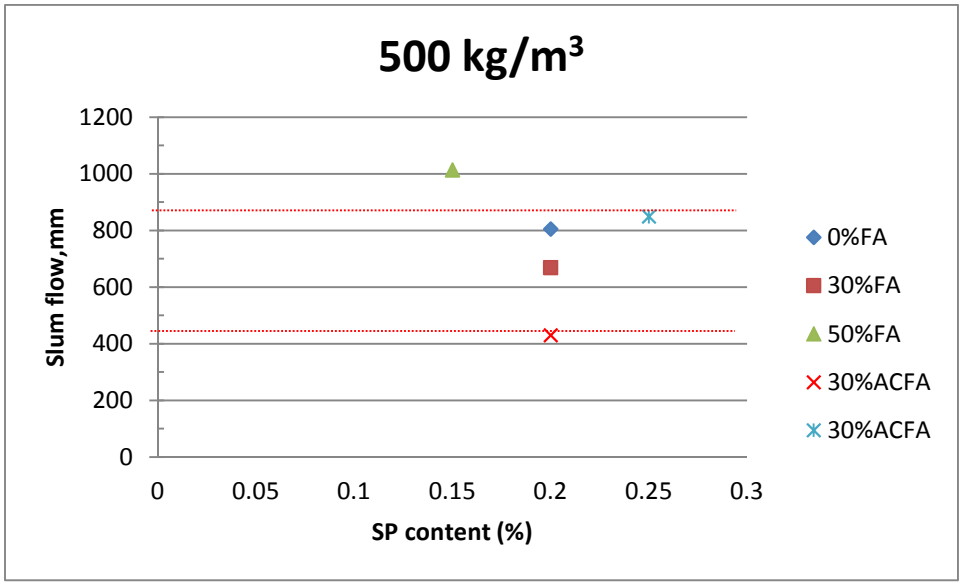

(b)

Figure 64. Slump flow of SCC with cementitious material content of 400 kg/m^3 (a) and 500 kg/m^3 (b)

Excellent correlation between the slump flow and J-ring test was observed as represented by *Figure 65*. Here the increased slump flow is directly proportional to the increase in the J-ring value for all investigated SCC.

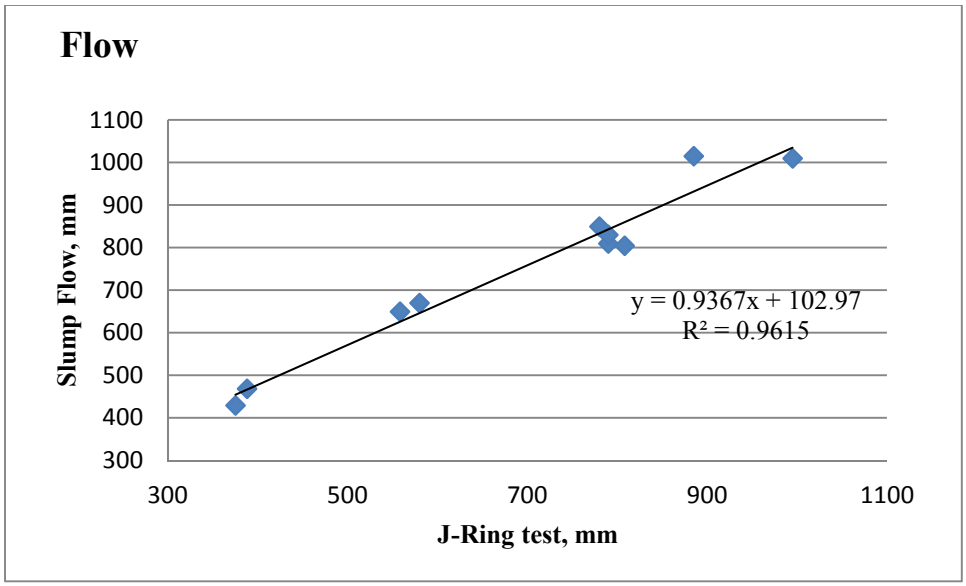

Figure 65. Correlation between the slump flow and J-ring test

5.2.3. Strength Development

The highest 28-day compressive strength of 64 MPa and 89 MPa was achieved by SCC based on activated fly ash at superplasticizer dosage of 0.25% and cementitious material content of 400 kg/m^3 and 500 kg/m^3, respectively, *Figure 66*. These values exceed the strength of reference portland cement based SCC and are an indication that the mechanical activation can improve the compressive strength of SCC. Indeed, it can be concluded that such improvement is due to the use of ultrafine particles of fly ash and nanosilica.

The strength of SCC with 50% of fly ash was low, especially only early ages of hardening. However, concrete with 30% of fly ash demonstrated slightly reduced early-age strength and, also exceeded the 28-day strength of reference SCC (without fly ash).

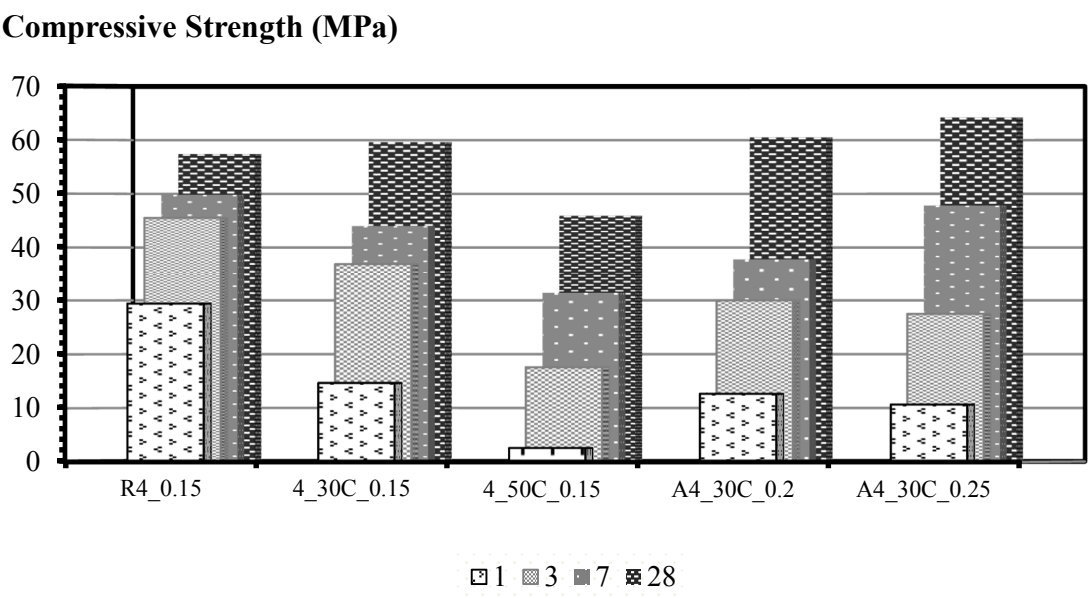

(a)

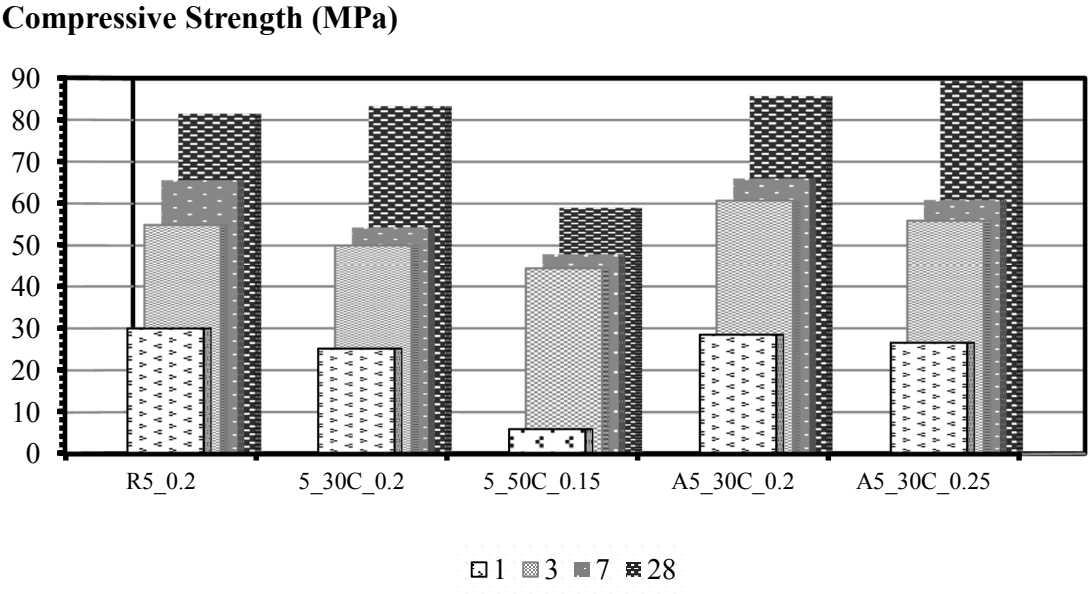

(b)

Figure 66. Strength of SCC produced at cementitious material content of 400 kg/m^3 (a) and 500 kg/m^3 (b)

Table 30. Mixture proportions for SCC with cementitious material content of 400 kg/m3 and 500 kg/m3

Cement Factor	Mix ID		Dosage of Admixture, %		Mixture Proportions, kg/m^3									
					Cement	Fly Ash	Activated Ash	Aggregate (SSD)				Admixtures		Total Water
			PCE	Nano silica				CA	IA	FA	Total	PCE	Nano silica	
400 kg/m^3	SCC1	R4_0.15	0.15	0.15	400	0	0	764	188	898	1850	0.938	3.427	181
	SCC3	4_30C_0.15	0.15	0.15	280	120	0	759	187	891	1837	0.938	3.427	181
	SCC9	4_50C_0.15	0.15	0.15	200	200	0	755	186	887	1828	0.938	3.427	181
	SCC7	A4_30C_0.2	0.20	0.15	280	0	120	758	186	891	1835	1.251	3.427	181
	SCC5	A4_30C_0.25	0.25	0.15	280	0	120	758	186	890	1834	1.564	3.427	181
500 kg/m^3	SCC4	R5_0.2	0.20	0.15	500	0	0	733	180	861	1775	1.564	4.284	179
	SCC8	5_30C_0.2	0.20	0.15	350	150	0	711	175	835	1722	1.564	4.284	179
	SCC11	5_50C_0.15	0.15	0.15	250	250	0	711	175	835	1722	1.173	4.284	179
	SCC6	A5_30C_0.2	0.20	0.15	350	0	150	727	179	853	1759	1.564	4.284	179
	SCC10	A5_30C_0.25	0.25	0.15	350	0	150	727	179	853	1759	1.955	4.284	178

Table 31. Fresh and hardened properties of SCC with cementitious material content of 400 kg/m^3 and 500 kg/m^3

Cement Factor	Mix ID		W/CM	Vol. of AGG	Yield	Air, %	Temp., F	Bulk Density, kg/m^3	V-funnel, s	Slump flow, mm	J-Ring, mm	Compressive Strength, MPa at the Age of			
												1 day	3 days	7 days	28 days
400 kg/m^3	SCC1	R4_0.15	0.375	0.700	0.98	2.4	70	2485.8	15	469	388	29.4	45.5	49.8	57.4
	SCC3	4_30C_0.15	0.375	0.694	1.02	4.2	69	2475.5	14	650	558	14.7	36.9	44.0	59.6
	SCC9	4_50C_0.15	0.375	0.691	0.98	3.5	70	2457	4	810	790	2.6	17.6	31.4	45.9
	SCC7	A4_30C_0.2	0.375	0.694	1.01	2.3	70	2398	5	530	490	12.7	30.0	37.8	60.5
	SCC5	A4_30C_0.25	0.375	0.693	0.99	3.3	68	2419.4	5	1010	995	10.7	27.5	47.8	64.2
500 kg/m^3	SCC4	R5_0.2	0.3	0.671	1.04	3.4	69	2372.5	11	805	808	30.0	54.9	65.6	81.5
	SCC8	5_30C_0.2	0.3	0.651	0.98	3.4	69	2443.2	10	1015	885	25.2	50.0	54.3	83.3
	SCC11	5_50C_0.15	0.3	0.647	0.98	3.4	70	2430.7	4	670	580	6.0	44.3	47.9	59.0
	SCC6	A5_30C_0.2	0.3	0.665	0.99	3	69	2454	13	430	375	28.5	60.7	66.0	85.7
	SCC10	A5_30C_0.25	0.3	0.650	0.98	2.8	70	2400.9	8	850	780	26.6	55.9	60.9	89.3

6. CONCLUSIONS

The heat of hydration along with the investigation of mechanical performance of cement paste and mortars can be used as very effective approach for the optimization of dosage of chemical admixtures, nanoparticles and SCM prior to their application of these components in concrete. Such optimization is essential when the combination of cements, SCM and nanoparticles is used.

It can be concluded that the use of nano-SiO_2 particles such as Cembinder 50 and Cembinder 8 can increase the performance of portland cement composites. For example, at the dosage increased to 2% Cembinder 50 demonstrated a better performance in terms of acceleration of hydration and compressive strength. Here, the product with higher surface area provided a better performance due to introduction of the nucleation sites for the formation C-S-H resulting in densified structure.

It can be concluded that the use of nano-SiO_2 particles obtained from the hydrothermal solutions can improve the performance of portland cement mortars. As detected by FTIR, powder nano-SiO_2 products had a lower intensity of Si-O-Si bonds compared with nano-SiO_2 sol products. The degree of disorder (as opposite to crystallinity) of nano-SiO_2 structure can play a role in the reactivity and strength development of mortars with nanomaterials. Due to higher surface area and adequate dispersion of nanoparticles the hydration of portland cement systems can be accelerated by nano-SiO_2. The C_3S hydration rate can be correlated with the BET surface area of nano-SiO_2 particles, as the higher surface area accelerated the formation of C-S-H gel due to seeding effect. With the addition of nano-SiO_2 the setting time is shortened due to accelerated hydration.

The rheological behavior of the pastes was enhanced with incorporation of nanosilica resulting in fluid systems with zero segregation. The addition of fly ash (up to 50%) to superplasticized cement pastes with nanosilica resulted in the reduction of shear stress vs. the reference (without fly ash). The pastes demonstrated shear thickening thixotropic response with quick structure buildup upon unloading. For this reason, for modelling of concrete workability, the cement paste shear stress can be used at the shearing rate of $1s^{-1}$.

Powder nano-SiO_2 products with higher surface area can accelerate the hydration of cement and provide enhancement of early-age strength of portland cement systems. Due to ongoing pozzolanic reactions, nano-SiO_2 additives can modify the structure and morphology of C-S-H products resulting in denser structure and improved mechanical performance of mortars. The addition of nano-SiO_2 at a very small dosage such as 0.25% by the weight of cementitious materials combined with 0.15% of PCE superplasticizer (partially used for the dispersion of nano-SiO_2) can provide consistent, up to 10% improvement of mortar strength in all ages of hardening.

The use of effective combination of PCE admixture at (0.2%), nanosilica at (0.25%) and fly ash at (30%) enables the reduction of the W/CM ratio and, at the same time, enhances the workability of portland cement systems. Optimal combination of these components enhances the mechanical performance at all ages of hardening, enabling to achieve a concrete with 28-day compressive strength up to 90 MPa.

The use of mechano-chemical activation (MCA) of fly ash with superplasticizer and nanosilica in aqueous solution enabled the formation of new activated cementitious product capable of considerable enhancement of strength performance of blended portland cement

systems. In all investigated systems class C fly ash has demonstrated a better performance than class F fly ash. Still, activation was very effective in class F fly ash systems, considerably enhancing the early-age and long-term performance.

The boost of performance of cementitious systems with activated fly ash is due to the presence of ultrafine of ultrafine super-reactive particles of fly ash and nanosilica resulting in the acceleration of cement hydration. This approach may require future investigation to explain the observed behavior and further improve the activity of fly ash.

The effective use of fly ash requires the application of liquid state MCA of fly ash-nanosilica-superplasticizer blends; this enables considerable reduction of W/CM ratio and at the same time, provides excellent workability (to the levels required for SCC) as well as the achievement of very high early-age strength with 1-day compressive strength of 47 MPa.

The developed nano composites can potentially use the SP in the range of up to 0.25%, the nanosilica in the range of less than 1% (for economical reason) and the activated fly ash of up to 30% in the blends with nanosilica and SP for nano-engineered concrete mixtures.

The developed approaches for nano-engineering of concrete, research results and optimization can serve as a solid foundation for the specification and application of sustainable concrete with high volumes of supplementary cementitious materials and enhanced performance as required for modern civil and transportation infrastructure applications.

7. FUTURE RESEARCH

The various aspects of reported research can be further extended:

1. Better understanding of the effects of Class F fly ash on concrete performance and new methods for activation of fly ash must be investigated.

2. Further research is necessary to identify the effects of activated fly ash on composition and morphology of hardened cement matrix including the time periods over 28 days.

3. Durability investigation for developed SCC based on activated fly ash is necessary.

REFERENCES

1. *Report Card for America's Infrastructure*, 2013, ASCE.

2. Chockalingam, M., *Experimental Investigation on Self Compacting Concrete (SCC) using marble powder and silica fume.* International Journal and Magazine of Engineering, Technology, Management and Research.

3. Collepardi, M., Ogoumah, J.J., Skarp, U., and Troli, R. *Influence of Amorphous Colloidal Silica on the Properties of Self-Compacting Concretes*. in *Proceedings of the International Conference, Challenges in Concrete Construction - Innovations and Developments in Concrete Materials and Construction*. 2002. Dundee, UK.

4. Bjornstrom, J. and Panas, I., *Antagonistic effect of superplasticizer and colloidal nano-silica in the hydration of Alite and Belite paste.* Material Science, 2007. **11**(42): p. 3901-3907.

5. Qing, Y., Zenan, Z., Deyu, K., and Rongshen, C., *Influence of nano-SiO2 addition on properties of hardened cement paste as compared with silica fume.* Construction and Building Materials, 2007. **21**: p. p. 539-545.

6. Flores, I., Sobolev, K., Torres-Martinez, L.M., Cuellar, E.L., Valdez, P.L., and Zarazua, E., *Performance of Cement Systems with Nano- SiO2 Particles Produced Using Sol-gel Method.* Journal of the Transportation Research Board, 2010. **1**: p. p.10-14.

7. Moini M., F.V.I., Amirjanov A., Sobolev K., *The Optimization of Aggregate Blends for Sustainable Low Cement Concrete, Construction and Building Materials 93 (2015): 627-634.* 2015.

8. *Global Climate Change*, 2013, Geothermal Energy.

9. Kutepov, A.M. and Potapov, V.V., *Movement and mass exchange of liquid drop in spinned flow of geothermal medium.* Teor. Osnovy. Tekh., 2000. **34**(2).

10. Flores-Vivian, I., Pradoto, R., Moini, M., Kozhukhova, M., Potapov, V., and Sobolev, K., *The Effect of SiO_2 Nanoparticles Derived from Hydrothermal Solutions on the Performance of Portland Cement Based Materials.* Composites Part B: Engineering (under review), 2015.

11. Langan, B.W., Weng, K., and Ward, M.A., *Effect of silica fume and fly ash on heat of hydration of portland cement.* Cement and Concrete Research, 2002. **32**: p. 1045-1051.

12. Flores-Vivian, I., Pradoto, R., Moini, M., and Sobolev, K. *The use of nanoparticles to improve the performance of concrete*. in *Nano Conference*. 2013. Brno, Czech Republic, EU.

13. Flores, I., Sobolev, K., Torres-Martinez, L.M., Cuellar, E.L., Valdez, P.L., and Zarazua, E., *Performance of Cement Systems with Nano- SiO2 Particles Produced Using Sol-gel Method.* Journal of the Transportation Research Board, 2010. **1**: p. 10-14.

14. Worrell, E., Price, L., Martin, N., Hendriks, C., and Meida, L.O., *Carbon dioxide emissions from the global cement industry 1*, in *Annual Review of Energy and the Environment*2001. p. 303-329.

15. Sobolev, K., *Sustainable Development of the Cement Industry and Blended Cements to Meet Ecological Challenges.* The Scientific World Journal, 2003. **3**: p. 308-318.

16. Sobolev, K. and Ferrada-Gutiérrez, M., *How Nanotechnology Can Change the Concrete World: Part 2.* American Ceramic Society Bulletin, 2005. **No. 11**: p. pp. 16-19.

17. Collepardi, M., Skarp, U., and Troli, R. *Optimization of Silica Fume, Fly Ash and Amorphous Nano-Silica in Superplasticized High-Performance Concretes*. in *8th CANMET/ACI International Conference on Fly Ash, Silica Fume, Slag , SP-221*. 2004. Las Vegas, USA.

18. Li, H., Xiao, H.-G., Yuan, J., and Ou, J., *Microstructure of cement mortar with nanoparticles.* Composites: Part B, 2004. **35**: p. pp. 185-189.

19. Li, G., *Properties of high-volume fly ash concrete incorporating nano-SiO2.* Cement and Concrete Research, 2004. **34**: p. pp.1043-1049.

20. *UWM Center for By-Products Utilization*. Available from: http://cbu.ceas.uwm.edu/.

21. Sanchez, F. and Sobolev, K., *Nanotechnology in Concrete -A review.* Contruction and Building Materials, 2010. **24**: p. 2060-2071.

22. Sobolev, K. and Gutiérrez, M.F., *How nanotechnology can change the concrete world: Part 1.* American Ceramic Society Bulletin, 2005. **84**(10): p. 14.

23. Trtik, P. and Bartos, P. *Nanotechnology and concrete: What can we utilise from the upcoming technologies*. in *Anna Maria 2001 Workshop on Cement and Concrete: Trends and Challenges*. 2001.

24. Plassard, C., Lesniewska, E., Pochard, I., and Nonat, A., *Investigation of the surface structure and elastic properties of calcium silicate hydrates at the nanoscale.* Ultramicroscopy, 2004. **100**(3): p. 331-338.

25. Corradi, M., Khurana, R., and Magarotto, R., *Controlling performance in ready mixed concrete.* Concrete international, 2004. **26**(8): p. 123-126.

26. Sobolev, K., Zhiblin, L., Flores-Vivian, I., and Pradoto, R., *Nano-Engineered Cements with Enhanced Mechanical Performance.* Journal of the American Ceramic Society, 2015. **1-9**.

27. Thomas, J.J., Jennings, H.M., and Chen, J.J., *Influence of nucleation seeding on the hydration mechanisms of tricalcium silicate and cement.* The Journal of Physical Chemistry C, 2009. **113**(11): p. 4327-4334.

28. Tajuelo, E., Richardson, I.G., Black, L., and Nonat, A., *P8: Relationship between composition, structure and morphology in CSH.* 2010.

29. *BASF, From nanocrystals to concrete components: X-SEED® crystals from BASF make concrete harden faster and reduce carbon emissions*. Available from: https://www.basf.com/us/en/company/news-and-media/science-around-us/from-nanocrystals-to-concrete-components.html.

30. Royak, S.M. and Royak, G.S., *Special cements.* Stroyizdat, 1983(Moscow, Russia): p. p. 88–109.

31. Jonasson, J., Ronin, V., and Hedlund, H. *High strength concretes with energetically modified cement and modeling of shrinkage caused by self-desiccation*. in *Proceedings of the 4th international symposium on the utilization of high strength/high performance concrete, Paris, France*. 1996.

32. Ioudovitch, B., Dmitriev, A., Zoubekhine, S., Bashlykov, N., Falikman, V., and Serdyuk, V. *Low-Water Requirement Binders as New-Generation Cements*. in *10th International Congress on the Chemistry of Cement, Pub*. 1997.

33. Sobolev, K., *Effect of complex admixtures on cement properties and the development of a test procedure for the evaluation of high-strength cements.* Advances in cement research, 2003. **15**(2): p. 67-75.

34. Frigione, G. and Marra, S., *Relationship between particle size distribution and compressive strength in Portland cement.* Cement and Concrete Research, 1976. **6**(1): p. 113-127.

35. Osbaeck, B. and Johansen, V., *Particle size distribution and rate of strength development of Portland cement.* Journal of the American Ceramic Society, 1989. **72**(2): p. 197-201.

36. Pommersheim, J.M. *Effect of particle size distribution on hydration kinetics*. in *MRS Proceedings*. 1986. Cambridge Univ Press.

37. Škvára, F., Kolář, K., Novotný, J., and Zadak, Z., *Cement pastes and mortars with low water-to-cement ratio I.* Cement and Concrete Research, 1980. **10**(2): p. 253-262.

38. Sobolev, K. and Arikan, M., *High volume mineral additive for eco-cement.* American Ceramic Society Bulletin, 2002. **81**(1): p. 39-43.

39. Sobolev, K., *High performance cement: a solution for next millennium.* Materials Technology(UK)(UK), 1999. **14**(4): p. 191-193.

40. Schönert, K. *Physical and technical aspects of very and micro fine grinding*. in *Proceedings of the second world congress particle technology. Kyoto, Japan: Society of Technology*. 1990.

41. Fernandez-Bertran, J.F., *Mechanochemistry: an overview.* Pure and applied chemistry, 1999. **71**(4): p. 581-586.

42. Balema, V., Wiench, J., Dennis, K., Pruski, M., and Pecharsky, V., *Titanium catalyzed solid-state transformations in LiAlH 4 during high-energy ball-milling.* Journal of alloys and compounds, 2001. **329**(1): p. 108-114.

43. America, Y.C.o., *Geothermal Power*, 2015, Yokogawa Corporation.

44. Bhushan, B., *Springer handbook of nanotechnology*2010: Springer Science & Business Media.

45. Poole Jr, C.P. and Owens, F.J., *Introduction to nanotechnology*2003: John Wiley & Sons.

46. Gann, D., *A review of nanotechnology and its potential applications for construction.* SPRU, University of Sussex, 2002. **28**.

47. Klabunde, K.J. and Richards, R.M., *Nanoscale materials in chemistry*2009: John Wiley & Sons.

48. Calderón-Moreno, J.M., Schehl, M., and Popa, M., *Superplastic behavior of zirconia-reinforced alumina nanocomposites from powder alcoxide mixtures.* Acta materialia, 2002. **50**(16): p. 3973-3983.

49. Watanabe, T., Kojima, E., Norimoto, K., Kimura, T., Machida, M., Hayakawa, M., Kitamura, A., Chikuni, M., Saeki, Y., and Kuga, T., *Multi-functional material with photocatalytic functions and method of manufacturing same*, 2001, Google Patents.

50. Hosseini, T., Flores-Vivian, I., Sobolev, K., and Kouklin, N., *Concrete embedded dye-synthesized photovoltaic solar cell.* Scientific reports, 2013. **3**.

51. Sobolev, K., Flores, I., Hermosillo, R., and Torres-Martínez, L.M., *Nanomaterials and nanotechnology for high-performance cement composites.* Proceedings of ACI session on

nanotechnology of concrete: recent developments and future perspectives, 2006: p. 91-118.

52. Kang, S., Hong, S.I., Choe, C.R., Park, M., Rim, S., and Kim, J., *Preparation and characterization of epoxy composites filled with functionalized nanosilica particles obtained via sol–gel process.* Polymer, 2001. **42**(3): p. 879-887.

53. Bjornstrom, J., Martinelli, A., Matic, A., Borjesson, L., and Panas, I., *Accelarating effects of colloidal nano-silica for beneficial calsium-silicate-hydrate formation in cement.* Chemical Physics Letter, 2004.

54. Green, B.H. *Development of a high-density cementitious rock-matching grout using nano-particles*. in *Proceedings of ACI Session on "Nanotechnology of Concrete: Recent Developments and Future Perspectives, SP-254*. 2008.

55. Qing, Y., Zenan, Z., Deyu, K., and Rongshen, C., *Influence of nano-SiO2 addition on properties of hardened cement paste as compared with silica fume.* Construction and building materials, 2007. **21**: p. 539-545.

56. Gaitero, J.J., Campillo, I., and Guerrero, A., *Reduction of the calcium leaching rate of cement paste by addition of silica nanoparticles.* Cement and Concrete Research, 2008. **38**(8-9): p. 1112-1118.

57. Jansson, I., Skarp, U., and Bigley, C. *The value of colloidal silica for enhanced durability in high fluidity cement based mixes*. in *5 International RILEM simposium on self-compacting concrete*. 2007.

58. Titoria, P. and Groves, K., *Nanotechnology for the Food Industry*, NANO: The magazine for small science.

59. Kagel, A., *The State of Geothermal Technology Part II: Surface Technology, Geothermal Energy Association*, 2008. p. 78.

60. *Silicon Nanoparticles*, 2009.

61. Ramachandran, V., Lowery, M., and Malhotra, V., *Behaviour of ASTM Type V cement hydrated in the presence of sulfonated melamine formaldehyde.* Materials and structures, 1995. **28**: p. 133-138.

62. A. Lange, J.P. *Formation of Nano-Sized Ettringite Crystals Identified as Root Cause for Cement Incompatibility of PCE Superplasticizers*. in *Nanotechnology in Construction, NICOM 5*. 2015.

63. Collepardi, S., Coppola, L., Troli, R., and Collepardi, M., *Mechanisms of Actions of Different Superplasticizers For High Performance Concrete.* ACI Special Publication, 1999. **186**.

64. Shin, J.-Y., Hong, J.-S., Suh, J.-K., and Lee, Y.-S., *Effects of polycarboxylate-type superplasticizer on fluidity and hydration behavior of cement paste.* Korean Journal of Chemical Engineering, 2008. **25**(6): p. 1553-1561.

65. Yamada, K., Takahashi, T., Hanehara, S., and Matsuhisa, M., *Effects of the chemical structure on the properties of polycarboxylate-type superplasticizer.* Cement and Concrete Research, 2000. **30**(2): p. 197-207.

66. Bassioni, G., *The influence of cement composition on superplasticizers' efficiency.* International Journal of Engineering (IJE), 2010. **3**(6): p. 577.

67. Mikanovic, N. and Jolicoeur, C., *Influence of superplasticizers on the rheology and stability of limestone and cement pastes.* Cement and Concrete Research, 2008. **38**(7): p. 907-919.

68. Sakai, E., Yamada, K., and Ohta, A., *Molecular structure and dispersion-adsorption mechanisms of comb-type superplasticizers used in Japan.* Journal of Advanced Concrete Technology, 2003. **1**(1): p. 16-25.

69. Fennis, S.A. and Walraven, J.C., *Using particle packing technology for sustainable concrete mixture design.* Heron, 57 (2012) 2, 2012.

70. Kim, B.-G., Jiang, S., Jolicoeur, C., and Aïtcin, P.-C., *The adsorption behavior of PNS superplasticizer and its relation to fluidity of cement paste.* Cement and Concrete Research, 2000. **30**(6): p. 887-893.

71. Malhotra, V.M. and Mehta, P.K., *Pozzolanic cementitious materials.* Advances in Concrete Technology, 1996. **vol 1**(Gordon and Breach, London): p. p.11.

72. Celik, O., Damci, E., and Piskin, S., *Characterization of fly ash and it effects on the compressive strength properties of Portland cement.* Indian Journal of Engineering and Materials Sciences, 2008. **15**(5): p. 433.

73. Thongsanitgarn, P., Wongkeo, W., Chaipanich, A., and Poon, C.S., *Heat of hydration of Portland high-calcium fly ash cement incorporating limestone powder: Effect of limestone particle size.* Construction and Building Materials, 2014. **66**: p. 410-417.

74. Lin, Z., Sobolev, K., and Flores-Vivian, I. *Nano-Engineered Cements with Improved Early Strength*. in *4th International Symposium on Nanotechnology in Construction 4 (NICOM4)*. 2012. Greece, May 20-22.

75. Felekoğlu, B., Türkel, S., and Kalyoncu, H., *Optimization of fineness to maximize the strength activity of high-calcium ground fly ash-Portland cement composites.* Construction and Building Materials, 2009. **2053-2061**(23(5)).

76. Hela, R. and Orsáková, D. *The Mechanical Activation of Fly Ash*. in *CONCRETE AND CONCRETE STRUCTURES 2013 - 6th International Conference, Slovakia*. 2013.

77. Kawashima, S., Hou, P., Wang, K., Corr, D.J., and Shah, S.P. *Activation of fly ash through nanomodification*. in *American Concrete Institute, ACI Special Publication*. 2012. Dallas, USA.

78. Ramseyer, C.C. and Kiamanesh, R., *Optimizing Concrete Mix Designs to Produce Cost Effective Paving Mixes*, 2009, Civil Engineering and Environmental Science, University of Oklahoma.

79. Rached, M., De Moya, M., and Fowler, D.W., *Utilizing aggregates characteristics to minimize cement content in portland cement concrete.* International Center for Aggregates Research (ICAR 401), University of Texas, Austin, USA, 2009.

80. Quiroga, P.N. and Fowler, D.W., *The effects of aggregates characteristics on the performance of Portland cement concrete*, 2004, International Center for Aggregates Research, University of Texas at Austin.

81. De Larrard, F. and Sedran, T., *Mixture-proportioning of high-performance concrete.* Cement and Concrete Research, 2002. **32**(11): p. 1699-1704.

82. Sobolev, K. and Soboleva, S., *High-Performance Concrete Mixture Proportioning.* ACI Special Publication, 1998. **179**.

83. Peterson, K., Sutter, L.L., and Anzalone, G., *Reduction of Minimum Required Weight of Cementitious Materials in WisDOT Concrete Mixes*, 2011.

84. Ji, T., Chen, C.-Y., Zhuang, Y.-Z., and Chen, J.-F., *A mix proportion design method of manufactured sand concrete based on minimum paste theory.* Construction and Building Materials, 2013. **44**: p. 422-426.

85. Noguchi, T., Maruyama, I., and Kanematsu, M. *Performance based design system for concrete mixture with multi-optimizing genetic algorithm*. in *Proceedings of the 11th International Congress on the Chemistry of Cement "Cements Contribution to the Development in the 21st Century", Durban*. 2003.

86. Yeh, I.-C., *Computer-aided design for optimum concrete mixtures.* Cement and Concrete Composites, 2007. **29**(3): p. 193-202.

87. Cheng, M.-Y., Prayogo, D., and Wu, Y.-W., *Novel Genetic Algorithm-Based Evolutionary Support Vector Machine for Optimizing High-Performance Concrete Mixture.* Journal of Computing in Civil Engineering, 2013. **28**(4).

88. Moini, M. and Lakizadeh, A., *Concrete Workability: An Investigation on Temperature effects Using Artificial Neural Networks*2011: AuthorHouse.

89. Van Dam, T., Taylor, P., Fick, G., VanGeem, M., and Lorenz, E., *Sustainable concrete pavements: A manual of practice.* 2012.

90. Liu, R., Durham, S.A., Rens, K.L., and Ramaswami, A., *Optimization of cementitious material content for sustainable concrete mixtures.* Journal of Materials in Civil Engineering, 2011. **24**(6): p. 745-753.

91. Easa, S.M. and Can, E.K., *Optimization model for aggregate blending.* Journal of construction engineering and management, 1985. **111**(3): p. 216-230.

92. Richardson, D.N., *Aggregate gradation optimization: literature search.* 2005.

93. Cordon, W.A. and Gillespie, H.A. *Variables in concrete aggregates and Portland cement paste which influence the strength of concrete*. in *ACI Journal Proceedings*. 1963. ACI.

94. Koehler, E.P., *Aggregates in self-consolidating concrete*2007: ProQuest.

95. Fu, G. and Dekelbab, W., *3-D random packing of polydisperse particles and concrete aggregate grading.* Powder Technology, 2003. **133**(1): p. 147-155.

96. Moini, M., Muzenski, S., Flores-Vivian, I., and Sobolev, K., *Aggregate Optimization for Concrete Mixtures with Low Cement Factor, 2014*

97. Moini, M., Lakizadeh, A., and Mohaqeqi, M., *Effect of mixture temperature on slump flow prediction of conventional concretes using artificial neural networks.* Australian Journal of Civil Engineering, 2012. **10**(1).

98. Simon, M.J., Lagergren, E.S., and Snyder, K.A. *Concrete mixture optimization using statistical mixture design methods*. in *Proceedings of the PCI/FHWA international symposium on high performance concrete*. 1997.

99. Kwan, A. and Wong, H., *Packing density of cementitious materials: part 2—packing and flow of OPC+ PFA+ CSF.* Materials and structures, 2008. **41**(4): p. 773-784.

100. Bergman, L.A. *Optimization of Portland-Pozzolan Concrete, Airport Runways*. in *Construction and Materials Issues 2001*. 1962. ASCE.

101. Aydın, S., *A ternary optimisation of mineral additives of alkali activated cement mortars.* Construction and Building Materials, 2013. **43**: p. 131-138.

102. *Aggregate suspension mixture proportioning method.* TechNote, ACI 211.6T-14. 68.

103. Sobolev, K., *The development of a new method for the proportioning of high-performance concrete mixtures.* Cement and Concrete Composites, 2004. **26**(7): p. 901-907.

104. Quercia, G., Hüsken, G., and Brouwers, H.J.H., *Water demand of amorphous nano silica and its impact on the workability of cement paste.* Cement and Concrete Research, 2012. **42(2)**: p. 344-357.

105. Nobel, A., *Cembinder for the oil field industry, colloidal silica dispersions - uses and benefits*

106. Potapov, V.V., Shitikov, E.S., Trutnev, N.S., Gorbach, V.A., and Portnyagin, N.N., *Influence of Silica Nanoparticles on the Strength Characteristics of Cement Samples.* Glass Physics and Chemistry, 2001. **37**(1): p. pp. 98–105.

107. Brazhnikov, S.M., Generalov, M.B., and Taitnev, N.S., *Vacuum Sublimation Technique for Preparing Ultradispersed Powders of Inorganic Salts.* Khim. Mashinoslr. (Moscow), 2004. **12**: p. 12–15.

108. Sobolev, K., Moini, M., Cramer, S., Flores-Vivian, I., Muzenski, S., Pradoto, R., Fahim, A., Pham, L., and Kozhukhova, M., *Laboratory Study of Optimized Concrete Pavement Mixtures*, 2015, UW-Milwaukee, UW- Madison, Temple University/ Bloom.

109. C989, A., *Standard Specification for Slag Cement for Use in Concrete and Mortars.*

110. American Society for Testing and Materials, A.C.-. *Standard Specification for Coal Fly Ash and Raw or Calcined Natural Pozzolan for Use in Concrete*, 2003.

111. Fennis, S., *Design of ecological concrete by particle packing optimization*2011: TU Delft, Delft University of Technology.

112. Paul J. Tikalsky, A.J.S., David G. Tepke, *Potential Concrete Mixture Designs for the I-99 Corridor Final Report, Issues 2003-2029*, P.T. Institute and R.P.T. Institute), Editors.

113. P. Tikalsky, V.S., K. Wang, B. Scheetz, T. Rupnow, A. St. Clair, M. Siddiqi, and S. Marquez, , *Development of Performance Properties of Ternary Mixes: Phase I Final Report. FHWA Pooled Fund Study TPF-5 (117)*2007.

114. Mehta, P.K. and Monteiro, P.J.M., *Concrete, Microstructure, Properties and Materials*2006, New York: McGraw Hill Companies.

115. Banfill, P., *Rheology of Fresh Cement and Concrete: Proceedings of an International Conference, Liverpool, 1990*1990: CRC Press.

116. Munoz, J., Silva, J., Perry, L., Youtcheff, J., and Sobolev, K., *Interaction of Amorphous Nano-aluminosilicates with Cement Pore Solution and the Effect on the Early Hydration*

Reaction of Portland Cement, in *Nanotechnology in Construction*2015, Springer. p. 161-166.

CURRICULUM VITAE

Rani G. K. Pradoto

Education

B.S., Civil Engineering (Structures), Bandung Institute of Technology, Indonesia, 1997.
M.S., Civil Engineering (Structures and Wind Engineering), Colorado State University (CSU), 2001.
Ph.D., Civil Engineering (Materials and Structures), University of Wisconsin Milwaukee (UWM), May 2016.

Ph.D. Dissertation Title

The Effect of Mechano-Chemical Activation of Fly Ash- Nanoparticles Blends on Performance of Cement Based Composites and Self-Consolidating Concrete

Awards
Grant Award from Portland Cement Association Education Foundation (PCAEF) on research "*Engineering of Nano C-S-H Seed to Enhance Structure and Performance of Cementitious Materials"* (August 2015)

UW-Milwaukee Chancellor's Awards Recipient (Fall 2015)

Professional Affiliations
Member of American Concrete Institute
Voting member of Committee 241: Nanotechnology of concrete

Brief statement of experience related to the work

As a Ph.D. student at University of Wisconsin-Milwaukee, my primary research project was to develop nano-engineered cement (NEC) binders using the mechano-chemical activation (MCA) of fly ash blended with nanoparticles and superplasticizer. The activated fly ash system with nanoparticles was beneficially used in self-consolidating concrete. The experimental results were compared with the performance of reference DOT grade concrete and demonstrated the advantage of self-compacting mixes. The developed NEC concept resulted in a concrete of better performance vs. reference with regard to a) improved early strength, b) utilization of SCM, c) reduction of portland cement, d) improved durability, d) improved long-term mechanical performance.

As a research assistant at the Advanced Nano-Cement Lab, I was involved in a DOT project on "Laboratory Study of Optimized Concrete Pavement Mixtures". The project developed the optimized concrete with supplementary cementitious materials to improving the performance and sustainability of pavement materials used in Wisconsin.

Research Achievements

- Development of activated fly ash with nanosilica for cement systems with improved early strength;
- Investigation of the effects of SiO_2 nanoparticles from hydrothermal solutions on performance of portland cement based materials;
- Investigation of optimized concrete pavement mixtures;
- Optimization of SCC mixtures with nanosilica and fly ash;
- The design and physical model comparison for wind loads on a high rise building.

Research and Teaching Experience

Teaching Assistant for "Strength of Materials" class, at UW- Milwaukee, Spring 2013 - Spring 2015

Research Assistant at Advance Cement-Based Materials Laboratory, UW-Milwaukee, January 2013-December 2015

Publications

1. Sobolev, K., Lin, Z., Flores-Vivian, I., Pradoto, R. "*Nano-Engineered Cements with Enhanced Mechanical Performance."* Journal of American Ceramics Society, 2015: p. 1-9.
2. Flores-Vivian, I., Pradoto, R.,Moini., M., Sobolev., K., "*The use of Nanoparticles to improve the performance of concrete.", Proceeding of* 5th International Conference of NANOCOM 2013, Oct 16-18, 2013, Czech Republic, EU
3. Flores-Vivian, I., Pradoto, R.,Moini., M., Kozhukhova , M., Potapov, V. Sobolev., K., "*The Effect of SiO_2 Nanoparticles Derived from Hydrothermal Solutions on the Performance of Portland Cement Based Materials"*. Under review for Journal Composites Part B.
4. Sobolev, K., Moini, M., Cramer, S., Flores-Vivian, I., Muzenski, S., Pradoto, R., Fahim, A., Pham, L., Kozhukhova, M., "*Laboratory Study of Optimized Concrete Pavement Mixtures*", WisDOT DOT Report (2015)
5. Meroney, R., N., Neff, D., Chang, C.H., Pradoto, R. "*Computational Fluid Dynamics and Physical Model Comparisons of Wind Loads and Pedestrian Comfort around a High Rise Building*", PROCEEDINGS OF THE 2002 STRUCTURES CONGRESS, Performance of Structures: from research to design, April 4-6, 2002, Denver, Colorado.
6. Activation of fly ash with nanosilica for cement systems with improved early strength (in preparation)

Presentations

"Performance of SiO2 nanoparticles from hydrothermal solutions in portland cement based materials," Poster at 5th International Symposium on Nanotechnology in Construction (NICOM 5), May 2015, Chicago USA.

Engineering Experience

Design engineering experience:

- Evaluation of the design of bridges using SAP;
- Analysis and design of ferry terminal for the port of Sumatra Island, Indonesia;
- Design and physical model comparisons of wind loads around a high rise building;
- Design of 3-storey residential building.

Construction Experience:

- Supervised the construction of Barelang Cable-Stayed Bridge (span 200 m) at Batam Island, Indonesia (1999).